Imperial College London

Department of Mathematics

Axisymmetric ferrofluids falling under gravity

JAVIER CHICO VÁZQUEZ

CID: 01577631

Supervised by DEMETRIOS T. PAPAGEORGIOU

The work contained in this thesis is my own work unless otherwise stated.

June 13, 2023

Submitted in partial fulfilment of the requirements for the MSci in Mathematics of Imperial College London

The work contained in this thesis is my own work unless otherwise stated.

Signed: JAVIER CHICO VÁZQUEZ Date: June 13, 2023

Abstract

In this paper, we present results on the widely applicable topic of falling axisymmetric ferrofluids. Combining two independent widely studied problems: falling viscous fluids and axisymmetric ferromagnetic flows, a reduced order model is developed and the flow stability is considered. The problem is further generalized by considering the effect of displacing the wire, and running time-varying and stochastic currents through it. Finally, a pseudo-spectral method is developed to resolve the nonlinear initial boundary value problems.

Acknowledgements

I am grateful to Demetrios for his support and guidance through the different stages for the project. He has been a constant source of wisdom, advice and inspiration. I am further grateful to the many people who I had the pleasure of speaking about my work: Dr. Sarah Ferguson Briggs, Anna Katsiavria, Dr. Michael Cornish, Yanghan Meng, Jose Luis Narbona, Dr. Gunnar Peng, Prof. Xuesong Wu and Prof. Darryl Holm. Thank you all for your advice and discussion on the project.

Last but not least I am immensely grateful to my partner Ana and my family for their continuous support in all stages of my degree.

Contents

1. Introduction

In the last few decades, the fields of falling viscous flows and ferrofluids have seen remarkable progress, with numerous applications in engineering, biomedicine, and environmental sciences. A thorough understanding of the dynamics and stability of coating fluid films falling under gravity's influence has been achieved through the work of various researchers, including Craster and Matar, Duprat et al., and Kliakhandler et al. (10; 13; 28; 53). Meanwhile, the study of ferrofluids has also experienced significant advancements, as demonstrated by the theories developed by Rosensweig (45) and others (3; 5; 7; 9).

While the majority of the literature on ferrofluids has focused on the inviscid case, recent research by Cornish (8) and Ferguson Briggs (16) has shifted attention to the study of viscous effects in ferrofluids. This transition has led to new insights and an enhanced understanding of the complexities involved in ferrofluid systems.The ferrofluid literature often neglects gravitational body forces, which are essential in the study of falling viscous fluids.

This Master's thesis aims to bridge the gap between these two areas of research by addressing a natural question: how can the long-wave theories for falling viscous fluids be combined with the ferrofluid results? Specifically, this study will investigate the behavior of axisymmetric ferrofluids that coat a small conducting wire and fall under the influence of gravity. To achieve this objective, the research will draw upon and extend existing theoretical frameworks, numerical methods, and experimental data, as well as the foundational works on fluid dynamics and electromagnetism by Batchelor (6), Grant and Phillips (20), and (54). Ultimately, this work will contribute to a more comprehensive understanding of the interaction between ferrofluids and gravitational forces and may lead to novel applications and innovations in related fields.

Before continuing to the next section we will present a brief introduction to the field of ferrofluids, as this is not covered in most undergraduate and graduate Fluid Dynamics courses.

A ferrofluid is a colloidal suspension of nanoscale ferromagnetic particles dispersed in a carrier fluid, typically an organic solvent or water (45) . These particles, often composed of materials such as magnetite, or cobalt ferrite, are coated with a surfactant to prevent aggregation and ensure their even distribution within the fluid (45) . Due to their magnetic nature, ferrofluids exhibit unique and fascinating properties. for instance, in the presence of external magnetic fields, they respond by forming of spikes and patterns as a result of an energy minimisation procedure. (45; 54). These intriguing characteristics have led to a diverse range of applications, including sealing and lubrication in rotating machinery, targeted drug delivery, magnetic resonance imaging (MRI) contrast agents, and cooling systems for electronic devices (9; 45).

It is important to note ferrohydrdynamics is not the same as magnetohydrodynamics (MHD), a research area the reader might be more familiar with due to its central role in astrophysical fluid dynamics. Ferrohydrodynamics and magnetohydrodynamics (MHD) both involve the study of fluids in the presence of magnetic fields, but they differ fundamentally in their underlying physics and applications. Ferrofluids, as mentioned earlier, are colloidal suspensions of nanoscale ferromagnetic particles dispersed in a carrier fluid (45). Their unique properties arise from the interaction between the dispersed magnetic particles and applied external magnetic fields (45). In contrast, magnetohydrodynamics deals with the macroscopic behavior of electrically conducting fluids, such as plasmas, liquid metals, and some electrolytes, in the presence of both magnetic and electric fields (12; 42). MHD studies the interplay between fluid dynamics and electromagnetism, taking into account the fluid's motion, electric currents, and the induced magnetic fields (12; 42).

While ferrofluids are primarily used in applications such as sealing, lubrication, drug delivery, and cooling systems (9; 45), MHD has broader applications in areas such as astrophysics, geophysics, and engineering. MHD is essential for understanding phenomena like solar flares, the Earth's magnetic field, and the behavior of plasmas in nuclear fusion reactors (12; 42). Although both ferrofluids and MHD involve the interaction of fluids with magnetic fields, their distinct material properties, scales, and underlying physical mechanisms lead to different research fo-

cuses and practical applications.

Finally, we will briefly comment on viscous falling flows, also known as falling films or coating flows, involve the study of fluid films flowing down solid surfaces or fibers under the influence of gravity. Over the past few decades, significant progress has been made in understanding the fundamental physics, stability, and dynamics of these flows (4; 26). Early investigations primarily focused on the behavior of thin films flowing down flat, inclined, or curved surfaces. Subsequent research expanded the scope to include viscous beads flowing down vertical fibers, leading to the development of long-wave theories and the investigation of various instabilities, such as absolute and convective instabilities (10; 13; 28; 53).

Recent studies have also considered the effects of various factors on viscous falling film flows, including viscosity contrasts, and non-Newtonian fluids (2; 4). Furthermore, the development of advanced experimental techniques and numerical simulations has allowed researchers to gain deeper insights into the complex behavior of these flows in real-world situations (18; 48). The progress made in the field of viscous falling flows has led to a wide range of applications, including coating processes in the manufacturing industry, heat exchangers, and biomedical devices (2; 26).

Now the scene is set to start our search for the answer to our research questions. In the first two chapters the equations governing the problem of falling ferrofluids will be derived and nondimensionalised. This will be followed by a thorough discussion of the problem in the long wave limit, where the axial length scale is much larger than the radial length scale. Then, the Stokes limit will be analysed to compare the results with the long wave limit. Finally, several complexifications of the problem are explored: a tranlsating wire, a time dependent magnetic field and the stochastic current case. The penultimate chapter is a brief showcase of the numerical methods used throughout the text and the final chapter presents the conclusions and future work avenues of the investigation.

2. Governing equations

In this section we will derive the governing equations and the corresponding boundary conditions for the problem in mind. Consider a situation as shown in Figure 2.1. Here a viscous fluid coats a thin conducting wire of dimensional radius $\hat{\alpha}$. We define our axisymmetric cylindrical coordinates coordinates with the z axis pointing downwards (i.e. gravity acts in the positive direction). Several equations must be considered to fully close the free boundary problem. First, we must consider the Maxwell equations for the Electromagnetic field induced by the current in the wire. Second, we must consider the continuity equation to satisfy conservation of mass in the fluid bulk. Further, we consider Newton's second law in continuum form to derive a dynamic equation for the fluid variables, integrating the ferrohydrodynamic effects. Finally, we derive the accompanying boundary conditions at the wire surface and the free boundary at $\hat{r} = \hat{S}$. In this text, the hatted variables represent dimensional variables unless stated otherwise. We will begin by considering the Maxwell equations, followed by the Navier Stokes equations.

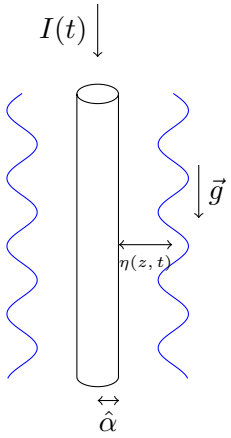

Figure 2.1.: A schematic of the problem.

2.1. Maxwell equations and the electromagnetic field

As first derived by James Clerk Maxwell (22), the electromagnetic field satisfies the Maxwell equations (20; 54), given by (2.1)

$$\begin{aligned} \nabla \cdot \hat{\mathbf{E}} &= \frac{\hat{\rho}_e}{\epsilon_0} \qquad & \nabla \cdot \hat{\mathbf{B}} &= 0 \\ \nabla \times \hat{\mathbf{E}} &= -\frac{\partial \hat{\mathbf{B}}}{\partial \hat{t}} \qquad & \nabla \times \hat{\mathbf{H}} &= \mu_0 \hat{\mathbf{J}} + \frac{1}{c^2}\frac{\partial \hat{\mathbf{E}}}{\partial \hat{t}} \end{aligned} \tag{2.1}$$

In what follows we assume the electromagnetic field is not affected by the fluid variables, in particular the fluid is non conducting (45). In equation 2.1 $\hat{\mathbf{E}}$ is the electric field, $\hat{\mathbf{H}}$ is the magnetic field, $\hat{\mathbf{B}}$ is the induced magnetic field and $\hat{\mathbf{J}}$ is the electric current density. Furthermore the scalar parameters are:

- $\hat{\rho}_e$ is the electric charge density of free space.
- ϵ_0 is the electric permittivity of free space, given by $\epsilon_0 \approx 8.85 \times 10^{-12}\ \mathrm{C^2\,N^{-1}\,m^{-2}}$.(20)
- μ_0 is the magnetic permeability of free space, given by $\mu_0 = \frac{2\alpha h}{e^2 c}$ (54), with α the fine structure constant, c the speed of light in a vacuum and e the elementary charge and h the Planck constant. Numerically, $\mu_0 \approx 4\pi \times 10^{-7}\ \mathrm{N\,A^{-2}}$. (20)
- The speed of light in a vacuum $c = (\mu_0 \varepsilon_0)^{-1/2} \approx 3 \times 10^8\ \mathrm{m\,s^{-1}}$. (25)

We further assume that the electric charge density is everywhere zero, so that the electric field is solenoidal. The magnetization vector $\hat{\mathbf{M}}$ is defined by the following relationship between the magnetic field and the induced magnetic field (16; 45):

$$\hat{\mathbf{B}} = \mu_0(\hat{\mathbf{H}} + \hat{\mathbf{M}}) \tag{2.2}$$

2.1.1. Colinearity

We will assume, as is standard in the ferrofluid literature is collinearity. This is that the induction vector $\hat{\mathbf{M}}$ and the magnetic field $\hat{\mathbf{H}}$ are parallel (9; 16; 45)

$$\hat{\mathbf{M}} = \chi \hat{\mathbf{H}} \tag{2.3}$$

and the dimensionless proportionality constant χ is known as the *magnetic susceptibility*. In this investigation it is further assumed that χ is independent of time, position and the magnitude of the field.

2.1.2. Jefimenko Integrals

We can construct the solution to the Maxwell equations using the Jefimeko integrals (under the Coulomb/Lorenz gauge). These are derived from the scalar and magnetic Liénard-Wiechert potentials, and more details are included in appendix A.2.1. In the case where $\hat{\rho}_e = 0$, but the current $\hat{\mathbf{J}} \neq 0$, these reduce to (20; 54)

$$\begin{aligned}\hat{\mathbf{B}}(\hat{\mathbf{x}}, \hat{t}) =& \frac{\mu_0}{4\pi} \int \left[\frac{\hat{\mathbf{J}}(\hat{\mathbf{x}}', \hat{t}_r) \times (\hat{\mathbf{x}} - \hat{\mathbf{x}}')}{|\hat{\mathbf{x}} - \hat{\mathbf{x}}'|^3} - \frac{\hat{\mathbf{x}} - \hat{\mathbf{x}}'}{|\hat{\mathbf{x}} - \hat{\mathbf{x}}'|^2} \times \frac{1}{c} \frac{\partial \hat{\mathbf{J}}(\hat{\mathbf{x}}', \hat{t}_r)}{\partial \hat{t}} \right] d^3\hat{x}' \\ \hat{\mathbf{E}}(\hat{\mathbf{x}}, \hat{t}) =& -\frac{1}{4\pi\varepsilon_0} \int \frac{1}{|\hat{\mathbf{x}} - \hat{\mathbf{x}}'| c^2} \frac{\partial \hat{\mathbf{J}}(\hat{\mathbf{x}}', \hat{t}_r)}{\partial \hat{t}} d^3\hat{x}'\end{aligned} \tag{2.4}$$

where the integrals are taken over $\mathbb{R}^3$ and the retarded time $\hat{t}_r$ is defined as

$$\hat{t}_r = \hat{t} - \frac{|\hat{\mathbf{x}} - \hat{\mathbf{x}}'|}{c} \approx t + \mathcal{O}(1/c) \tag{2.5}$$

In our case, $\hat{\mathbf{J}}$ will always point in the z direction, so that $\hat{\mathbf{E}}$ will always point in the z direction as well, and as the problem is axisymmetric the triple integrals can be reduced into double integrals by transforming to cylindrical coordinates and integrating out the angular differential.

2.1.3. Constant electric current

In the case of an infinitely long wire of radius $\hat{\alpha}$ carrying a constant current I, in the magnetostatic limit we recover the following well known azimuthal solution to the Maxwell equations (45): $\hat{\mathbf{B}} = (0, \hat{B}_\phi, 0)^\intercal$ and

$$\hat{B}_\phi = \begin{cases} \frac{\mu_0 I \hat{r}}{2\pi\hat{\alpha}^2} & \hat{r} < \hat{\alpha} \\ \frac{\mu_0 I}{2\pi\hat{r}} & \hat{r} > \hat{\alpha} \end{cases} \tag{2.6}$$

This is because $\hat{\mathbf{J}} = 0$ everywhere except in the wire itself, and $\hat{\mathbf{E}} = 0$ identically. We are only interested in the magnetic field outside of the wire, which satisfies the $\frac{1}{\hat{r}}$ law.

2.1.4. Time-dependent electric current

Let us assume there is an alternating current in the wire, so that $\mathbf{I}(t) = I_0 \cos(\Omega \hat{t}) \mathbf{e}_z$. We can compute the electromagnetic using the aforementioned Jefimenko's equations, in the case where $\hat{\rho}_e = 0$ as given by 2.4. However, as we are dealing with non-relativistic velocities and distances, $c \approx 3 \cdot 10^8$ ms^{-1} is much larger than any of the characteristics speeds in our problem. This motivates a Taylor expansion of the integrand for $\hat{\mathbf{B}}$, to second order in the first summand ($\hat{\mathbf{J}}$) and first order in the second summand ($\partial_{\hat{t}} \hat{\mathbf{J}}$), in powers of $\frac{1}{c}$. More precisely, we expand

$$\hat{\mathbf{J}}(\hat{\mathbf{x}}, \hat{t}_r) = \hat{\mathbf{J}}(\hat{\mathbf{x}}, \hat{t}) + \Delta\hat{t} \frac{\partial \hat{\mathbf{J}}(\hat{\mathbf{x}}, \hat{t})}{\partial \hat{t}} + \frac{1}{2} \frac{\partial^2 \hat{\mathbf{J}}(\hat{\mathbf{x}}, \hat{t})}{\partial \hat{t}^2} (\Delta\hat{t})^2 \tag{2.7}$$

With $\Delta\hat{t} = \hat{t}_r - \hat{t} = -\frac{|\hat{\mathbf{x}} - \hat{\mathbf{x}}'|}{c}$. The first derivative terms cancel and we obtain

$$\hat{\mathbf{B}}(\hat{\mathbf{x}}, \hat{t}) = \frac{\mu_0}{4\pi} \int \left[\frac{\mathbf{J}(\hat{\mathbf{x}}, \hat{t}) \times (\hat{\mathbf{x}} - \hat{\mathbf{x}}')}{|\hat{\mathbf{x}} - \hat{\mathbf{x}}'|^3} + \mathcal{O}\left(\frac{1}{c^2}\right) \right] d^3\hat{x}' = \left(0, \frac{\mu_0 I\left(\hat{t}\right)}{2\pi \hat{r}} + \mathcal{O}\left(\frac{1}{c}\right), 0 \right)^{\mathsf{T}} \tag{2.8}$$

so to leading order the magnetic field has the same form as the time independent case, with some small corrections (recall $c \approx 3 \cdot 10^8 \, \mathrm{m} \cdot \mathrm{s}^{-1}$)

Electric field

At first glance, it seems like we can neglect the electric field to leading order, as it contains a $\frac{1}{c^2}$ factor in the integrand. However, it is also divided by ϵ_0, and we must consider the scale of the quantity $\frac{1}{\epsilon_0 c^2}$ and we cannot compare this to $\mathcal{O}(1)$, but to $\mathcal{O}(\mu_0)$, for this is the leading order scale of the magnetic field, and the scale of the electromagnetic field in our problem. Indeed, as $c^2 = \frac{1}{\epsilon_0 \mu_0}$ it turns out that $\hat{\mathbf{E}} = \mathcal{O}(\mu_0)$, and we must consider it when the current changes in time. Recall from the Jefimenko equations 2.4 that

$$\hat{\mathbf{E}}(\hat{\mathbf{x}}, \hat{t}) = -\frac{\mu_0}{4\pi} \int \frac{1}{|\hat{\mathbf{x}} - \hat{\mathbf{x}}'|} \frac{\partial \mathbf{J}(\hat{\mathbf{x}}, \hat{t})}{\partial \hat{t}} d^3\hat{x}' \tag{2.9}$$

The appereance of the retarded time and its dependence on c^{-1} suggests that we Taylor expand the integral and proceed as before. To leading order

$$\hat{\mathbf{E}}(\hat{\mathbf{x}},\hat{t}) = -\frac{\mu_0}{4\pi}\int\left[\frac{1}{|\hat{\mathbf{x}}-\hat{\mathbf{x}}'|}\frac{\partial\hat{\mathbf{J}}(\hat{\mathbf{x}},\hat{t})}{\partial\hat{t}} + \mathcal{O}\left(\frac{1}{c}\right)\right]d^3\hat{x}' \tag{2.10}$$

However, this is problematic, as the integral will not be convergent. Therefore, an alternative procedure to extract the leading order electric field is required. From the above expression we see that $\hat{\mathbf{E}}$ and $\hat{\mathbf{J}}$ are collinear, motivating an Ansatz for the electric field that is purely longitudinal and axisymmetric (independent of φ): $\hat{\mathbf{E}} = (0,0,\hat{E}_z(\hat{r},\hat{t}))^\intercal$. Next from the third Maxwell equations (Faraday's law) we can see that

$$\nabla\times\hat{\mathbf{E}} = -\frac{\partial\hat{\mathbf{B}}}{\partial\hat{t}} = \left(0, \frac{I_0\mu_0\Omega\sin(\Omega\hat{t})}{2\pi\hat{r}}, 0\right)^\intercal \tag{2.11}$$

And taking into account the form for $\hat{\mathbf{E}}$, we see that

$$\frac{\partial\hat{E}_z}{\partial\varphi} = 0 \quad -\frac{\partial\hat{E}_z}{\partial\hat{r}} = \frac{I_0\mu_0\Omega\sin(\Omega\hat{t})}{2\pi\hat{r}} \tag{2.12}$$

Integrating this for $\hat{E}_z$, and take into account that the integration constant f might be a function of t

$$\hat{E}_z = -\frac{I_0\mu_0\Omega\sin(\Omega\hat{t})}{2\pi}\log\hat{r} + f(\hat{t}) + \mathcal{O}(1/c) \tag{2.13}$$

where we know f is not a function of $\hat{z}$ from symmetry.

2.1.5. Exact Solution to the full Maxwell equations and higher order approximation

Although the leading order behaviour is sufficient for our setting, using powerful symbolic calculators like `Mathematica` we can integrate the Jefimenko equations 2.4. Recall that the current density is non-zero in the longitudinal direction, and in particular given by

$$\hat{\mathbf{J}} = \left(0,0,\frac{I_0}{A}\cos(\Omega\hat{t})\right)^\intercal \tag{2.14}$$

Electric Field

Where A = Wire cross sectional area. We can first integrate the second Jefimenko equation, listed here for convenience

$$\hat{\mathbf{E}}(\hat{\mathbf{x}},\hat{t}) = -\frac{\mu_0}{4\pi}\int \frac{1}{|\hat{\mathbf{x}}-\hat{\mathbf{x}}'|}\frac{\partial \hat{\mathbf{J}}(\hat{\mathbf{x}},\hat{t})}{\partial \hat{t}} d^3\hat{x}'$$

Introducing cylindrical coordinates, the volume integral can be explicited and factored to

$$\hat{E}_z = \frac{\mu_0 I_0 \Omega}{4\pi A}\int_0^{2\pi} d\varphi' \int_0^{\hat{\alpha}} \hat{r}' d\hat{r}' \int_{-\infty}^{\infty} d\hat{z}' \left[\frac{1}{\sqrt{\hat{r}^2+(\hat{z}-\hat{z}')^2}}\sin\Omega\left(\hat{t}-\frac{\sqrt{\hat{r}^2+(\hat{z}-\hat{z}')^2}}{c}\right)\right]$$

This integral is evaluated in detail in appendix A.2.2. The result is

$$\hat{E}_z = \frac{I_0\mu_0\Omega}{2\pi}\left(\sin(\Omega\hat{t})I_1(\hat{r}) - \cos(\Omega\hat{t})I_2(\hat{r})\right)$$

with

$$\begin{aligned} I_1(\hat{r}) &= \frac{\pi c}{\Omega\hat{r}} G^{0,2}_{3,1}\left(\begin{matrix} \frac{1}{2},\frac{1}{2} & 0 \\ & 0 \end{matrix}\middle| \frac{4c^2}{\Omega^2\hat{r}^2}\right) \\ &= \log\left(\frac{2c}{\hat{r}\Omega}\right) J_0\left(\frac{\hat{r}\Omega}{c}\right) - \text{Hypergeometric0F1Regularized}^{(1,0)}\left(1,-\frac{\hat{r}^2\Omega^2}{4c^2}\right) \end{aligned} \tag{2.15}$$

$$I_2(\hat{r}) = \frac{\pi}{2} J_0\left(\frac{\Omega\hat{r}}{c}\right) \tag{2.16}$$

Where $G^{0,2}_{3,1}$ is the Meijer-G function (35), "Hypergeometric0F1Regularized" is regularized confluent hypergeometric function $F_{0,1}(a;z)/\Gamma(a)$ (44) and J_0 is a Bessel function of the first kind of order 0. Hence we have obtained an exact expression for the electric field $\hat{\mathbf{E}}$. In our case however, c is large compared to the other physical variables so we can expand $I_2(\hat{r})$ in powers of c

$$I_2 = \frac{\pi}{2} - \frac{\pi\Omega^2\hat{r}^2}{8c^2} + \mathcal{O}\left(\frac{1}{c^3}\right) \tag{2.17}$$

repeating the same expansion for $I_1(\hat{r})$ we discover the leading order solution has the expected logarithmic dependence on $\hat{r}$ from 2.13, and furthermore, there is no $\mathcal{O}(c^{-1})$ term in any of the expansions. (If you inspect at Ampere's law this makes sense, because the electric field there acts in second order in c^{-1}, so there is no "room" for an $\mathcal{O}(c^{-1})$ term in any of the fields, as this would automatically mean they have an $\mathcal{O}(c)$ term)

$$I_1 = (-\gamma + \log(c) - \log(\hat{r}\Omega) + \log(2)) + O\left(\frac{1}{c^2}\right) \tag{2.18}$$

Further, from the leading order terms for I_1 and I_2 we can deduce the $f(\hat{t})$ term hypothesized in the previous section. Indeed, we see

$$f(\hat{t}) = \frac{I_0\mu_0\Omega}{2\pi}\left(\sin(\Omega\hat{t})(\log(2c) - \log(\Omega) - \gamma) - \cos(\Omega\hat{t})\frac{\pi}{2}\right)$$

Magnetic field

This is slightly more convoluted than the calculation for the electric field, as we must consider the contribution from both $\hat{\mathbf{J}}$ and $\partial_{\hat{t}}\hat{\mathbf{J}}$ terms to the Jefimenko integral (2.4). First we consider the contribution from the current density, given by

$$\frac{\mu_0}{4\pi}\int\left[\frac{\hat{\mathbf{J}}(\hat{\mathbf{x}},\hat{t})\times(\hat{\mathbf{x}}-\hat{\mathbf{x}}')}{|\hat{\mathbf{x}}-\hat{\mathbf{x}}'|^3}\right]d^3\hat{x}' \tag{2.19}$$

Inspecting the cross product in the integrand we can deduce that only the second component will be non-zero. Thus we proceed by only computing the itnegral for this component. Integrating out the radial and azimuthal contributions, we reach

$$= \frac{\mu_0}{4\pi}\int_{-\infty}^{\infty}\left[\frac{I(\hat{t}_r)\hat{r}}{(\hat{r}^2+(\hat{z}-\hat{z}')^2)^{3/2}}\right]d\hat{z}' \tag{2.20}$$

Using the same change of variables as for the electric field this simplifies to

$$\frac{\mu_0 I_0\hat{r}}{2\pi}\int_r^{\infty}\left[\frac{\cos(\Omega(\hat{t}-\frac{u}{c}))}{u^2\sqrt{u^2-\hat{r}^2}}\right]du \tag{2.21}$$

we can now proceed with the symbolic calculations, reaching a very complicated analytical expression, available in the Appendix A.2.3. However, it can be expanded to

$$\frac{I_0\mu\cos(\Omega\hat{t})}{2\pi\hat{r}}+\frac{I_0\mu\Omega\sin(\Omega\hat{t})}{4c}+O\left(\frac{1}{c^2}\right) \tag{2.22}$$

so in particular we recover the expected solution to leading order. Now moving to the second part of the integral in Jefimenko's formula, we consider the contribution of $\partial_t\mathbf{J}$. The integral is given by

$$-\frac{\mu_0}{4\pi}\int\left[\frac{\hat{\mathbf{x}}-\hat{\mathbf{x}}'}{|\hat{\mathbf{x}}-\hat{\mathbf{x}}'|^2}\times\frac{1}{c}\frac{\partial\mathbf{J}(\hat{\mathbf{x}},\hat{t})}{\partial\hat{t}}\right]d^3\hat{x}'=-\frac{\mu_0}{4\pi c}\int_{-\infty}^{\infty}\left[\frac{I'(\hat{t}_r)\hat{r}}{\hat{r}^2+(\hat{z}-\hat{z}')^2}\right]d\hat{z}' \tag{2.23}$$

We will proceed in the same way as for the other two integrals. Integrating our the radial and azimuthal components we apply the same change of variables.The result after the aforementioned change of variables is

$$\frac{\mu_0 I_0\hat{r}\Omega}{2\pi c}\int_r^{\infty}\left[\frac{\sin(\Omega(\hat{t}-\frac{u}{c}))}{u\sqrt{u^2-\hat{r}^2}}\right]du \tag{2.24}$$

We can split the integral in two simpler integrals using identities for the sine function.

$$\begin{aligned}&\frac{\mu_0 I_0\hat{r}\Omega}{2\pi c}\left(\sin\Omega t\int_r^{\infty}\left[\frac{\cos(\frac{\Omega u}{c})}{u\sqrt{u^2-r^2}}\right]du-\cos\Omega t\int_r^{\infty}\left[\frac{\sin(\frac{\Omega u}{c})}{u\sqrt{u^2-r^2}}\right]du\right)\\&=\frac{\mu_0 I_0\hat{r}\Omega}{2\pi c}\left(\sin\Omega\hat{t}I_3(\hat{r})-\cos\Omega\hat{t}I_4(\hat{r})\right)\end{aligned} \tag{2.25}$$

The exact form of I_3 and I_4 is given in the appendix A.2.3, we are more interested in the expansions:

$$I_3(\hat{r})=\frac{\pi}{2\hat{r}}-\frac{\pi\Omega}{2c}+\mathcal{O}\left(\frac{1}{c^2}\right) \tag{2.26}$$

It is important to note the $1/c$ factor in equation 2.23, so only the leading order term is relevant to approximated the first order corrections to the magnetic field. Now, for the second integral, expanding in powers of c

$$\begin{aligned}I_4(\hat{r})&=-\frac{(\Omega(-\log(c)+\log(\hat{r})+\log(\Omega)+\gamma-1-\log(2)))}{c}+\mathcal{O}\left(\frac{1}{c^2}\right)\\&=-\frac{\Omega}{c}\left(\gamma-1+\log\left(\frac{\Omega\hat{r}}{2c}\right)\right)+\mathcal{O}(c^{-2})\end{aligned} \tag{2.27}$$

Considering again the $1/c$ factor in 2.23 we see this does not contribute to the first order correction.

2.1.6. Summary of the approximations to the electromagnetic field

So we deduce that to leading order the non-zero components of the electric and magnetic fields are:

$$\begin{aligned}\hat{B}_\phi(\hat{r},\hat{t}) &= \frac{I_0\mu_0\cos(\Omega\hat{t})}{2\pi\hat{r}} + \mathcal{O}\left(\frac{1}{c}\right)\\ \hat{E}_z(\hat{r},\hat{t}) &= \frac{I_0\mu_0\Omega}{2\pi}\left(\sin(\Omega\hat{t})\left(-\gamma+\log\left(\frac{2c}{\Omega\hat{r}}\right)\right)-\cos(\Omega\hat{t})\frac{\pi}{2}\right)+\mathcal{O}\left(1/c^2\right)\end{aligned} \tag{2.28}$$

We can indeed check this satisfies the Maxwell equations to leading order. We know Faraday's Law is satisfied by construction. Both of the fields are solenoidal, so the first two equations are satisfied. Finally, for Ampere's law, we know that to leading order the magnetic field satisfies

$$\nabla\times\hat{\mathbf{H}} = \mu_0\hat{\mathbf{J}} \tag{2.29}$$

and adding $\frac{1}{c^2}\frac{\partial^2\hat{\mathbf{E}}}{\partial\hat{t}^2}$, this is $\mathcal{O}\left(\frac{\log c}{c^2}\right)$ at worst, which is not leading order, and smaller than $\mathcal{O}(1/c)$. An important remark is that from here we observe that the length scale associated with the oscillating current ($\sim\frac{c}{\Omega}$) is much larger than that lengthscale associated with the fluid flow (the radial lengthscale $\sim R$). This means that the electric field can be taken to be quasi-steady in space, i.e. slowly varying.

A second important remark, is that the electric field can be made negligible, as Ω can be chosen so that both terms $\sim\Omega\log\Omega$ and $\sim\Omega\log c$ are arbitrarily small, given that $\lim_{x\to0}x\log x=0$. This is useful as it will allow us to consider the electric field as negligible and greatly reduce the complexity of some of our equations. Moreover, $\hat{r}$ is bounded away from zero, so the log singularity is not dangerous.

2.2. Fluid equations

Once the equations for the electromagnetic field are established and solved we can turn our attention to the equations governing the fluid variables: $\hat{\rho}, \hat{p}, \hat{\mathbf{u}}$, density, pressure and velocity respectively. We will first derive the equations for the bulk. As stated previously, a hat denotes a dimensional variable. Once this is done we will turn our attention to the conditions the variables must satisfy on the boundaries of the domain. Although in the present study we only consider the second fluid as being passive, the governing equations are derived for two arbitrary fluids. In particular, the index $\iota = 1$ labels the interior fluid, bounded between $\hat{\alpha} < \hat{r} < \hat{S}$, and the index $\iota = 2$ labels the exterior fluid, located in the region $\hat{r} > \hat{S}$. Further, the axisymmetric velocity vector is given by $\hat{\mathbf{u}}^{(\iota)} = (\hat{u}^{(\iota)}(\hat{r}, \hat{z}, \hat{t}), 0, \hat{w}^{(\iota)}(\hat{r}, \hat{z}, \hat{t}))^{\mathsf{T}}$

2.2.1. Bulk equations

In this investigation it is assumed at all times that the fluid is incompressible, that is that

$$\frac{D\hat{\rho}^{(\iota)}}{D\hat{t}} = \partial_{\hat{t}}\hat{\rho}^{(\iota)} + (\hat{\mathbf{u}}^{(\iota)} \cdot \nabla)\hat{\rho}^{(\iota)} = 0 \tag{2.30}$$

Where we have defined the material derivative $\frac{D}{D\hat{t}}$. With this in mind the equations for the bulk of fluid in the region $\hat{\alpha} < \hat{r} < \hat{S}$ can be derived. By considering the conservation of mass for an arbitrary control volume and using the incompressibiliy condition 2.30, the continuity equation is derived. In differential form it is given by (6)

$$\nabla \cdot \hat{\mathbf{u}}^{(\iota)} = 0 \tag{2.31}$$

Considering now conservation of momentum, with a similar argument and applying Gauss' divergence theorem to the integrals resulting from surface forces on arbitrary control volumes, we can derive the second Navier-Stokes equation, which we write in the following form (6; 8) for an incompressible fluid:

$$\hat{\rho}^{(\iota)} \frac{D\hat{\mathbf{u}}^{(\iota)}}{D\hat{t}} = \nabla \cdot \hat{T} + \hat{\rho}^{(\iota)}\mathbf{f} \tag{2.32}$$

where $\frac{D}{Dt}$ denotes the material derivative as given in eq. (2.30). The stress tensor T can be split into four components, representing the pressure, viscous stresses, the ferrofluid stress tensor and the Maxwell stress tensor:

$$\hat{T} = \hat{T}_p + \hat{T}_v + \hat{T}_f + \hat{T}_m \tag{2.33}$$

First, the pressure term is just an isotropic tensor $\hat{T}_p = -\hat{p}^{(\iota)}\delta_{ij}$ and its divergence is given by the pressure gradient $\nabla \cdot \hat{T}_p = -\nabla\hat{p}$. The viscous stress tensor is (6)

$$\hat{T}_v = \mu^{(\iota)}(\nabla\hat{\mathbf{u}}^{(\iota)} + (\nabla\hat{\mathbf{u}}^{(\iota)})^T)$$

where $\mu^{(\iota)}$ is the dynamic viscosity of the fluid. Taking the divergence of this tensor its contribution to equation 2.32 is found to be $\mu^{(\iota)}\nabla^2\hat{\mathbf{u}}^{(\iota)}$, where ∇^2 is the vector Laplacian. For convenience we write the gradient of the velocity:

$$\nabla\hat{\mathbf{u}} = \begin{pmatrix} \partial_{\hat{r}}\hat{u} & 0 & \partial_{\hat{z}}\hat{u} \\ 0 & \frac{\hat{u}}{\hat{r}} & 0 \\ \partial_{\hat{r}}\hat{w} & 0 & \partial_{\hat{z}}\hat{w} \end{pmatrix}$$

The ferrofluid stress tensor, is defined by (45)

$$\hat{T}_f = -\mu_0 \left(\int_0^{\hat{H}} \nu \left(\frac{\partial \hat{M}}{\partial \nu} \right)_{\hat{H},\hat{\Theta}} d\hat{H} + \int_0^{\hat{H}} \hat{M} d\hat{H} \right) \delta_{ij} = -\mu_0(\hat{p}_s + \hat{p}_m)\delta_{ij} \tag{2.34}$$

Here, $\hat{H} = |\hat{\mathbf{H}}|$, $\hat{M} = |\hat{\mathbf{M}}|$ and ν is the specific volume of ferrofluid particles in the fluid and $\hat{\Theta}$ is the temperature. For isothermal flow fields we can compute the divergence of each of the pressures. For the fluid magnetic pressure, we reach

$$\nabla\hat{p}_m = -\mu_0\nabla\int_0^{\hat{H}} \hat{M} d\hat{H} = -\mu_0\hat{M}\nabla\hat{H} \tag{2.35}$$

The Maxwell stress tensor is is given in general by (25)

$$\hat{T}_m = \epsilon_0\hat{\mathbf{E}}\hat{\mathbf{E}}^\intercal + \hat{\mathbf{B}}\hat{\mathbf{H}}^\intercal - \frac{1}{2}(\mu_0|\hat{\mathbf{H}}|^2 + \epsilon_0|\hat{\mathbf{E}}|^2)\delta_{ij} \tag{2.36}$$

In the magnetostatic case, the Maxwell stress tensor simplifies to (8):

$$\hat{T}_m = \hat{\mathbf{B}}\hat{\mathbf{H}}^\intercal - \frac{1}{2}\mu_0|\hat{\mathbf{H}}|^2\delta_{ij} \tag{2.37}$$

and in general it the divergence of this tensor can be computed to obtain its contributions to the Navier Stokes equations. Considering first the Magnetostatic case

$$\nabla\cdot(\hat{\mathbf{B}}\hat{\mathbf{H}}^\intercal) - \nabla\cdot(\frac{1}{2}\mu_0|\hat{\mathbf{H}}|^2\delta_{ij}) = \hat{\mathbf{H}}\nabla\cdot\hat{\mathbf{B}} + (\hat{\mathbf{B}}\cdot\nabla)\hat{\mathbf{H}} - \frac{1}{2}\mu_0\nabla|\hat{\mathbf{H}}|^2 \tag{2.38}$$

The first of the three terms will be zero as a consequence of the Maxwell equations. Now recall, $\hat{\mathbf{B}} = \mu_0(\hat{\mathbf{H}} + \hat{\mathbf{M}})$, so that

$$\nabla\cdot\hat{T}_m = \mu_0((\hat{\mathbf{H}} + \hat{\mathbf{M}})\cdot\nabla)\hat{\mathbf{H}} - \frac{1}{2}\mu_0\nabla|\hat{\mathbf{H}}|^2 = \mu_0(\hat{\mathbf{H}}\cdot\nabla)\hat{\mathbf{H}} + \mu_0(\hat{\mathbf{M}}\cdot\nabla)\hat{\mathbf{H}} - \frac{1}{2}\mu_0\nabla|\hat{\mathbf{H}}|^2 \tag{2.39}$$

and we can cancel the first and third terms using the following vector identity (34)

$$\mathbf{A}\times(\nabla\times\mathbf{A}) = (\mathbf{A}\cdot\nabla)\mathbf{A} - \frac{1}{2}\nabla(\mathbf{A}\cdot\mathbf{A}) \tag{2.40}$$

with $\mathbf{A} = \hat{\mathbf{H}}$ and recalling the second Maxwell equation for the electrostatic limit, $\nabla\times\hat{\mathbf{H}} = 0$, to get

$$\nabla\cdot\hat{T}_m = \mu_0(\hat{\mathbf{M}}\cdot\nabla)\hat{\mathbf{H}} \tag{2.41}$$

This will cancel with $\nabla\hat{p}_m \approx \nabla\cdot\hat{T}_f$ from equation 2.35, so that in the fluid bulk we have standard Navier-Stokes equation for a Newtonian fluid:

$$\hat{\rho}^{(\iota)}\frac{D\hat{\mathbf{u}}^{(\iota)}}{D\hat{t}} = -\nabla\hat{p}^{(\iota)} + \mu^{(\iota)}\nabla^2\hat{\mathbf{u}}^{(\iota)} + \hat{\rho}^{(\iota)}\mathbf{f} \tag{2.42}$$

By taking the divergence of eq. (2.42) we can find a Poisson equation for the pressure in the fluid bulk

$$\hat{\rho}^{(\iota)}\left(\frac{(\hat{u}^{(\iota)})^2}{\hat{r}^2} + (\partial_r\hat{u}^{(\iota)})^2 + +2\partial_z\hat{u}^{(\iota)}\partial_r\hat{w}^{(\iota)} + (\partial_z\hat{w}^{(\iota)})^2\right) = -\nabla^2\hat{p}^{(\iota)} \tag{2.43}$$

2.2.2. Boundary Conditions

We have derived four (one + three) partial differential equations for the fluid variables: $\hat{p}, \hat{\mathbf{u}}$. To fully define the evolution of the system boundary conditions on the boundaries of the domain of the problem must be specified. Starting at the wall of the cylindrical wire, situated at $\hat{r} = \hat{\alpha}$, the no slip condition is imposed, as is standard in problems with viscous fluids (10; 28)

$$\hat{\mathbf{u}} = 0 \quad \text{at} \quad \hat{r} = \hat{\alpha} \tag{2.44}$$

The boundary conditions on the moving boundary, situated at $\hat{r} = \hat{S}(\hat{t}, \hat{z})$, are more intricate. As the moving boundary must be computed as part of the solution we require additional equations. The most straightforward condition is the kinematic condition (6)

$$\frac{D\hat{S}}{D\hat{t}} = \partial_{\hat{t}}\hat{S} + (\hat{\mathbf{u}} \cdot \nabla)\hat{S} = 0 \quad \text{at} \quad \hat{r} = \hat{S} \tag{2.45}$$

To obtain additional equations we will impose a stress balance. The curvature of the surface will induce a normal stress jump. It is useful to compute the unit normal and tangential vector to the moving surface. Recall the moving boundary $\hat{S} = \hat{S}(\hat{z}, \hat{t})$ in the axisymmetric framework will have normal and tangential vectors given by (the subscript denotes differentiation by $\hat{z}$) (8)

$$\mathbf{n} = \frac{1}{\sqrt{1 + \hat{S}_{\hat{z}}^2}} \left(1, 0, -\hat{S}_{\hat{z}}\right)^\intercal \quad \mathbf{t} = \frac{1}{\sqrt{1 + \hat{S}_{\hat{z}}^2}} \left(\hat{S}_{\hat{z}}, 0, 1\right)^\intercal$$

In general, the aforementioned condition on the stress across the interface reads (6; 8)

$$\mathbf{n} \cdot [\hat{T}]_1^2 = \sigma \mathbf{n}(\nabla \cdot \mathbf{n}) - \nabla\sigma \tag{2.46}$$

where $[f]_1^2 = f_2 - f_1$ denotes the difference or jump in a quantity between the interface. Two scalar equations can be obtained from 2.46 by considering the normal and tangential components of the equation. Considering the tangential component first,

$$\mathbf{n} \cdot [\hat{T}]_1^2 \cdot \mathbf{t} = \nabla\sigma \cdot \mathbf{t} = 0 \tag{2.47}$$

As we are assuming there are no gradients in the surface tension, $\nabla\sigma = 0$. This dot product will only select entries in the offdiagonal of T, so we can forget momentarily about all the elements of the tensor multiplied by δ_{ij}, so in particular the entire ferrofluid stress tensor $\hat{T}_f$ and the pressure term. Further, we assume the outer fluid is not magnetic, so $\mathbf{M}^{(2)} = 0$, and we can find that (8)

$$\mathbf{n} \cdot [\hat{T}_m]_1^2 \cdot \mathbf{t} = 0 \tag{2.48}$$

hence the only contributing comes from viscosity, giving the final form of the stress condition (see appendix A.3.1 for a detailed calculation, and dropping the index in the velocities for convenience.)

$$\mathbf{n} \cdot [\hat{T}_v]_1^2 \cdot \mathbf{t} = \left[\frac{\mu^{(\iota)}}{1 + \hat{S}_{\hat{z}}^2} \left(2\hat{S}_{\hat{z}} \left(\partial_{\hat{r}} \hat{u} - \partial_{\hat{z}} \hat{w} \right) + \left(1 - \hat{S}_{\hat{z}}^2 \right) \left(\partial_{\hat{z}} \hat{u} + \partial_{\hat{r}} \hat{w} \right) \right) \right]_1^2 = 0 \tag{2.49}$$

When the second fluid is passive, as is assumed in this investigation, the above tangential stress condition reduces to

$$\begin{aligned} \frac{\mu^{(1)}}{1 + \hat{S}_{\hat{z}}^2} \left(2\hat{S}_{\hat{z}} \left(\partial_{\hat{r}} \hat{u} - \partial_{\hat{z}} \hat{w} \right) + \left(1 - \hat{S}_{\hat{z}}^2 \right) \left(\partial_{\hat{z}} \hat{u} + \partial_{\hat{r}} \hat{w} \right) = 0 \right) = 0 \\ \implies 2\hat{S}_{\hat{z}} \left(\partial_{\hat{r}} \hat{u} - \partial_{\hat{z}} \hat{w} \right) + \left(1 - \hat{S}_{\hat{z}}^2 \right) \left(\partial_{\hat{z}} \hat{u} + \partial_{\hat{r}} \hat{w} \right) = 0 \end{aligned} \tag{2.50}$$

For the normal stress balance, also known as the Laplace-Young equation, taking the dot product of eq. (2.46) and $\mathbf{n}$ we obtain

$$\mathbf{n} \cdot [\hat{T}]_1^2 \cdot \mathbf{n} = \sigma \nabla \cdot \mathbf{n} \tag{2.51}$$

The left hand side will select diagonal entries of the stress tensor, so we will have the dynamic pressure p for both fluids, $\mathbf{n} \cdot [\hat{T}_v]_1^2 \cdot \mathbf{n}$, $\mathbf{n} \cdot [\hat{T}_f]_1^2 \cdot \mathbf{n}$ and $\mathbf{n} \cdot [\hat{T}_m]_1^2 \cdot \mathbf{n}$ contributions. Each of these terms can be associated to a pressure. The capillary pressure, i.e. the right hand side in Laplace-Young eq. (2.51), is evaluated to be (detailed calculation in appendix A.3.2)

$$\hat{p}_c = \sigma \nabla \cdot \mathbf{n} = \frac{\sigma}{\sqrt{1 + \hat{S}_{\hat{z}}^2}} \left(\frac{1}{\hat{S}} - \frac{S_{zz}}{1 + \hat{S}_{\hat{z}\hat{z}}^2} \right) \tag{2.52}$$

The viscous pressure (detailed calculation in appendix A.3.2)

$$\hat{p}_v = \mathbf{n} \cdot \hat{T}_v \cdot \mathbf{n} = \frac{2\mu}{1 + \hat{S}_{\hat{z}}^2}(\partial_{\hat{r}}\hat{u} - \hat{S}_{\hat{z}}(\partial_{\hat{z}}\hat{u} + \partial_{\hat{r}}\hat{w}) + \hat{S}_{\hat{z}}^2\partial_{\hat{z}}\hat{w}) \tag{2.53}$$

Furthermore, the magnetic normal pressure is evaluated to be

$$\hat{p}_n = \mathbf{n} \cdot \hat{T}_m \cdot \mathbf{n} = \frac{1}{2}\mu_0(\mathbf{n} \cdot \mathbf{M}^{(1)})^2 \tag{2.54}$$

We still have p_m the fluid magnetic pressure and p_s, the magnetorestrictive pressure as defined above

$$\mathbf{n} \cdot \hat{T}_f \cdot \mathbf{n} = \hat{p}_m + \hat{p}_s \tag{2.55}$$

We can write the Laplace-Young equation in terms of the pressures

$$\hat{p}^{(1)} - \hat{p}^{(2)} + \hat{p}_m + \hat{p}_s + \hat{p}_n + \hat{p}_v^{(2)} - \hat{p}_v^{(1)} = \hat{p}_c \quad \text{at} \quad \hat{r} = \hat{S} \tag{2.56}$$

This simplifies greatly in the case the outer fluid is passive. Then $p_v^{(2)} = 0$ and $p^{(2)} = p_a$, the atmospheric pressure which we can set to zero without loss of generality. Moreover, the magnetorestrictive pressure p_s is negligible in the non-relativistic limit. Finally, we require continuity of velocities across the interface:

$$\begin{aligned} [\hat{\mathbf{u}} \cdot \mathbf{t}]_1^2 = 0 \quad \text{at} \quad \hat{r} = \hat{S} \\ [\hat{\mathbf{u}} \cdot \mathbf{n}]_1^2 = 0 \quad \text{at} \quad \hat{r} = \hat{S} \end{aligned} \tag{2.57}$$

2.3. Summary of the governing equations

In this section we list the governing equations, expanding the vector quantities for the case of axisymmetrical flow, where $\hat{\mathbf{u}} = (\hat{u}, 0, \hat{w})^\intercal$. For continuity, equation (2.31) is

$$\partial_{\hat{r}}\hat{u}^{(\iota)} + \frac{1}{\hat{r}}\hat{u}^{(\iota)} + \partial_{\hat{z}}\hat{w}^{(\iota)} = 0 \tag{2.58}$$

For the momentum equations, now with the stress tensor also expanded, equation (2.32) is

$$\begin{aligned}\partial_{\hat{t}}\hat{u}^{(\iota)} + \hat{u}^{(\iota)}\partial_{\hat{r}}\hat{u}^{(\iota)} + \hat{w}^{(\iota)}\partial_{\hat{z}}\hat{u}^{(\iota)} &= -\frac{1}{\hat{\rho}^{(\iota)}}\partial_{\hat{r}}\hat{p}^{(\iota)} + \frac{\mu^{(\iota)}}{\hat{\rho}^{(\iota)}}\left(\partial_{\hat{r}}^2\hat{u}^{(\iota)} + \frac{1}{\hat{r}}\partial_{\hat{r}}\hat{u}^{(\iota)} + \partial_{\hat{z}}^2\hat{u}^{(\iota)} - \frac{\hat{u}^{(\iota)}}{\hat{r}^2}\right)\\ \partial_{\hat{t}}\hat{w}^{(\iota)} + \hat{u}^{(\iota)}\partial_{\hat{r}}\hat{w}^{(\iota)} + \hat{w}^{(\iota)}\partial_{\hat{z}}\hat{w}^{(\iota)} &= -\frac{1}{\hat{\rho}^{(\iota)}}\partial_{\hat{z}}\hat{p}^{(\iota)} + \frac{\mu^{(\iota)}}{\hat{\rho}^{(\iota)}}\left(\partial_{\hat{r}}^2\hat{w}^{(\iota)} + \frac{1}{\hat{r}}\partial_{\hat{r}}\hat{w}^{(\iota)} + \partial_{\hat{z}}^2\hat{w}^{(\iota)}\right) + g\end{aligned} \tag{2.59}$$

The no slip condition is as simple as before,

$$\hat{u}(\hat{\alpha}) = 0 \quad \hat{w}(\hat{\alpha}) = 0 \tag{2.60}$$

The kinematic condition (2.45) is expanded to give

$$\hat{S} + \hat{w}\hat{S}_{\hat{z}} = \hat{u} \quad \text{ on } \hat{r} = \hat{S} \tag{2.61}$$

Continuity of velocities on $\hat{r} = \hat{S}$ gives $[\hat{\mathbf{u}} \cdot \mathbf{t}]_1^2 = [\hat{\mathbf{u}} \cdot \mathbf{n}]_1^2 = 0$. The tangential stress condition was already expanded in equation (2.50). It is repeated here for convenience

$$2\hat{S}_{\hat{z}}\left(\partial_{\hat{r}}\hat{u} - \partial_{\hat{z}}\hat{w}\right) + \left(1 - \hat{S}_{\hat{z}}^2\right)\left(\partial_{\hat{z}}\hat{u} + \partial_{\hat{r}}\hat{w}\right) = 0 \quad \text{ on } \hat{r} = \hat{S} \tag{2.62}$$

Finally, the normal stress balance was already expanded in equation (2.56), repeated here for convenience

$$\hat{p} - \frac{2\mu}{1+\hat{S}_{\hat{z}}^2}(\partial_{\hat{r}}\hat{u} - \hat{S}_{\hat{z}}(\partial_{\hat{z}}\hat{u} + \partial_{\hat{r}}\hat{w}) + \hat{S}_{\hat{z}}^2\partial_{\hat{z}}\hat{w}) = \frac{\sigma}{\sqrt{1+\hat{S}_{\hat{z}}^2}}\left(\frac{1}{\hat{S}} - \frac{\hat{S}_{\hat{z}\hat{z}}}{1+\hat{S}_{\hat{z}}^2}\right) - \frac{\mu_0\chi B^2}{8\pi^2\hat{S}^2} \text{ on } \hat{r} = \hat{S} \tag{2.63}$$

3. Nondimensionalisation of the equations

Once the governing equations have been introduced it is convenient to introduce nondimensional variables to work with them. This raises an interesting point: what should the characteristic length and time scales be? In this study the characteristic velocity is chosen from a balance between gravity and viscosity. In particular, the reference velocity is

$$V = \frac{\hat{\rho} g R^2}{\mu^{(1)}}$$

and the reference pressure is given by the hydrostatic pressure balance, $\hat{\rho} g R$.

3.1. Standard nondimensionalisation

As a first guess, the following scalings are chosen, using only the radial lengthscale, R:

$$\hat{r} = Rr \quad \hat{z} = Rz \quad \hat{u} = V \quad \hat{w} = Vw \quad \hat{t} = \frac{R}{V} t \quad \hat{p} = \hat{\rho} g R p$$

The hatted variables are dimensional, the standard variables are dimensionless. Applying these scalings to the equations in the previous section a set of nondimensional governing equations is derived. In particular, the continuity equation, no slip condition and kinematic equation remain unchanged (i.e. no nondimensional groups appear), as they are not dynamic equations:

$$\begin{aligned} \frac{1}{r}\partial_r(ru) + \partial_z w &= 0 \\ \partial_t S + w S_z = u \quad &\text{on } r = S(z,t) \\ u = 0 \quad \text{and} \quad w = 0 \quad &\text{on } r = \alpha = \frac{\hat{\alpha}}{R} \end{aligned} \tag{3.1}$$

However, for the Navier-Stokes equations the Reynolds number Re (defined below) will appear in the equations.

$$\begin{aligned} \mathrm{Re}(u_t + uu_r + wu_z) &= -p_r + (u_{rr} + u_{zz} + \frac{1}{r}u_r - \frac{u}{r^2}) \\ \mathrm{Re}(w_t + uw_r + ww_z) &= 1 - p_z + (w_{rr} + \frac{1}{r}w_r + w_{zz}) \end{aligned} \tag{3.2}$$

For the dynamic boundary conditions, the tangential stress remains unchanged from the dimensional form, as the outer fluid is taken as passive, implying:

$$(1 - S_z^2)(u_z + w_r) + 2S_z(u_r - w_z) = 0 \quad \text{on } r = S(z,t) \tag{3.3}$$

However a number of nondimensional quantities appear in the normal stress balance, and the equation is transformed to:

$$\mathrm{Bo}\, p - 2\mathrm{Ca}\frac{1}{1+S_z^2}(S_z^2 w_z - 2S_z(w_r + u_z) + u_r) = \frac{1}{\sqrt{1+S_z^2}}\left(\frac{1}{S} - \frac{S_{zz}}{1+S_z^2}\right) - \frac{\mathrm{Ma}}{S^2} \quad \text{on } r = S(z,t) \tag{3.4}$$

It is important to analyse the meaning of each of the dimensionless numbers that appear in the equations.

- The Reynolds number, $\mathrm{Re} = \frac{\hat{\rho}VR}{\mu}$, the famous ratio between the inertial and viscous forces in the fluid bulk.
- The Bond number, $\mathrm{Bo} = \frac{\hat{\rho}gR^2}{\sigma}$, the ratio between gravity and surface tension forces.
- The capillary number, $\mathrm{Ca} = \frac{\mu V}{\sigma}$, a ratio between inertial and capillary timescales.
- The magnetic Bond number, $\mathrm{Ma} = \frac{\mu_0 \chi J_0^2}{8\pi^2 R\sigma}$. This is the ratio between the magnetic forces and surface tension forces.
- The non-dimensional radius $\alpha = \frac{\hat{\alpha}}{R}$. This parameter is of paramount importance, for it determines if we are dealing with a thin fluid or not. In particular, when α is close to 1 it means that the wire is thick compared to the fluid, or equivalently, that the fluid film is thin.

3.2. Introducing a second lengthscale: the Long-Wave nondimensionalisation

Motivated with the aim of making analytical progress in nonlinear flows when the waves are long (38) we modify the scalings to introduce a second lengthscale L associated with the z coordinate. In particular,

$$\hat{r} = Rr \quad \hat{z} = Lz \quad \hat{u} = \frac{R}{L}Vu \quad \hat{w} = Vw \quad \hat{t} = \frac{L}{V}t \quad \hat{p} = \hat{\rho}gLp \tag{3.5}$$

We see that this introduces a new non-dimensional number, $\epsilon = \frac{R}{L}$. In the long-wave limit, we work in the formal limit $\epsilon \to 0$. This new scaling will give rise to a different set of non-dimensional equations. The continuity equation, the no-slip condition and the kinematic equation are unchanged. However, the Navier-Stokes equations can be verified to transform to:

$$\begin{aligned} \epsilon^4 \mathrm{Re}(u_t + uu_r + wu_z) &= -p_r + \epsilon^2(u_{rr} + \epsilon^2 u_{zz} + \frac{1}{r}u_r - \frac{u}{r^2}) \\ \epsilon^2 \mathrm{Re}(w_t + uw_r + ww_z) &= 1 - p_z + (w_{rr} + \frac{1}{r}w_r + \epsilon^2 w_{zz}) \end{aligned} \tag{3.6}$$

The dynamic boundary conditions also change with the introduction of ϵ. The tangential stress balance transforms to:

$$(1 - \epsilon^2 S_z^2)(\epsilon^2 u_z + w_r) + 2\epsilon^2 S_z(u_r - w_z) = 0 \text{ on } r = S(z,t) \tag{3.7}$$

and finally the normal stress condition becomes

$$\mathrm{Bo}\, p - \mathrm{Ca}\frac{2\epsilon^2}{1+\epsilon^2 S_z}(\epsilon^2 S_z^2 w_z - 2S_z(w_r + \epsilon^2 u_z) + u_r) = \frac{\epsilon}{\sqrt{1+\epsilon^2 S_z^2}}\left(\frac{1}{S} - \frac{\epsilon^2 S_{zz}}{1+\epsilon^2 S_z^2}\right) - \frac{\epsilon \mathrm{Ma}}{S^2} \tag{3.8}$$

evaluated at $r = S(z,t)$. These scalings lay the groundwork for taking the tempting $\epsilon \to 0$ limit, as it is clear this would significantly simplify the equations in question. We will proceed with this in the following chapter.

4. Long Wave limit

In the previous chapter, section 3.2 we reached a set of nondimensional equations that take into account the different lengthscales in the problem, R and L. In this chapter we will explore what can be deduced when one of those, L is much larger than R. We will do this with the aim of deducing an evolution equation for $S(z,t)$, the film's thickness and the position of the free boundary. Our method is inspired by the one presented by Craster and Matar in (10). We will go through similar steps as them, but including the new magnetic term in eq. (2.63).

Long wave theories have been hugely successful in aiding to the resolution of viscous flow problems in the last couple of decades (37; 38; 39). By exploiting disparities between the lengthscales in a problem equations can be drastically simplified leading to far simpler and less expensive numerical problems (50), as is the case here.

Looking at the normal stress balance (3.8), we see that fixing $\mathrm{Bo} = \mathrm{Ca} = \epsilon$, allows us to write the equation as

$$p - \frac{2\epsilon^2}{1+\epsilon^2 S_z}(\epsilon^2 S_z^2 w_z - 2S_z(w_r + \epsilon^2 u_z) + u_r) = \frac{1}{\sqrt{1+\epsilon^2 S_z^2}}\left(\frac{1}{S} - \frac{\epsilon^2 S_{zz}}{1+\epsilon^2 S_z^2}\right) - \frac{\mathrm{Ma}}{S^2}$$

Forcing this scaling for the nondimensional parameters is equivalent to setting $L = \frac{\sigma}{\rho g R}$, or in physical terms, imposing a surface tension dominated setting. Once this is done, we can proceed by taking the limit $\epsilon \to 0$ of the Navier Stokes equations and the dynamic boundary conditions.

4.1. Equations in the long wave limit

Taking the aforementioned limit, with the Reynolds number fixed, the continuity equation, no-slip condition and kinematic equation remain the same, as they do not depend on ϵ. The Navier Stokes equation simplify greatly, to give

$$\begin{aligned} 0 &= -\partial_r p \\ 0 &= 1 - \partial_z p + \partial_r^2 w + \frac{1}{r}\partial_r w \end{aligned} \tag{4.1}$$

The tangential stress balance (3.7), to leading order is given by a stress free condition, implyign that the normal derivative of the velocity to be zero at the interface.

$$\partial_r w = 0 \quad r = S(z,t) \tag{4.2}$$

The normal stress balance must be treated very carefully. In particular, the limit is found to be

$$p = \frac{1}{S} - \epsilon^2 S_{zz} - \frac{\mathrm{Ma}}{S^2} \quad \text{on} \quad r = S(z,t) \tag{4.3}$$

This appears inconsistent, as it includes an ϵ^2 term. We keep this term as previous literature does so (for good reason), and in this way we can compare our predictions with the existing literature. In particular, this term is kept for a purely mathematical reason: without it all modes would be linearly unstable, an unphysical and undesirable feature for our model, leading to an ill-posed initial value problem. We can see this in part because it is a singular limit, meaning removing it removes the dependence from the highest order derivative.

4.2. Solving the long wave equations

4.2.1. Solving for the axial velocity.

We can solve equations (4.1) with standard techniques. The first equation just can be integrated to give $p = p(z)$. This is useful, as it means we can integrate the second equation in r. We can

find a homogeneous solution by considering

$$\partial_r^2 w + \frac{1}{r}\partial_r w = 0 \tag{4.4}$$

which we can identify as a linear first order ordinary differential equation (ODE) in $v = \partial_r w$,

$$\partial_r v + \frac{1}{r}v = 0 \Longrightarrow \frac{dv}{v} = -\frac{1}{r}dr \Longrightarrow \log v = -\log r + C_1 \Longrightarrow v = \partial_r w = \frac{C_2}{r} \tag{4.5}$$

From here, after another integration we obtain a general solution to the homogeneous problem

$$w(r) = A\log r + B \tag{4.6}$$

To find a particular solution to the inhomogeneous problem with constant forcing, we see that the ansatz $w(r) = Cr^2$ is a appropriate, as the second derivative is constant (like the forcing), the first derivative is linear, and when divided by r again we get a constant. Thus

$$2C + 2C = \partial_z p - 1 \Longrightarrow C = \frac{1}{4}(\partial_z p - 1) \tag{4.7}$$

to obtain the constants A, B we can make use of the boundary conditions given by no-slip, $w(\alpha) = 0$, and the tangential stress (4.2). Using this we find

$$\frac{A}{S} + \frac{1}{4}(\partial_z p - 1)2S = 0 \Longrightarrow A = -\frac{1}{2}(\partial_z p - 1)S^2 \tag{4.8}$$

and finally, applying no-slip on the wire,

$$A\log\alpha + B + \frac{1}{4}(\partial_z p - 1)\alpha^2 = 0 \Longrightarrow B = -A\log\alpha - \frac{1}{4}(\partial_z p - 1)\alpha^2 \tag{4.9}$$

Hence our solution is given by

$$w(r,z) = -\frac{1}{4}(\partial_z p - 1)\left(2S^2\log\left(\frac{r}{\alpha}\right) + \alpha^2 - r^2\right) \tag{4.10}$$

4.2.2. Solving for for the radial velocity

Using the continuity equation (2.58), we can solve for $u(z,t)$. In particular,

$$\frac{1}{r}\partial_r(ru) + \partial_z w = 0 \Longrightarrow u(r,z) = -\frac{1}{r}\int dr\,[r\partial_z w] \tag{4.11}$$

The z derivative of w comes from p and S. In particular,

$$\partial_z w = -\frac{1}{4}\partial_z^2 p\left(2S^2\log\left(\frac{r}{\alpha}\right) + \alpha^2 - S^2\right) - \frac{1}{2}(\partial_z p - 1)\left(2S\log\left(\frac{r}{\alpha}\right) - S\right)\partial_z S \tag{4.12}$$

and we can perform the integration with the aid of a symbolic calculator. The result is

$$\begin{aligned} u(r,z) &= \frac{1}{r}\int dr\,[r\partial_z w] \\ &= -\frac{1}{r}\int r\left\{\frac{1}{4}\partial_z^2 p\left(2S^2\log\left(\frac{r}{\alpha}\right) + \alpha^2 - S^2\right) - \frac{1}{2}(\partial_z p - 1)\left(2S\log\left(\frac{r}{\alpha}\right) - S\right)\partial_z S\right\} dr \\ &= r\left(-\frac{1}{8}\alpha^2\partial_z^2 p - \left(\frac{1}{4}S\partial_z^2 p + \frac{1}{2}\partial_z S\partial_z p - \frac{1}{2}\partial_z S\right)S\log\left(\frac{r}{\alpha}\right)\right) \\ &+ \frac{1}{4}S^2\partial_z^2 p + \frac{1}{2}S\partial_z S\partial_z p - \frac{1}{2}S\partial_z S + A \end{aligned} \tag{4.13}$$

We can compute the value of the integration constant by imposing the no-slip condition $u(\alpha) = 0$. This gives

$$\begin{aligned} u(r,z,t) &= \frac{S}{4r}(\partial_z p - 1)\left(\alpha^2 + 2r^2\log\left(\frac{r}{\alpha}\right) - r^2\right)S_z \\ &+ \frac{\partial_z^2 p}{16r}\left(2S^2\left(\alpha^2 + 2r^2\log\left(\frac{r}{\alpha}\right) - r^2\right) + \left(r^2 - \alpha^2\right)^2\right) \end{aligned} \tag{4.14}$$

From here on, we are interested in deriving an evolution equation for $S(z,t)$, so we will be interested in the value of u and w at $r = S$, which we list here for convenience

$$\begin{aligned} w(S,z) &= -\frac{1}{4}(\partial_z p - 1)\left[\alpha^2 - S^2 + 2S^2\log\frac{S}{\alpha}\right] \\ u(S,z) &= \frac{(S^2(\partial_z p - 1))_z}{8S}\left[\alpha^2 - S^2 + 2S^2\log\frac{S}{\alpha}\right] - \frac{p_{zz}}{16S}(\alpha^2 - S^2)^2 \end{aligned} \tag{4.15}$$

The only remaining boundary conditions are the kinematic equation (2.61) and the normal stress balance (4.3). We can substitute eq. (4.15) in the kinematic equation: $\partial_t S + w(S,z)\partial_z S =$

$u(S,z)$. Multiplying by S and with some algebraic manipulation we can reach the following conservation-type equation for S^2

$$\begin{aligned} 8(S^2)_t &= \frac{\partial}{\partial z}\left((\partial_z p - 1)\left(2S^2\left(\alpha^2 - S^2 + 2S^2\log\left(\frac{S}{\alpha}\right)\right) - (\alpha^2 - S^2)^2\right)\right) \\ p &= \frac{1}{S} - \epsilon^2 S_{zz} - \frac{\mathrm{Ma}}{S^2} \end{aligned} \tag{4.16}$$

This is a partial differential equation that completely determines the spatiotemporal evolution of $S(z,t)$. Once S is found using the numerical schemes outlined in chapter 11, the leading order velocity fields follows from eq. (4.14) and eq. (4.10), repeated here for convenience

$$\begin{aligned} u(r,z,t) &= \frac{S}{4r}(\partial_z p - 1)\left(\alpha^2 + 2r^2\log\left(\frac{r}{\alpha}\right) - r^2\right)S_z \\ &\quad + \frac{\partial_z^2 p}{16r}\left(2S^2\left(\alpha^2 + 2r^2\log\left(\frac{r}{\alpha}\right) - r^2\right) + \left(r^2 - \alpha^2\right)^2\right) \\ w(r,z) &= -\frac{1}{4}(\partial_z p - 1)\left(2S^2\log\left(\frac{r}{\alpha}\right) + \alpha^2 - r^2\right) \end{aligned} \tag{4.17}$$

Further, to plot the streamlines it might be interesting to obtain an analytical formula for the streamfunction, in particular the Stokes streamfunction as introduced in section 7.4. The details of the calculation are omitted as they are simple but tedious integrations, but are available in appendix A.6. The final result is

$$\psi(r,t) = \frac{(\partial_z p - 1)}{16}\left(2S^2\left(\alpha^2 + 2r^2\log\left(\frac{r}{\alpha}\right) - r^2\right) - \left(r^2 - \alpha^2\right)^2\right) \tag{4.18}$$

4.3. The thin film limit

Equation (4.16) is a good equation to consider when studying the linear stability of the problem, or to simulate using numerical methods. However, it is highly nonlinear and fairly intractable in that form. A natural simplification to make is to consider the limit as the film's thickness is small. Mathematically, setting $S = \alpha + \eta$, with η small (physically this is a thin film limit, i.e. the surface is close to α) we get (detailed calculation in appendix A.4)

$$(1 + \frac{\eta}{\alpha})\eta_t + \frac{1}{3}\frac{\partial}{\partial z}\left[\eta^3\left(\left(1 + \frac{\eta}{\alpha}\right)(1 + \frac{\eta_z}{\alpha^2(1+\frac{\eta}{\alpha})^2}(1 - \frac{2\mathrm{Ma}}{\alpha(1+\frac{\eta}{\alpha})}) + \epsilon^2\eta_{zzz}\right)\right] = 0 \tag{4.19}$$

Finally, taking the limit $\eta/\alpha << 1$, we reach a Benney type (18) equation

$$\partial_t \eta + \frac{1}{3}\frac{\partial}{\partial z}(\eta^3(1 + (1 - 2\mathrm{Ma})\eta_z + \epsilon^2 \eta_{zzz}) = 0 \tag{4.20}$$

Although this equation is structurally very similar to others in the literature as in (10; 28; 38), the presence of the magnetic bond number as a parameter enables the stabilisation of all modes, as will be shown in the preceding pages. This is a significant difference not present in non-ferrohydrodynamic models.

4.4. Linear Dispersion Relations

4.4.1. Dispersion relation associated with arbitrary thickness

In this section we will derive the linear dispersion relation associated with eq. (4.16). The system is linearised with respect to a steady state where the pressure is constant $p = 1$, and the film is perfectly cylindrical, $S = 1$. This greatly simplifies the expressions for u and w from (4.15). In particular,

$$u(S, z)^* = 0 \quad w(S, z)^* = \frac{1}{4}\left[\alpha^2 - 1 + 2\log\left(\frac{1}{\alpha}\right)\right] \tag{4.21}$$

and we introduce a normal mode

$$S = 1 + \delta\tilde{S}\exp(\lambda t + ikz) = 1 + \delta\tilde{S}\phi(t, z) \tag{4.22}$$

When we substitute in eq. (4.16) and we linearise the equations (discarding terms which are not linear in δ), we get the following (detailed calculation in appendix A.5)

$$\lambda(k) = \frac{k^2}{16}\left(\epsilon^2 k^2 + 2\mathrm{Ma} - 1\right)\left((\alpha^2 - 1)^2 + 2(2\log\alpha + 1 - \alpha^2)\right) - \frac{ik}{2}(2\log\alpha + 1 - \alpha^2) \tag{4.23}$$

To study this dispersion relation, and the stability properties of the system it is important to understand the real part of this equation. In particular, focusing on

$$f(\alpha) = (\alpha^2 - 1)^2 + 2(2\log\alpha + 1 - \alpha^2), \alpha \in (0, 1] \tag{4.24}$$

as $f(\alpha = 1) = 0$ and $f(\alpha) \to -\infty$ as $\alpha \to 0$, and this is an increasing function, we see that $f(\alpha) \leq 0$ when $\alpha \in (0, 1]$. We can confirm this by plotting the function $f(\alpha)$, available in fig. 4.1. This facilitates the stability analysis, as when focusing on the real part, we see the

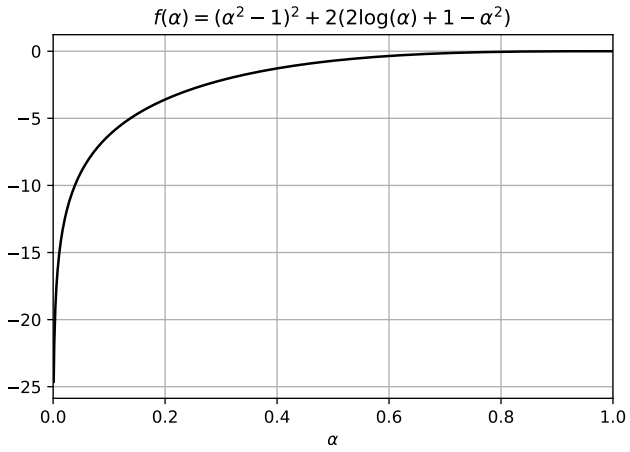

Figure 4.1.: The function $f(\alpha)$. We observe indeed it is negative in the domain $\alpha \in [0, 1]$

system is unstable when

$$k^2(\epsilon^2 k^2 + 2\mathrm{Ma} - 1) < 0 \iff \epsilon^2 k^2 + 2\mathrm{Ma} - 1 < 0 \tag{4.25}$$

Here, we see directly that $2\mathrm{Ma} > 1$ implies linear stability for all modes, as then the above quantity is always positive. Thus there is a critical value of the Magnetic number at $Ma_{\mathrm{crit}} = \frac{1}{2}$. Further, we see that when this is not the case, and the system configuration allows unstable modes, they are located in the interval $\left(0, \frac{1-2\mathrm{Ma}}{\epsilon}\right)$. Furthermore, taking a derivative of the real part of the dispersion relation (4.23) with respect to the wave number k, we find that the most unstable mode is given by

$$\partial_k \lambda(k^*) = 0 \quad \Longrightarrow \quad k^* = \frac{\sqrt{1/2 - \mathrm{Ma}}}{\epsilon} \tag{4.26}$$

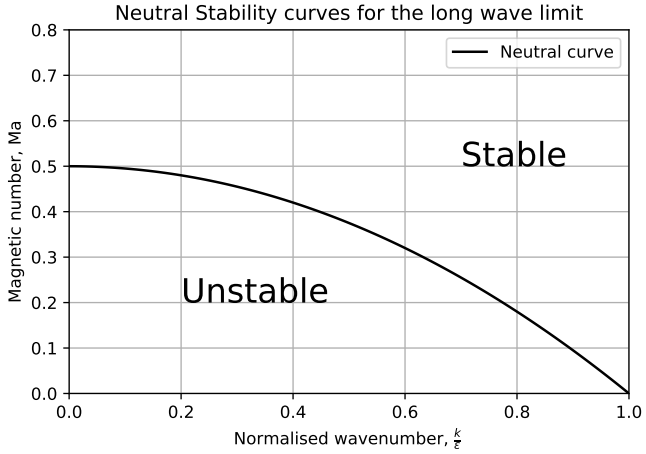

Figure 4.2.: Neutral Curve for the long wave limit.

substituting this in the dispersion relation we find that the maximum growth rate is given by

$$\lambda^* = \mathrm{Re}(\lambda(k^*)) = -\frac{f(\alpha)}{16\epsilon^2}\left(\mathrm{Ma} - \frac{1}{2}\right)^2 \tag{4.27}$$

4.4.2. Thin film limit

When the film is thin, α is close to one. Thus, let $\Delta = 1 - \alpha > 0$, and $\Delta << 1$. Solving for $\alpha = 1 - \Delta$, and substituting in (4.23), focusing on the real part only and taking the limit as Δ is small, we obtain the dispersion relation for the thin film limit

$$\lambda = \frac{k^2}{16}\left(\epsilon^2 k^2 + 2\mathrm{Ma} - 1\right)(\Delta)^3 = \frac{k^2}{16}\left(\epsilon^2 k^2 + 2\mathrm{Ma} - 1\right)(1-\alpha)^3 + \mathcal{O}((1-\alpha)^4) \tag{4.28}$$

We can also recover this limit from the thin-film equation 4.20. The most interesting fact about this relation is that it tells us that the critical Magnetic number is the same as for the thick film case. In particular, the "shape" of the dispersion relation is the same, with the only difference being the magnitude. Moreover, both dispersion relations will share the same neutral curve. As for the imaginary part of the dispersion relation, we find that $\lambda_i = k(1-\alpha)^2 + \mathcal{O}((1-\alpha)^3)$ We compare the thin film limit with the standard dispersion relation in fig. 4.3. In particular, it is interesting to note how it is appreciable that the cubic error in section 4.4.2 is larger than the qubic error in eq. (4.28).

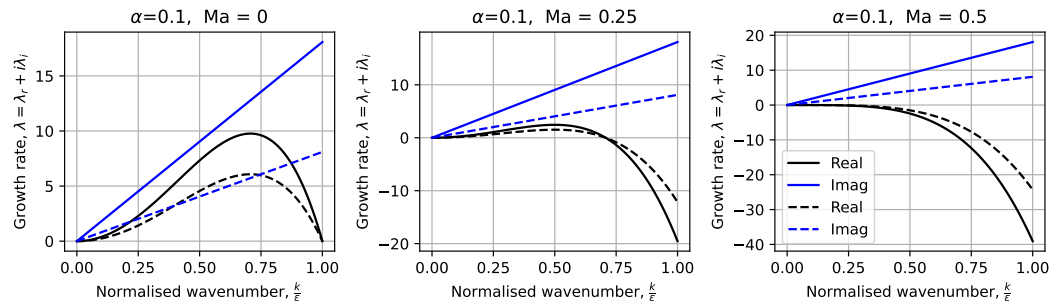

Figure 4.3.: Dispersion relation for a thick film, $\alpha = 0.1$. The solid lines represent the dispersion relation for arbitrary thickness (eq. (4.23)) and the dashed lines the dispersion relation in the thin film limit (eq. (4.28)). Black lines represent the growth rate - the real part of the dispersion relations - and blue lines the wave speed, i.e. the imaginary part of the dispersion relations. As the film is thick the dashed and solid lines are far apart. The stabilising effect of increasing the magnetic bond number and the stability threshold of Ma = 0.5 is confirmed.

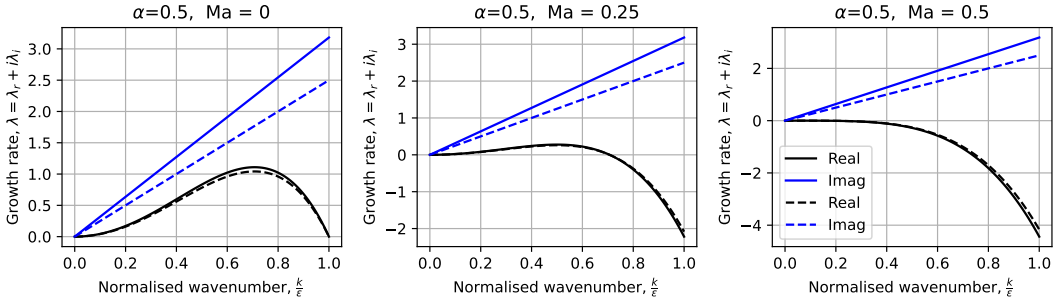

Figure 4.4.: Dispersion relation for a medium thickness film, $\alpha = 0.5$. The legend is the same as in fig. 4.3. We observe the magnetic bond number still has a stabilising effect and the stability threshold is Ma = 0.5.

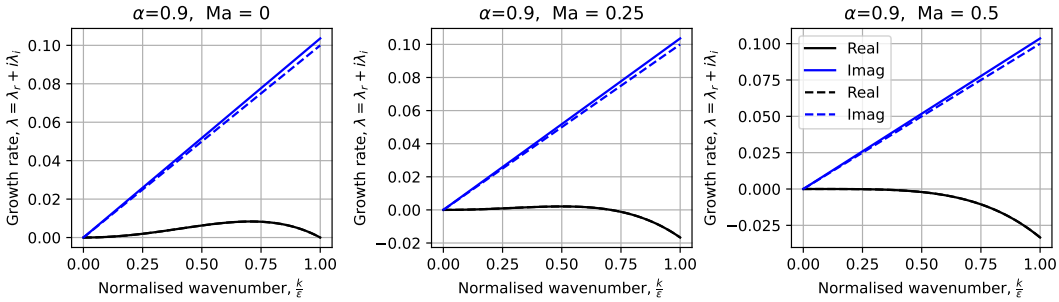

Figure 4.5.: Dispersion relation for a thin film, $\alpha = 0.9$. The legend is the same as in fig. 4.3. We appreciate how close the real part (growth rate) curves due to the qubic convergence. The imaginary curves however, are not as close, owing to the quadratic convergence, but overall the solid and dashed lines are very close to each other, and the same stabilising pattern as in the other figures is visible.

5. The long wave limit for a time dependent magnetic field.

A natural extension to chapter 4 is to consider the effect of a time dependent current, $I(t)$. Many electrical circuits in every day applications run on alternating current (AC), so this question is relevant. In particular we will consider the effect of oscillating time dependent currents of the form

$$I(t) = I_0(1 + \beta\cos(\Omega t))$$

With this form, we have an average current I_0 that is being disturbed sinusoidally. It is important to remark that we will not consider the effects of the electric field in this section as computed in section 2.1.5, assuming it negligible. In particular, this can be done by assuming Ω is small enough, as the electric field is proportional to the magnitude of Ω. Recalling that $\mathrm{Ma} = \mu I^2$, where μ is a constant, we will now have to consider $\mathrm{Ma} = \mathrm{Ma}(t)$.

5.1. Linear stability analysis

Proceeding as before, with the same base flow and spatially constant leading order pressure, we perform a similar linearity analysis as before, but we now consider normal modes of the form

$$S = 1 + \delta S(t)e^{ikz}$$

where the growth rate is now a function of time $S(t)$. Performing a similar linearisation calculation as before in equation (4.16), the right hand side will be the same, for the derivatives are only spatial. However on the left hand side $S'(t)$ will appear. In particular the new "dispersion

relation" will now be a temporal ordinary differential equation for $S(t)$ (this is the real part only):

$$\frac{dS}{dt} = \frac{k^2}{16}(\epsilon^2 k^2 - (1 - 2\,\mathrm{Ma}(t))f(\alpha)S(t) \tag{5.1}$$

where $f(\alpha) = (\alpha^2-1)^2+2(2\log\alpha+1-\alpha^2) < 0$ as in the previous chapter. Considering the form of the time dependent magnetic number, squaring the intensity and expanding into resonant modes (so only terms of the form $\cos(n\Omega t) \quad n \in \mathbb{Z}$), we obtain

$$\frac{dS}{dt} = \frac{k^2}{16}\left(\epsilon^2 k^2 - (1 - 2\,\mathrm{Ma}_0 - \mathrm{Ma}_0\,\beta^2) + 4\,\mathrm{Ma}_0\,\beta\cos(\Omega t) + \mathrm{Ma}_0\,\beta^2\cos(2\Omega t)\right) f(\alpha)S(t) \tag{5.2}$$

where we have written $\mathrm{Ma}_0 = \mu I_0^2$. This equation can be written as

$$\frac{dS}{dt} = (A + B\cos(\Omega t) + C\cos(2\Omega t))S \tag{5.3}$$

where A, B and C are obtained from eq. (5.2) in the straightforward way, by equation coefficients. As a remark, the reader might find eq. (5.3) familiar as it reminds us of Mathieu equations. However it is not a Mathieu equation, as it is first order equation. If we write $S(t) = \exp(\lambda(t))$, it can be integrated to give

$$\lambda(t) = \ln(S(t)) = At + \frac{B}{\Omega}\sin(\Omega t) + \frac{C}{2\Omega}\sin(2\Omega t)$$

In particular, we observe the sign of A will control the long time stability of the system, as the sinusoidal terms will modulate the amplitude but will never become unbounded. For stability $A < 0$ is required, and proceeding as in the previous chapter, considering $f(\alpha) < 0$, the stability criterion is equivalent to

$$\epsilon^2 k^2 - (1 - 2\,\mathrm{Ma}_0 - \beta^2\,\mathrm{Ma}_0) < 0$$

Thus we find the new critical value of the average magnetic bond number is

$$\mathrm{Ma}_0^* = \frac{1}{2+\beta^2} < \frac{1}{2} \tag{5.4}$$

which is smaller than the non-time dependent critical value! Thus, the oscillatory electric current has a further stabilising effect on the system, as all modes become stable to linear perturbations at a smaller critical value! A comparison is presented in fig. 5.1.

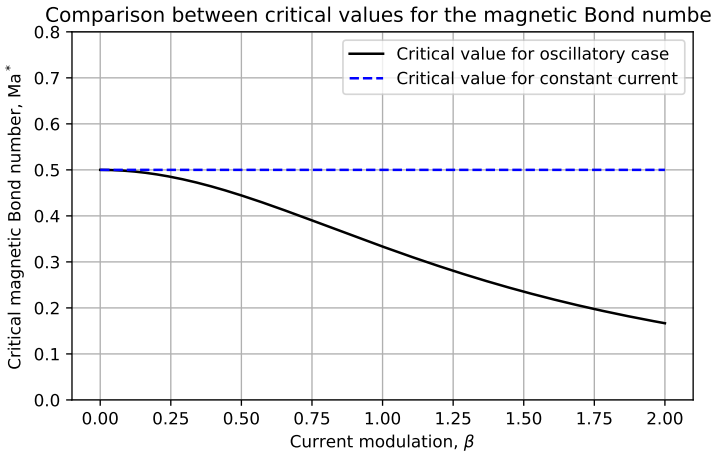

Figure 5.1.: Comparison of the critical value for the parameter Ma in the oscillatory and constant case.

In fig. 5.2 the curve $S(t)$ is displayed for a set of representative values of the parameters. The decay is often interrupted by the oscillations, but in the long term the system ends up decaying.

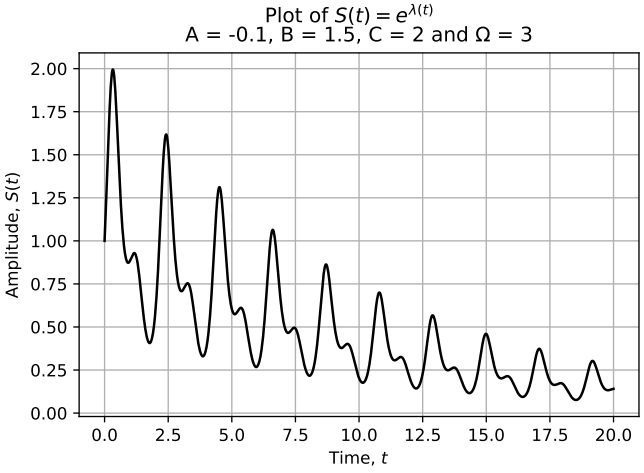

Figure 5.2.: Plot of the amplitude $S(t) = \exp(\lambda(t))$ for some representative values.

6. Simulation of the long wave reduced order equations and travelling wave formation

In the previous chapters several reduced order partial differential equations were derived to model the fluid thickness. Although these equations are interesting from a physical perspective, they are perhaps even richer from a purely mathematical perspective. In particular, these equations develop travelling waves with impressive properties from seemingly arbitrary initial conditions. In this chapter we briefly present our findings for the formation of travelling waves. Moreover, we are interested in considering how well the thin film equation approximated the more complicates conservation equation in eq. (4.16).

6.1. Accuracy of the thin film approximation

The partial differential equations obtained in the long-wave limit (eq. (4.16) and eq. (4.20)) were simulated using a pseudospectral method, as detailed in section 11.1 with periodic boundary conditions for $z \in [-L, L]$ and $N = 256$ or $N = 512$ modes. In particular, we are interested in seeing how well the thin film equation eq. (4.20) approximates the more complicated equation eq. (4.16) for arbitrary thickness.

Starting from equation eq. (4.20), we initialize the system with an initial condition

$$S(z, 0) = 1 + \delta \cos(k^* z) \tag{6.1}$$

where k^* is the wave number that selects the fastest growing mode according to linear theory, as derived in eq. (4.28).

The equations were solved for thin films with $\alpha = 0.99$ and $\alpha = 0.95$ as well as for thicker films with $\alpha = 0.75$. Although, eq. (4.20) is independent of α the parameter must enter through the initial conditions, as $S = \eta + \alpha$ and S is centered around 1. Moreover, they were simulated for unstable regimes, Ma $= 0$ as well as at the stability threshold Ma$= \frac{1}{2}$. As for the other parameters, $\epsilon = 0.1$ and $\delta = \frac{1-\alpha}{2}$. This is presented in fig. 6.1 through fig. 6.6. Time is in the vertical axis and space is in the horizontal axis in the contour plots. The final panel showcases the final profile for each of the two equations superimposed, with the dashed lined representing the thin film equation eq. (4.20) and the solid line the arbitrary thickness equations eq. (4.16).

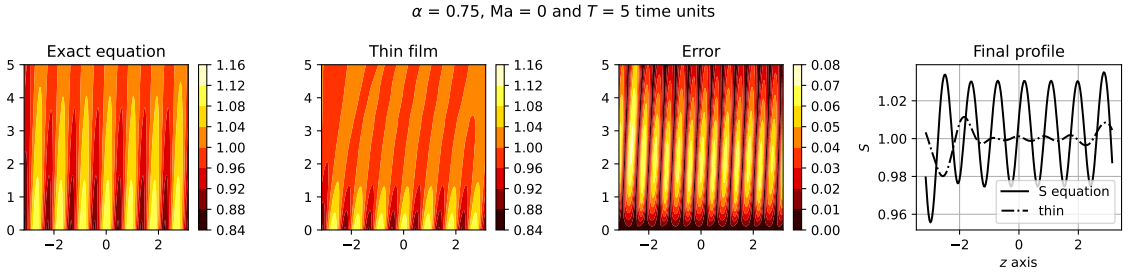

Figure 6.1.: Simulation of a thick film outside of the stability threshold. The final panel showcases the final profiles for each of the two equations.

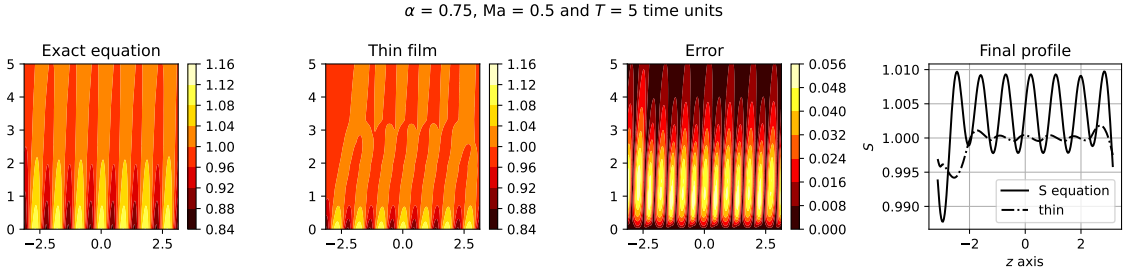

Figure 6.2.: Simulation of a thick film at the stability threshold. There is rapid convergence.

In fig. 6.1 and fig. 6.2 the equations are simulated for a relatively thick film, and thus the error in the thin film approximation is considerable, as expected.

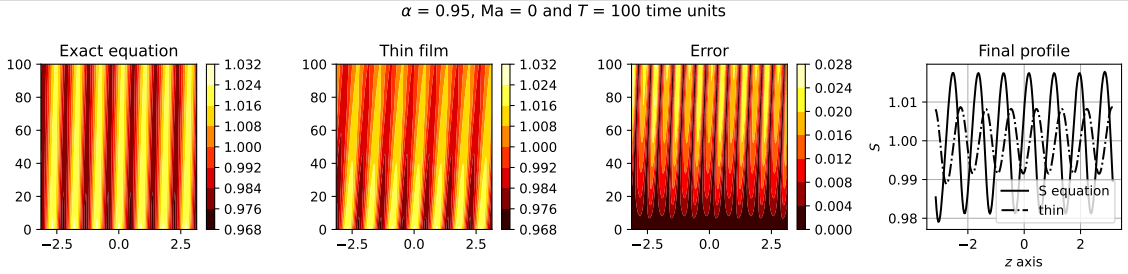

Figure 6.3.: Simulation of thin film.

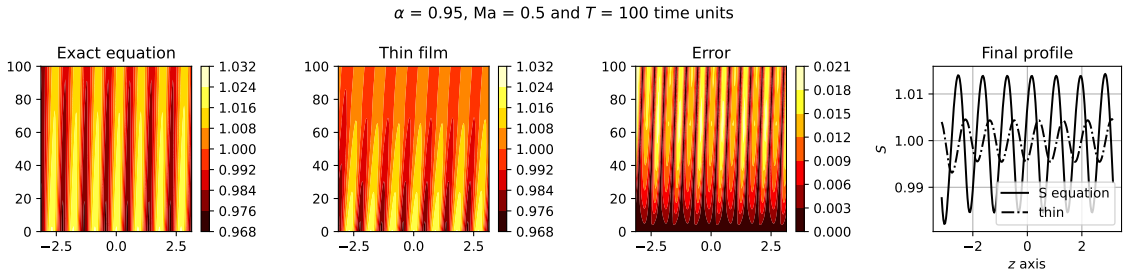

Figure 6.4.: Simulation of a thin film at the stability threshold.

In fig. 6.3 and fig. 6.4 are simulated for a thinner film, and thus the error decreases significantly, as expected from the thin film analysis.

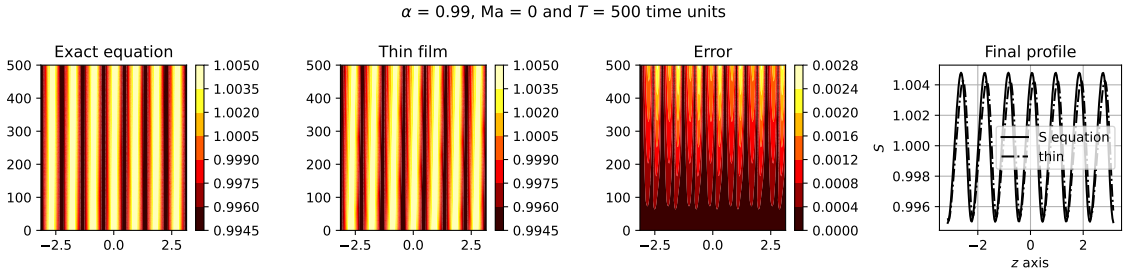

Figure 6.5.: Simulation of a very thin film.

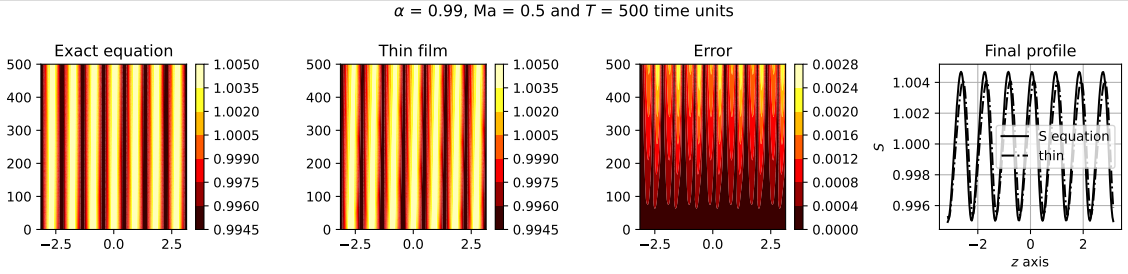

Figure 6.6.: Simulation of a very thin film at the stability threshold. The simulation time was extended to $T = 500$ to account for the fact that the growth rate goes like $\mathcal{O}((1-\alpha)^3)$

In fig. 6.5 and fig. 6.6 the equations are simulated for an extremely thin film and thus error is very small. Note that the decay rate is very small, but this is expected from the dispersion relations in chapter 4, as the absolute size of the growth rate (whether positive or negative) is proportional to the function $f(\alpha)$ that converges to 0 as $\alpha \to 1$, and it does so with a small quadratic error.

6.2. Travelling wave formation

Once we have compared eq. (4.16) to eq. (4.20) we can seek solutions with interesting mathematical properties. In the thin film limit, for a certain parameter range, the equation is initialised with a linearly unstable wavenumber with the aim of seeking travelling wave solutions. In particular, the following parameter values are used:

- $\epsilon = 0.1$, a small value but large enough so that the fourth derivative term is large enough that the numerics are not unstable.
- $D = 1 - 2\,\mathrm{Ma} = 0.6$, or equivalently $\mathrm{Ma} = 0.2$. This means we have a weak current that is not strong enough to stabilise the free surface, but the ferrohydrynamic effect is not negligible.
- The interval length L is varied.
- The thickness parameter α is varied, between $\alpha = 0.4$ and $\alpha = 0.6$

- The initial conditions are similar to those in the previous section, with

$$\eta(z,0) = (1-\alpha)(1+0.95\sin(k^* z))$$

where as previously mentioned k^* is the most unstable wavenumber according to the linear theory developed in chapter 4.

First, we study a film of medium thickness, $\alpha = \frac{1}{2}$

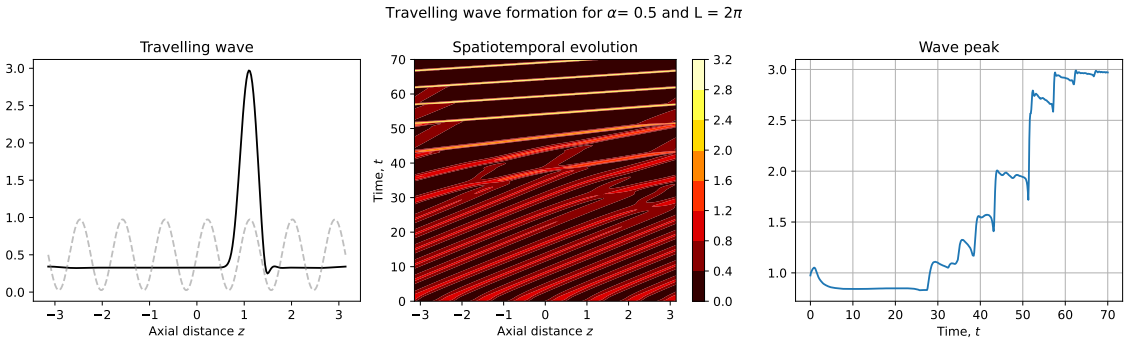

Figure 6.7.: The travelling wave solution remains unaltered in time.

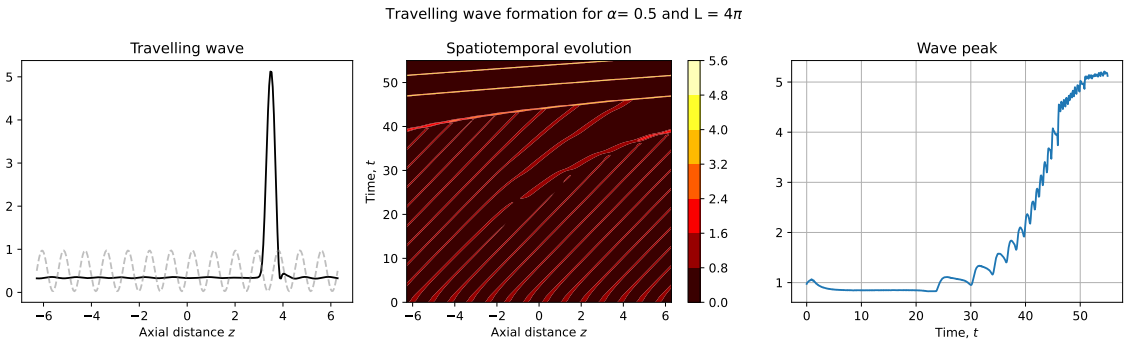

Figure 6.8.: The travelling wave solution remains unaltered in time.

In fig. 6.7 and fig. 6.8 we observe that a travelling wave forms. Moreover, as L increases the travelling wave forms more quickly and it is more peaked. This is because there is more mass available for the travelling wave to accumulate. When α is increased the rate of formation decreases, as this means the film is thinner and thus less mass is available for the mechanism. We can observe this in fig. 6.9 and fig. 6.10. In particular, in fig. 6.9 the wave has not formed yet and two clear waves are present after $t = 200$ time units of iteration. For $L = 4\pi$ however

the added mass induced by the increased interval allows the wave to form faster.

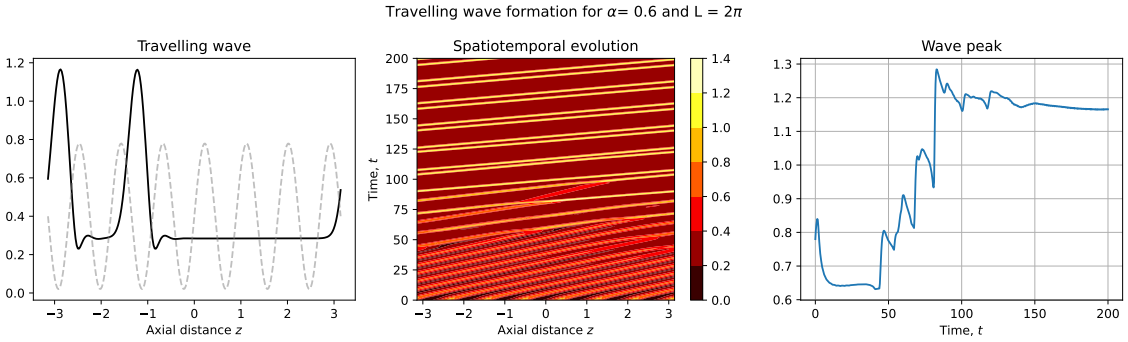

Figure 6.9.: The travelling wave solution remains unaltered in time.

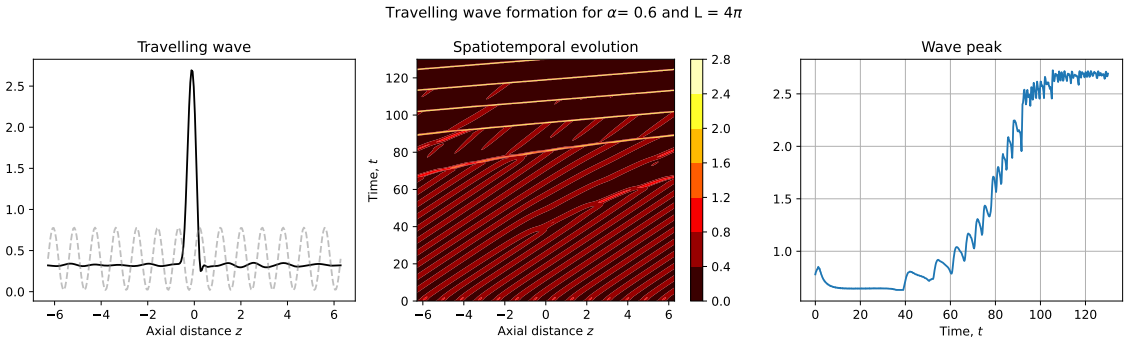

Figure 6.10.: The travelling wave solution remains unaltered in time.

Finally, decreasing α (increasing the fluid thickness) increases the rate of convergence, as seen in the very detailed simulation for $\alpha = 0.4$ displayed in fig. 6.11

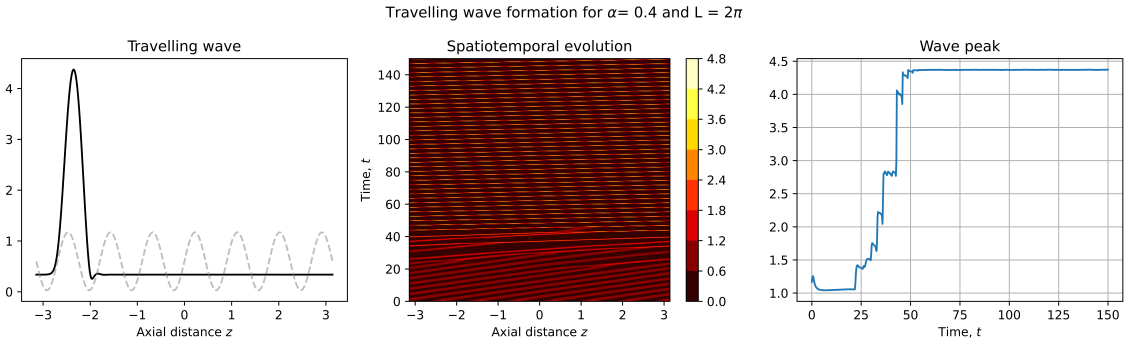

Figure 6.11.: The travelling wave solution remains unaltered in time.

Moreover we can suspect this solution is stable as if it is supplied as an initial condition it simply remains unchanged, as evident in fig. 6.12

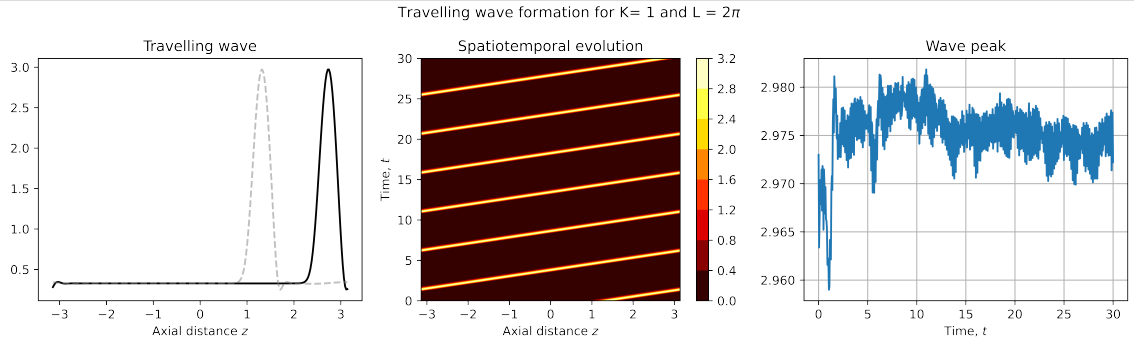

Figure 6.12.: The travelling wave solution remains unaltered in time.

Further, if we perturb the travelling wave, so that the initial condition is the travelling wave with some sinusoidal noise it is still stable, at least from a numerical perspective, as seen in fig. 6.13. Proving the stability of the solution more generally is complicated as it has a rich structure and the linearised perturbation equations have non constant coefficients.

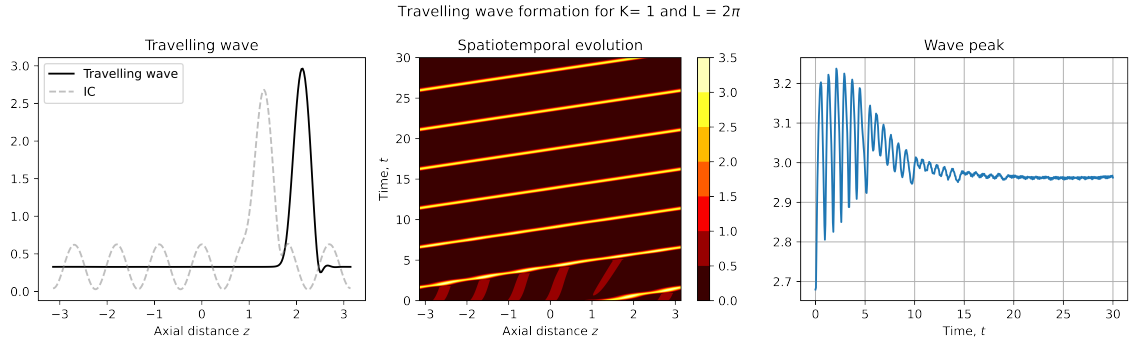

Figure 6.13.: The travelling wave solution is stable to perturbations of the form $\cos(kz)$.

As a final remark, it is interesting to note that the travelling wave is not a symmetric profile. This is expected, as if eq. (4.20) is transformed into a travelling frame, with $\xi = x - ct$, the equation obtained is

$$-c\partial_\xi \eta + \frac{1}{3}\frac{\partial}{\partial \xi}\left(\eta^3\left(1 + (1 - 2\,\mathrm{Ma})\partial_\xi \eta + \epsilon^2 \partial_\xi^3 \eta\right)\right) = 0 \tag{6.2}$$

And this equation does not admit symmetric solutions.

6.2.1. Time periodic travelling waves

Following the spirit of chapter 5, a natural question to ask is what effect will a time dependent current $I(t) = 1 + \delta\cos(\Omega t)$ on the travelling waves obtained in the previous section. This experiment was run for $\alpha = 0.4, 0.5$, $\Omega \in \{0.1, 0.5, 1, 2\}$ and $\delta \in \{0.1, 0.5, 0.7\}$, but a limited number of examples are shown in fig. 6.14, fig. 6.15 and fig. 6.16. The travelling wave still forms but it now has a temporal structure. In particular, the wave's amplitude oscillates periodically in phase with the time dependent current.

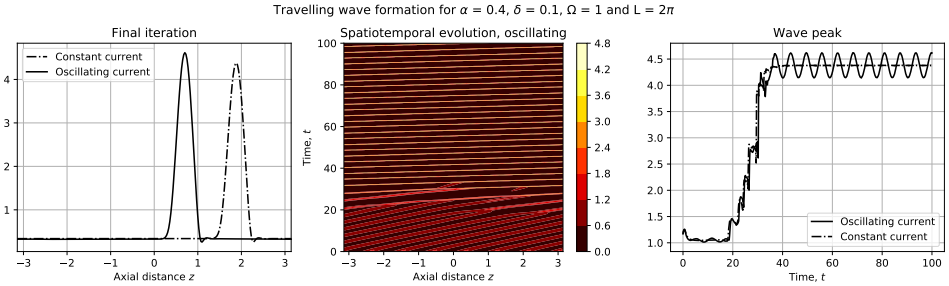

Figure 6.14.: Time periodic travelling wave, with $\Omega = 1$ (fast oscillation) and $\delta = 0.1$ (small forcing). The wave maximum barely deviates from the deterministic case.

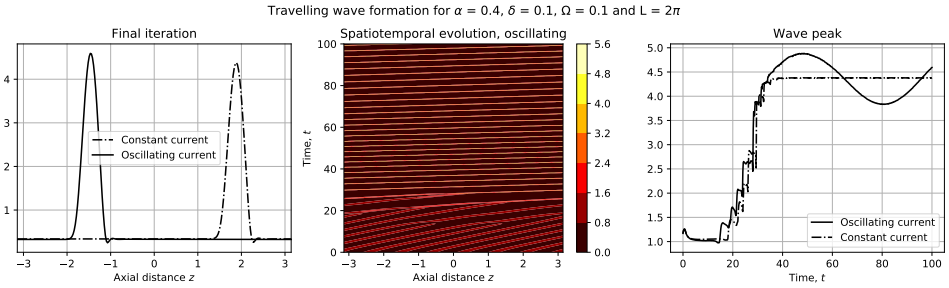

Figure 6.15.: Time periodic travelling wave, with $\Omega = .1$ (slow oscillation) and $\delta = 0.1$ (small forcing). The wave maximum oscillates on a much larger timescale.

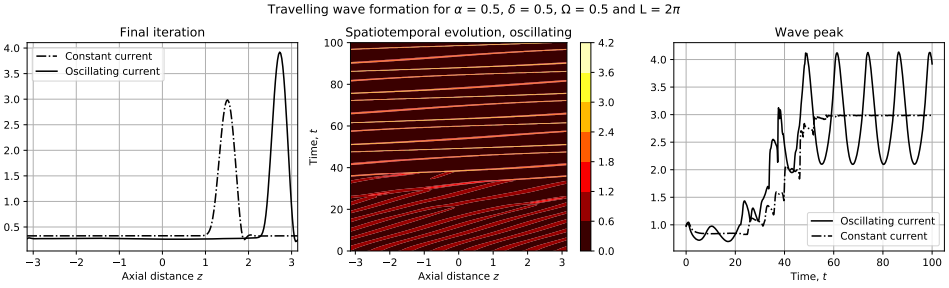

Figure 6.16.: Time periodic travelling wave, with $\Omega = 0.5$ (fast oscillation) and $\delta = 0.5$ (large forcing). The wave maximum heavily deviates from the deterministic case.

7. The Stokes stream function and derivation of the linearised equations

In this short chapter we will linearise the Navier-Stokes equations for arbitrary Reynolds number, alongside the linearised boundary conditions. The base flow is chosen specifically to counter gravity at leading order. The derivations presented here will be useful to consider in the upcoming chapters. Further, another useful concept is presented here: the Stokes stream function.

Starting from the Navier-Stokes equations and the corresponding boundary conditions nondimensionalised in the natural way (with a single spatial lengthscale), as in section 3.1, we can perform the following expansion: To obtain the dispersion relation, we perform an expansion around the perfectly cylindrical solution with (unknown) uniform pressure.

$$S = 1 + \epsilon S_1(z,t) \quad \text{and} p = p_0 + \epsilon p_1(r,z,t) \tag{7.1}$$

For the velocities, we will need some non-zero leading order component in the z direction to counteract gravity (as $\nabla p_0 = 0$), but we can restrict this to $w_0 = w_0(r)$ only, so that

$$w = w_0(r) + \epsilon w_1(r,z,t) \quad u = \epsilon u_1(r,z,t)$$

It is important to remark that this ϵ term is different to the one in previous chapters and has no direct physical interpretation.

7.1. Deriving the leading order equations

7.1.1. Body equations

The continuity equation is trivially satisfied at $\mathcal{O}(1)$, as w_0 is a function of r only and u_0 is identically 0. Likewise the leading order radial momentum equation is also trivially satisfied, as it only involves $u_0 = 0$ and derivatives of p_0, which are identically zero as the pressure is assumed constant. However, the leading order z momentum equation is not trivial:

$$\mathrm{Re}(w_t + uw_r + ww_z) = 1 - p_z + w_{rr} + \frac{1}{r}w_r + w_{zz}$$

at $\mathcal{O}(1)$, we retain the following terms:

$$1 + \frac{1}{r}\partial_r(r\partial_r w_0(r)) = 0$$

and the system is subject to the following leading order boundary conditions. The tangential stress balance at leading order (recall $S = 1 + \epsilon S_1$)

$$\partial_r w_0 = 0 \quad r = 1$$

No slip becomes $w_0(r = \alpha) = 0$. The solution to this boundary value problem is known to us from the previous discussion

$$w_0(r) = \frac{1}{4}\left[2\log\left(\frac{r}{\alpha}\right) - (r^2 - \alpha^2)\right]$$

Finally, the normal stress balance at leading order is

$$\mathrm{Bo}\, p_0 + \mathrm{Ma} - 1 = 0 \Longrightarrow p_0 = \frac{1}{\mathrm{Bo}} - \frac{\mathrm{Ma}}{\mathrm{Bo}} \tag{7.2}$$

7.2. Deriving the perturbation equations

We can now consider the $\mathcal{O}(\epsilon)$ equations. It is easy to see the continuity equation translates readily to the perturbed variables

$$\frac{\partial}{\partial r}u_1(r,z,t) + \frac{\partial}{\partial z}w_1(r,z,t) + \frac{u_1(r,z,t)}{r} = 0 \tag{7.3}$$

Considering Navier Stokes in the radial direction, terms where u is multiplied with u will be neglected at this order. The terms in the Laplace operator will be retained due to its linearity, as well as term in the ∂_t operator. Further,

$$w\partial_z u = (w_0(r) + \epsilon w_1)(\epsilon u_1) = \epsilon w_0(r)u_1 + \mathcal{O}(\epsilon^2)$$

hence we keep only the order ϵ term. Thus, the linearised equation is

$$\mathrm{Re}(\partial_t u_1 + w_0(r)\partial_z u_1) = -\partial_r p_1 + \frac{\partial^2 u_1}{\partial r^2} + \partial_z^2 u_1 + \frac{1}{r}\partial_r u_1 - \frac{u_1}{r^2} \tag{7.4}$$

Let us now consider the momentum equation in the axial direction. As before, the terms acted upon by linear operators will show up as normal. There two nonlinear terms to consider here:

$$u\partial_r w = \epsilon u_1 \partial_r(w_0(r) + \epsilon w_1) = \epsilon u_1 \partial_r w_0 + \mathcal{O}(\epsilon^2)$$

$$w\partial_z w = (w_0 + \epsilon w_1)(\epsilon \partial_z w_1) = \epsilon w_0 \partial_z w_1$$

where we have used the fact $\partial_z w_0(r) = 0$. Thus, the linearised equation is:

$$\mathrm{Re}(\partial_t w_1 + w_0(r)\partial_z w_1 + u_1\frac{dw_0}{dr}) = -\partial_z p_1 + \partial_r^2 w_1 + \frac{1}{r}\partial_r w_1 + \partial_z^2 w_1 \tag{7.5}$$

7.2.1. Boundary conditions

The no-slip condition is trivially evaluated at order ϵ: $u_1(\alpha) = w_1(\alpha) = 0$ Moving on to the free boundary conditions, the simplest is the kinematic condition. The linear terms are simply evaluated at order ϵ, but the nonlinear term:

$$w\partial_z S = (w_0(1) + \epsilon w_1(1))\partial_z(1 + \epsilon S_1) = \epsilon w_0(1)\partial_z S_1 + \mathcal{O}(\epsilon)$$

thus, the condition is

$$\partial_t S_1 + w_0(r=1)\partial_z S_1 = u_1(r=1) \quad \text{on } r = S(z,t) \tag{7.6}$$

Moving on to the tangential stress balance, we must proceed with care. Copying the condition here for convenience,

$$(1 - S_z^2)(u_z + w_r) + 2S_z(u_r - w_z) = 0 \quad \text{on } r = 1$$

We can immediately see that second term is $\mathcal{O}(\epsilon^2)$ and will not contribute at the desired order. On the first term, $S_z^2 = \mathcal{O}(\epsilon^2)$ so again it is not important. Thus we have

$$\partial_z u + \partial_r w = 0 \quad r = 1 + \epsilon S_1$$

Considering $\partial_z u = \epsilon \partial_z u_1 + \ldots$, this term will be present. As for $\partial_r w$, we can expand this

$$\partial_r w|_{r=1+\epsilon S_1} = \frac{dw_0}{dr}(1+\epsilon S_1) + \epsilon \partial_r w_1(1) = \frac{dw_0}{dr}(1) + \epsilon \frac{d^2 w_0}{dr^2}|_1 S_1 + \epsilon \partial_r w_1(1) = \epsilon \frac{d^2 w_0}{dr^2}|_1 S_1 + \epsilon \partial_r w_1(1)$$

Now, evaluating $\frac{d^2 w_0}{dr^2} = -1$ and rearranging, we reach the tangential stress balance at order ϵ.

$$S_1 = \partial_z u_1 + \partial_r w_1 \quad \text{on } r = 1 \tag{7.7}$$

Finally, the normal stress balance can be linearised to

$$\mathrm{Bo}\, p_1 - 2\mathrm{Ca}\, \partial_r u_1 = (2\mathrm{Ma} - 1)S_1 - \partial_z^2 S_1 \quad \text{on } r = 1 \tag{7.8}$$

7.3. Summary

Below we list the linearised perturbation equations for convenience

$$\begin{aligned}
\frac{\partial}{\partial r}u_1(r,z,t) + \frac{\partial}{\partial z}w_1(r,z,t) + \frac{u_1(r,z,t)}{r} &= 0 \\
\mathrm{Re}(\partial_t u_1 + w_0(r)\partial_z u_1) &= -\partial_r p_1 + \frac{\partial^2 u_1}{\partial r^2} + \partial_z^2 u_1 + \frac{1}{r}\partial_r u_1 - \frac{u_1}{r^2} \\
\mathrm{Re}\left(\partial_t w_1 + w_0(r)\partial_z w_1 + u_1\frac{dw_0}{dr}\right) &= -\partial_z p_1 + \partial_r^2 w_1 + \frac{1}{r}\partial_r w_1 + \partial_z^2 w_1 \\
u_1(\alpha) = w_1(\alpha) &= 0 \\
\partial_t S_1 + w_0(r)\partial_z S_1 &= u_1 \quad \text{on } r = 1 \\
S_1 &= \partial_z u_1 + \partial_r w_1 \quad \text{on } r = 1 \\
\mathrm{Bo}\, p_1 - 2\mathrm{Ca}\partial_r u_1 &= (2\mathrm{Ma} - 1)S_1 - \partial_z^2 S_1 \quad \text{on } r = 1
\end{aligned} \tag{7.9}$$

With this, we have the required equations to proceed with the stability analysis for the upcoming chapters, but we will have a brief detour to discuss a useful construction for numerical schemes.

7.4. The Stokes stream function

Another useful construction is finding a stream-function for the flow. Although the flow is three dimensional in the sense that it occupies a three dimensional region of space, the axisymmetric assumption implies that all dependent variables depend on at most two spatial variables and thus the flow is two dimensional mathematically speaking. Therefore, we know that a stream-function will exist (29). In particular, we introduce a Stokes stream-function that will automatically satisfy the continuity equation in cylindrical coordinates(51):

$$u = \frac{1}{r}\frac{\partial \psi}{\partial z} \quad w = -\frac{1}{r}\frac{\partial \psi}{\partial r}$$

It is easy to see that ψ will automatically satisfy the continuity equation (7.3), as it can be rewritten as

$$\frac{1}{r}\partial_r(ru) + \partial_z w = 0$$

and using the fact that $\partial_{rz}^2 = \partial_{zr}^2$ the proof is trivial.

This construction will be helpful for our task, for when it is substituted into the Navier-Stokes equations the pressure can be eliminated and we are left with a single scalar equation for a single scalar unknown, $\psi(r, z, t)$. It must be noted however that this equation will be a fourth order partial differential equation, and thus will require four boundary conditions to specify the solution.

7.5. Linearised equations in terms of the Stokes Stream Function

We will now make use of the Stokes stream-function to derive equivalent equations to those in section 7.3. First, note that the continuity equation will be satisfied automatically, so it can be safely ignored. Before proceeding, and with the foresight that we will be eventually interested in understanding the stability of this system, we introduce the following normal mode formulation (with a slight abuse of notation for convenience)

$$\psi(r, z, t) \longrightarrow \psi(r, t)e^{i\kappa z} \Longrightarrow \partial_z \to i\kappa$$

Now, we can substitute this form of the stream function into the linearised Navier-Stokes equations from eq. (7.9). The pressure is eliminated by multiplying the r equation by $i\kappa$ (which is the same as ∂_z)) and subtracting the z equation after differentiation by r. This will cancel the pressures and will return the following scalar equation for $\psi(r, t)$

$$\begin{aligned}
&\left(\frac{\partial^4}{\partial r^4}\psi(r,t)\right) r^3 - 2\left(\frac{\partial^3}{\partial r^3}\psi(r,t)\right) r^2 - \left(\frac{\partial^3}{\partial r^2 \partial t}\psi(r,t)\right) \mathrm{Re}\; r^3 \\
&+ \left(-iW_0(r)\,\mathrm{Re}\,k\, r^3 - 2k^2 r^3 + 3r\right)\left(\frac{\partial^2}{\partial r^2}\psi(r,t)\right) \\
&+ \left(\frac{\partial^2}{\partial r \partial t}\psi(r,t)\right) \mathrm{Re}\; r^2 + i\psi(r,t)\left(\frac{d^2}{dr^2}W_0(r)\right) \mathrm{Re}\, k\, r^3 \\
&+ \left(i\,\mathrm{Re}\,k\, r^2 W_0(r) + 2k^2 r^2 - 3\right)\left(\frac{\partial}{\partial r}\psi(r,t)\right) \\
&+ \left(\mathrm{Re}\, kr\left(\frac{\partial}{\partial t}\psi(r,t)\right) + \left(-i\,\mathrm{Re}\left(\frac{dW_0}{dr}(r)\right) + \left(i\,\mathrm{Re}\, W_0(r) + k\right) k^2 r\right)\psi(r,t)\right) k\, r^2 = 0
\end{aligned} \tag{7.10}$$

The no slip boundary conditions at $r = \alpha < 1$ transform to

$$\psi(\alpha, t) = 0 \quad \text{and} \quad \frac{\partial \psi}{\partial r}|_{r=\alpha} = 0$$

As for the free boundary conditions at $r = 1$, combining the tangential and kinematic equations we obtain:

$$\begin{aligned} &\frac{\partial^2}{\partial r \partial t}\psi(r,t) - \frac{\partial^3}{\partial r^2 \partial t}\psi(r,t) - k^2\left(\frac{\partial}{\partial t}\psi(r,t)\right) \\ &+ ikW_0(1)\left(\frac{\partial}{\partial r}\psi(r,t) - \frac{\partial^2}{\partial r^2}\psi(r,t) - k^2\psi(r,t)\right) - ik\psi(r,t) = 0 \end{aligned} \tag{7.11}$$

and combining the tangential and normal stress balance, substituting for the pressure in terms of ψ from the Navier-Stokes equations, yield the final boundary condition, to be evaluated at $r = 1$.

$$\begin{aligned} &-\frac{iBo}{k}\left(i\left(\frac{\partial}{\partial r}\psi(r,t)\right)W_0(1)\,\mathrm{Re}\,k - i\psi(r,t)\left(\frac{dW_0}{dr}(r)\right)Rk + k^2\left(\frac{\partial}{\partial r}\psi(r,t)\right) + \left(\frac{\partial^2}{\partial r \partial t}\psi(r,t)\right)\mathrm{Re}\right) \\ &-\frac{iBo}{k}\left(-\left(\frac{\partial^3}{\partial r^3}\psi(r,t)\right) + \left(\frac{\partial^2}{\partial r^2}\psi(r,t)\right) - \frac{\partial}{\partial r}\psi(r,t)\right) \\ &-2Ca\left(-ik\psi(r,t) + ik\left(\frac{\partial}{\partial r}\psi(r,t)\right)\right) + \left(k^2 - D\right)\left(\frac{\partial}{\partial r}\psi(r,t) - \frac{\partial^2}{\partial r^2}\psi(r,t) - k^2\psi(r,t)\right) = 0 \end{aligned} \tag{7.12}$$

Detailed derivations of these boundary conditions are included in appendix A.7

8. Linear Stokes Flow Analysis

In this section the Stokes limit of the problem is considered. In this case, the Reynolds number is still vanishingly small, however, unlike in the long wave limit there does not exist a disparity between the scales so a limit can not be taken as before. Hence, the full Stokes equations are considered.

The aim of this chapter is to derive a dispersion relation for the Stokes problem, to compare it and validate the analytical dispersion relations for the reduced model. The approach is motivated by the approach present by (10), but incorporating the Magnetic effect.

We can continue from the previous chapter, by setting $\mathrm{Re} = 0$ in the perturbation equations. We recall for convenience that the base flow is given by the balance between viscous forces and gravity, and the associated constant pressure is

$$w_0(r) = \frac{1}{4}\left[2\log\left(\frac{r}{\alpha}\right) - (r^2 - \alpha^2)\right] \quad p_0 = \frac{1 - \mathrm{Ma}}{\mathrm{Bo}} \tag{8.1}$$

8.1. Linearised Stokes equations

As the Reynolds number is not present in the continuity equation we have again

$$\partial_r u_1 + \frac{u_1}{r} + \partial_z w_1 = 0$$

And the momentum balance equations are eq. (7.9) but with Re = 0

$$\begin{aligned} 0 &= -\partial_r p_1 + \partial_r^2 u_1 + \partial_z^2 u_1 + \frac{1}{r}\partial_r u_1 - \frac{u_1}{r^2} \\ 0 &= -\partial_z p_1 + \partial_r^2 w_1 + \partial_z^2 w_1 + \frac{1}{r}\partial_r w_1 \end{aligned} \tag{8.2}$$

8.1.1. Linearised Boundary conditions

As Re is not present in the linearised boundary conditions (7.9), they will be exactly the same. They are repeated here for convenience. No-slip at the wire surface is given by $u_1(r = \alpha) = w_1(r = \alpha) = 0$, and at the free boundary (in this case evaluated at $r = 1$), the kinematic condition, tangential stress and normal stress condition are respectively:

$$\begin{aligned} \partial_t S_1 + w_0(r=1)\partial_z S_1 &= u_1(r=1) \\ -S_1 + \frac{\partial u_1}{\partial z} + \frac{\partial w_1}{\partial r} &= 0 \\ \mathrm{Bo}\, p_1 - 2\mathrm{Ca}\partial_r u_1 - 2\mathrm{Ma}S_1 + S_1 + \partial_z^2 S_1 &= 0 \end{aligned} \tag{8.3}$$

8.2. Stokes operator

As discussed in section 7.4, there exists a stream function for this axisymmetrical flow, recalled here for convenience.

$$u_1 = \frac{1}{r}\frac{\partial \psi}{\partial z} \quad w_1 = -\frac{1}{r}\frac{\partial \psi}{\partial r}$$

The partial differential equation in section 7.5 reduces to (after a logn and not very insightful calculation)

$$D(D\psi) = 0 \quad D = \frac{\partial^2}{\partial r^2} - \frac{1}{r}\frac{\partial}{\partial r} + \frac{\partial^2}{\partial z^2} \tag{8.4}$$

where D is known as the Stokes operator (8).

8.3. Normal mode formulation

With the aim of seeking a linear dispersion relation to study the instability of the Stokes problem, a normal mode configuration is introduced, following the idea already introduced in chapter 4

and section 7.5. This is equivalent to transforming the problem to Laplace space in t and to Fourier space in z. However the radial coordinate is not transformed (and more generally, the equations for arbitrary Reynolds number have coefficients that depend on r). When introducing the normal modes, it can either be done at the stream function level or at the velocity level, but it does not matter for the equations are equivalent. In particular,

$$\begin{gathered}\psi(r,z,t) = f(r)e^{i\kappa z+\Lambda t} + c.c. \quad \text{or} \\ u_1(r,z,t) = \tilde{u}(r)e^{i\kappa z+\Lambda t} + c.c. \quad w_1(r,z,t) = \tilde{w}(r)e^{i\kappa z+\Lambda t} + c.c.\end{gathered} \tag{8.5}$$

This means that the functions $f, \tilde{u}$ and $\tilde{w}$ are related via

$$\tilde{u}(r) = \frac{i\kappa}{r}f(r) \quad \tilde{w}(r) = -\frac{1}{r}\frac{\partial f(r)}{\partial r} \tag{8.6}$$

and similarly for the pressure field and the free surface: $p(r,z,t) = \tilde{p}(r)e^{i\kappa z+\Lambda t} + c.c.$ and $S(z,t) = \tilde{S}e^{i\kappa z+\Lambda t} + c.c.$, where $\tilde{S}$ is a constant (and not a function of r like all the other tilde variables). In this formulation, the governing equations will take the form of ordinary differential equations in r for the tilde variables. We must remark, that to connect the long wave formulation with the Stokes analysis we identify, $\kappa = \epsilon k$ and $\Lambda = \epsilon\lambda$, where k, λ are the perturbation variables from the long wave analysis in chapter 4. Further, the dispersion relation ($\Lambda(\kappa)$) will be found by forcing a solvability condition with the boundary conditions. In the stream function formulation the continuity condition is trivially satisfied. The momentum equations under this normal mode formulation are given by

$$\begin{aligned}0 &= -\partial_r\tilde{p} + \partial_r^2\tilde{u} - \kappa^2\tilde{u} + \frac{1}{r}\partial_r\tilde{u} - \frac{\tilde{u}}{r^2} \\ 0 &= -i\kappa\tilde{p} + \partial_r^2\tilde{w} - \kappa^2\tilde{w} + \frac{1}{r}\partial_r\tilde{w}\end{aligned} \tag{8.7}$$

Analytical Solution to the Ordinary Differential equations

To solve analytically the ordinary differential equations we could take two possible paths. First, using the factorised form of the equation for the stream function (8.4), or by exploiting the fact that the pressure field will be harmonic in the Stokes limit. We will present the second option here, but once the general solution has been found we will return to the stream function

formulation using the connection presented in (8.6) to impose the boundary conditions.

Taking the divergence (meaning applying the operator $\frac{1}{r}\partial_r(r\cdot)$ to the radial equation and multiplying the longitudinal equation by $i\kappa \leftrightarrow \partial_z$ and summing up the result) and using the continuity equation we deduce the following equation for the pressure:

$$\partial_r^2\tilde{p} + \frac{1}{r}\partial_r\tilde{p} - \kappa^2\tilde{p} = \nabla^2\tilde{p} = 0 \tag{8.8}$$

in other words, the pressure is harmonic. From the left hand side of equation 8.8 we identify a Bessel equation (multiplying by r^2). Thus the general solution is given by (1)

$$\tilde{p} = a_1 I_0(\kappa r) + a_3 K_0(\kappa r) \tag{8.9}$$

where I_0 and K_0 are modified Bessel functions of order 0 of the first and second kind, respectively, and a_1, a_3 are unknown constants. With the solution for $\tilde{p}(r)$ we can return to the momentum equations and solve for say $\tilde{w}$ (or $\tilde{u}$, we only need one to compute the stream function) The equation for $\tilde{w}$ is the longitudinal momentum equation, repeated here for convenience

$$0 = -i\kappa\tilde{p} + \partial_r^2\tilde{w} - \kappa^2\tilde{w} + \frac{1}{r}\partial_r\tilde{w}$$

Multiplying by r^2 and substituting the now known pressure

$$0 = -i\kappa r^2(a_1 I_0(\kappa r) + a_3 K_0(\kappa r)) + r^2\partial_r^2\tilde{w} - r^2\kappa^2\tilde{w} + r\partial_r\tilde{w}$$

we recognise an inhomogeneous Bessel equation. The homogeneous solution will be given by

$$\tilde{w}_h(r) = ia_2 I_0(\kappa r) + ia_4 K_0(r)$$

The arbitrary constants are rescaled by i for convenience. Now a particular solution must be found. Trying an Ansatz

$$\tilde{w}_p(r) = C_1 r I_1(\kappa r) + C_2 r K_1(r)$$

we find that the constants must be equal to $C_1 = \frac{ia_1}{2} \quad C_2 = -\frac{ia_3}{2}$. This gives the solution for

$\tilde{w}(r)$

$$\tilde{w}(r) = i\left(\frac{a_1 r I_1(\kappa r)}{2} + a_2 I_0(\kappa r) - \frac{a_3 r K_1(\kappa r)}{2} + a_4 K_0(\kappa r)\right) \tag{8.10}$$

now, recalling the relationship between $\tilde{w}$ and $f(r)$, the radial dependence of the stream function given in equation 8.6, we have

$$\tilde{w}(r) = -\frac{1}{r}\frac{\partial f}{\partial r} \Longrightarrow \frac{\partial f}{\partial r} = -r\tilde{w}(r)$$

and integrating, the stream function is found

$$f(r) = \frac{i}{2\kappa^2}\left(2a_1 I_1(\kappa r) - 2a_3 K_1(\kappa r) - \kappa a_1 r I_0(\kappa r) - 2\kappa a_2 I_1(\kappa r) - \kappa r a_3 K_0(\kappa r) + 2\kappa a_4 K_1(\kappa r)\right) \tag{8.11}$$

This integral has been computed with the aide of the formulas presented in (1). With the general solution in hand, we can impose the solvability condition by ensuring there are a non-zero set of constants that satisfies the boundary conditions.

8.3.1. Matrix Reformulation

Now that an analytical solution to the ordinary differential equations has been obtained, the dispersion relation is obtained by setting up the boundary conditions for an arbitrary values of κ and imposing a solvability condition. It is easier to see this by reformulating the problem with a matrix. This is motivated by the fact that in equation 8.11 the stream function is linear in the integration constants $\{a_i\}_{i\in\{1,2,3,4\}}$, so that the stream function can be written as

$$f(r) = \mathbf{v}(r)\cdot\mathbf{a} \quad \tilde{p}(r) = \mathbf{q}(r)\cdot\mathbf{a} \tag{8.12}$$

where

$$\mathbf{v}(r) = \begin{pmatrix} \frac{ir}{\kappa^2} I_1(\kappa r) - \frac{ir^2 I_0(\kappa r)}{2\kappa} \\ -\frac{ir I_1(\kappa r)}{2\kappa^2} \\ -\frac{ir K_1(\kappa r)}{\kappa^2} - \frac{ir^2 K_0(\kappa r)}{2\kappa} \\ \frac{ir K_0(\kappa r)}{\kappa} \end{pmatrix} \quad \mathbf{q}(r) = \begin{pmatrix} I_0(\kappa r) \\ 0 \\ K_0(\kappa r) \\ 0 \end{pmatrix} \quad \mathbf{a} = \begin{pmatrix} a_1 \\ a_2 \\ a_3 \\ a_4 \end{pmatrix}$$

To set up the solvability condition it is necessary to rewrite the boundary conditions from 8.1.1

in terms of the stream function $f(r)$. This has been done already in section 7.5, but we do not need to find an expression for the pressure as we already have one in terms of Bessel functions. We know from section 7.5 that the no-slip conditions at the wire will require that

$$\begin{aligned} \tilde{u}(\alpha) = \frac{\kappa i}{\alpha} f(\alpha) = 0 \implies f(\alpha) = 0 \\ \tilde{w}(\alpha) = -\frac{1}{\alpha}\frac{df}{dr}(\alpha) = 0 \implies f'(\alpha) = 0 \end{aligned} \tag{8.13}$$

Moving onto the free boundary, where we evaluate the functions and their derivatives at $r = 1$ (recall this is the first order perturbation). The tangential stress balance is

$$\partial_r w_1 + \partial_z u_1 = S_1 \implies -\partial_r(\frac{1}{r}\frac{df}{dr}) + i\kappa\frac{i\kappa}{r} f(r) = \tilde{S}$$

$$\frac{1}{r^2} f'(r) - \frac{1}{r} f''(r) - \kappa^2 f(r) = \tilde{S}$$

thus, the boundary condition ($r = 1$) becomes

$$\tilde{S} = f'(1) - f''(1) - \kappa^2 f(1) \tag{8.14}$$

For the normal stress balance, we define $D = 1 - 2\text{Ma}$ and compute

$$\text{Bo}\, p_1 - 2\text{Ca}\partial_r u_1 = -(DS_1 - \partial_z^2 S_1)\text{Bo}\,\tilde{p} - 2\text{Ca}\partial_r\left(\frac{i\kappa}{r} f\right) = -(D - \kappa^2)\tilde{S} \tag{8.15}$$

We can find the value of the pressure from the radial z momentum equation, and evaluate at $r = 1$

$$\text{Bo}\,\tilde{p}(1) + 2i\kappa\text{Ca}(f(1) - f'(1)) + (D - \kappa^2)\tilde{S} \tag{8.16}$$

Finally, the kinematic condition is

$$\begin{aligned} \partial_t S_1 + w_0(1)\partial_z S_1 = u_1(1) \\ \implies \Lambda\tilde{S} + w_0(1)i\kappa\tilde{S} = \tilde{u}(1) = i\kappa f(1) \end{aligned} \tag{8.17}$$

We can reduce this system from 5 equations and 5 unknowns (a_i's and $\tilde{S}$) to 4 equations and 4 unknowns by using the tangential stress balance 8.14 and substituting $\tilde{S}$ in the normal stress

balance and the kinematic equation, resulting in

$$\begin{aligned}\Lambda(f'(1)-f''(1)-\kappa^2 f(1))+w_0(1)i\kappa(f'(1)-f''(1)-\kappa^2 f(1))-i\kappa f(1)=0\\ f(1)(-\Lambda\kappa^2-w_0(1)i\kappa^3-i\kappa)+f'(1)(\Lambda+w_0(1)i\kappa)+f''(1)(-\Lambda-i\kappa w_0(1))=0\end{aligned} \tag{8.18}$$

and for the normal balance

$$\mathrm{Bo}\,\tilde{p}(1)+f(1)(-2i\kappa\mathrm{Ca}-D\kappa^2+\kappa^4)+f'(1)(-2i\kappa\mathrm{Ca}-\kappa^2+D)+f''(1)(\kappa^2-D)=0 \tag{8.19}$$

8.3.2. Dispersion relation formulation

We can now formulate a system of equations for the coefficients. The first two equations arise from imposing no-slip on the wire. In terms of the general solution they are given by:

$$\begin{aligned}\frac{a_1\alpha I_0(\alpha\kappa)}{2}-\frac{a_1 I_1(\alpha\kappa)}{\kappa}+a_2 I_1(\alpha\kappa)+\frac{a_3\alpha K_0(\alpha\kappa)}{2}+\frac{a_3 K_1(\alpha\kappa)}{\kappa}-a_4 K_1(\alpha\kappa)=0\\ \frac{a_1\alpha I_1(\alpha\kappa)}{2}+a_2 I_0(\alpha\kappa)-\frac{a_3\alpha K_1(\alpha\kappa)}{2}+a_4 K_0(\alpha\kappa)=0\end{aligned} \tag{8.20}$$

But we can write this more compactly using vector formulation:

$$\begin{aligned}\mathbf{v}(\alpha)\cdot\mathbf{a}=0\quad \frac{\partial\mathbf{v}}{\partial r}(\alpha)\cdot\mathbf{a}=0\\ \left[\mathbf{v}(1)(-\Lambda\kappa^2-w_0(1)i\kappa^3-i\kappa)+\frac{\partial\mathbf{v}}{\partial r}(1)(\Lambda+i\kappa w_0(1))+\frac{\partial^2\mathbf{v}}{\partial r^2}(1)(-\Lambda-i\kappa w_0(1))\right]\cdot\mathbf{a}=0\\ \left[\mathrm{Bo}\,\mathbf{q}(1)+\mathbf{v}(1)(-2\mathrm{Ca}i\kappa-D\kappa^2+\kappa^4)+\frac{\partial\mathbf{v}}{\partial r}(1)(-2\mathrm{Ca}i\kappa-\kappa^2+D)+\frac{\partial^2\mathbf{v}}{\partial r^2}(1)(\kappa^2-D)\right]\cdot\mathbf{a}=0\end{aligned} \tag{8.21}$$

This is indeed a linear system of equations for $\mathbf{a}$, in particular defining the rows matrix $M = M(\Lambda)$ as the transpose of the above equations, and the system is

$$M(\Lambda)\begin{pmatrix}a_1\\a_2\\a_3\\a_4\end{pmatrix}=0 \tag{8.22}$$

Where the exact analytical form of $M(\Lambda)$ is given in the appendix A.8. For this to have non trivial solutions we require that $\det(M(\Lambda)) = 0$. So for each κ the problem is set up and solved numerically using the secant method from Python's `Scipy` package.

8.3.3. Analytical solution to the Stokes Flow dispersion relation

Using a symbolic manipulation program, such as Mathematica (43), we can compute the determinant in eq. (8.22) exactly. Even in the matrix it is easy to see the determinant will be linear in Λ. Thus, given the determinant it is easy to solve for the growth rate Λ. However, the full analytical solution for Λ would not fit in a single page, so it has not been included as part of the report. A more interesting remark is that expanding the dispersion relation in the limit $\alpha \to 1$ we recover exactly the same dispersion relation as for the long wave formulation, eq. (4.28), so that the growth rate has size $\mathcal{O}((1-\alpha^3))$. This makes physical sense as when α is close to one the film is thin and the long wave results are expected to hold. This will be verified numerically in the next section.

8.4. Numerical Results for the Stokes flow dispersion relation

We can then plot the dispersion relation and compare with the reduced order models (which we have in closed form 4.23). In the forthcoming figures we will present results for three different α regimes and 3 different Magnetic Bond number values.

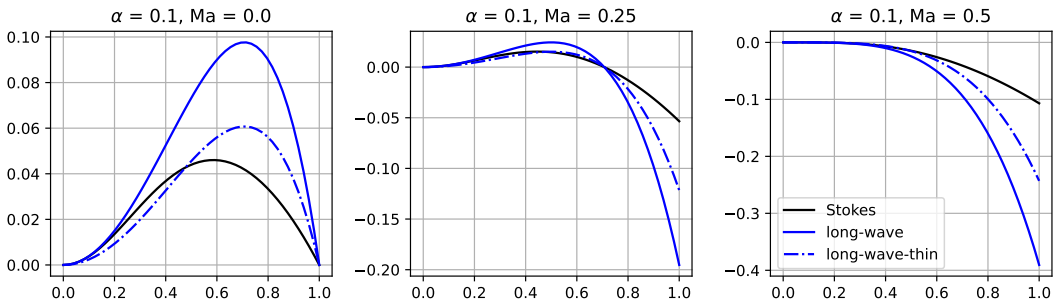

Figure 8.1.: Dispersion relations for a thin wire (thick film), where $\alpha = 0.1$, and several values of the magnetic number. The main appreciation here is that $Ma = 0.5$ is also a bifurcation point in the Stokes regime.

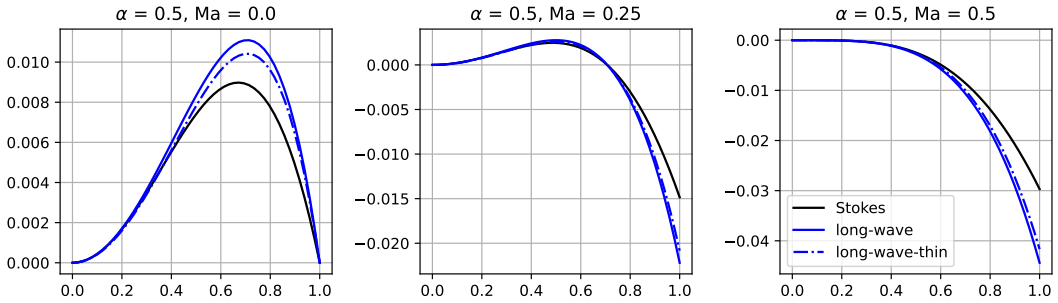

Figure 8.2.: Dispersion relations for $\alpha = 0.5$, and several values of the magnetic number. The main appreciation here is that Ma= 0.5 is also a bifurcation point in the Stokes regime.

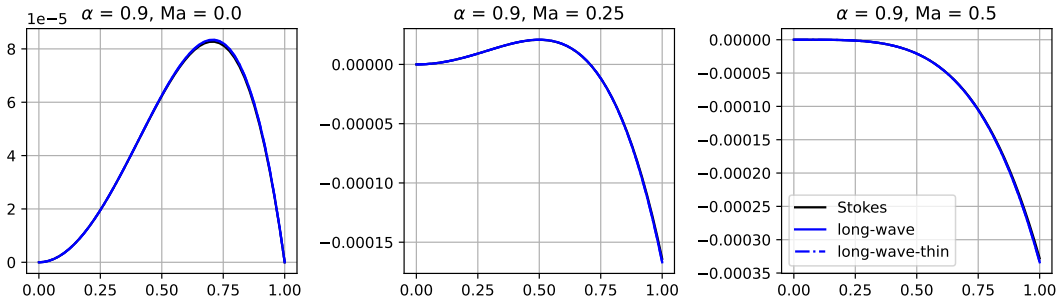

Figure 8.3.: Dispersion relations for a thick wire (thin film), where $\alpha = 0.9$, and several values of the magnetic number. We see great agreement between the thin film reduced order models and the Stokes flow, as expected from the fact the film is thin.

We can also plot the neutral curves for the Stokes limit. Extraordinarily, these match exactly with the long wave formulation, suggesting the stabilising role of the magnetic field is quite universal. We suspect this already from the above charts, as in all of them the intersection points with the x axis agree for all limits. This is confirmed visually below in fig. 8.4.

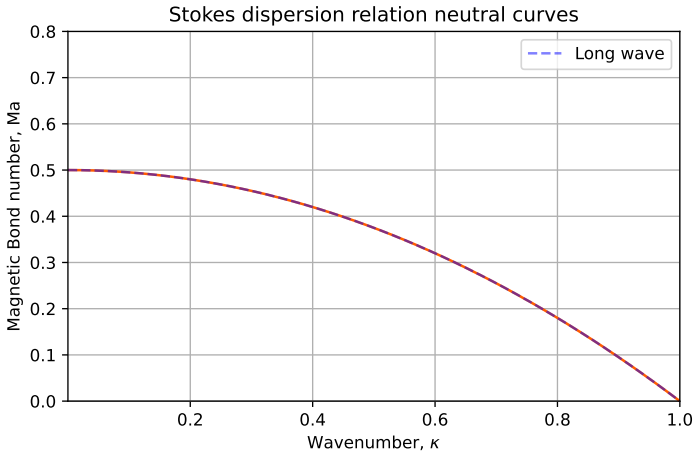

Figure 8.4.: Neutral curves for the Stokes limit (in orange) obtained as contours of the real part of $\Lambda = \Lambda(\kappa, \mathrm{Ma})$ match exactly with the neutral curves for the long wave limit (blue dashed line)

Once the dispersion relation has been obtained by imposing the solvability condition it is interesting to see how the eigenfunctions for the stream function look like for several values of κ and α. We repeat the same values for α as in the previous plots for consistency. It is important to note that the eigenfunctions are free up to a scaling, as when the solvability condition is imposed the linear system in eq. (8.21) has infinite solutions. In particular the eigenfunctions have been chosen so that $\mathrm{Im}(\psi) = 1$ at $r = 1$. This is displayed in fig. 8.5, fig. 8.6 and fig. 8.7

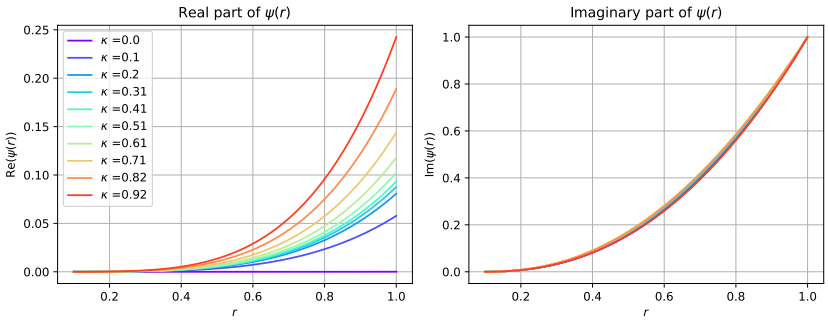

Figure 8.5.: Eigenfunctions for the stream function in the Stokes limit for $\alpha = 0.1$, the thick film limit.

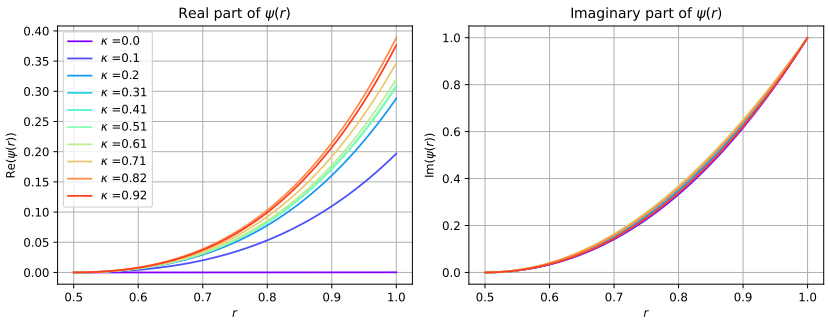

Figure 8.6.: Eigenfunctions for the stream function in the Stokes limit for $\alpha = 0.5$.

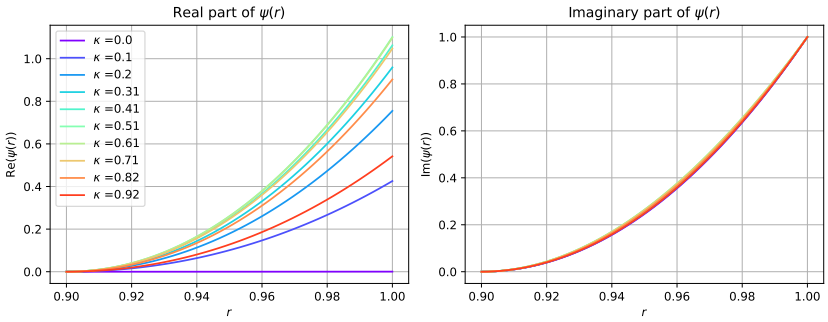

Figure 8.7.: Eigenfunctions for the stream function in the Stokes limit for $\alpha = 0.9$, the thin film limit.

The above figures further serve as a partial check that the solvability condition has been satisfied successfully, as we can see the boundary conditions at $r = \alpha$ are satisfied. This concludes our exploration of the stability of the system in the Stokes limit. This now makes us ponder what will the situation look like when the Reynolds number is not small? With this in mind we move on to the next chapter, studying stability for arbitrary Reynolds numbers.

9. Moving Cylinder

In this chapter we will study the effect of displacing the wire has on the solutions. This is a natural generalisation to make, as in many applications the wire is not stationary. In particular, we will focus on longitudinal displacement, meaning the wire moves with nondimensional velocity pointing in the axial component: $\mathbf{V} = (0, 0, V)^\intercal$.

This is a ferrohydrodynamic cylindrical analogue to the classical Landau-Levich drag out problem in flows where a plate is coated with a liquid film (30; 31). However, instead of adopting a matched asymptotic expansion approach, with one static layer and one layer solve under the lubrication assumption (47) we will follow a long wave philosophy.

9.1. Long wave limit

We can proceed as in chapter 4, with the equations from section 3.2. As for the stationary cylinder case, we can solve for u and w. The calculation is very similar, so it is omitted here, and the only difference is that when the boundary conditions are applied an additional constant term is included in $w(r, z, t)$. This follows from the linearity of the equations in the long wave limit. As before, we are interested in the value of the velocities at the interface $r = S$, given here, and compared with (4.13) and (4.10), which are labeled u_s and w_s respectively.

$$\begin{aligned} u(S,z) = u_s(S,z) &= \frac{(S^2(p_z-1))_z}{8S}\left[\alpha^2 - S^2 + 2S^2\log\frac{S}{\alpha}\right] - \frac{p_{zz}}{16S}(\alpha^2 - S^2)^2 \\ w(S,z) = w_s(S,z) + V &= -\frac{1}{4}(p_z - 1)\left[\alpha^2 - S^2 + 2S^2\log\frac{S}{\alpha}\right] + V \end{aligned} \tag{9.1}$$

Proceeding as in chapter 4, we now seek a conservation equation derived from the kinematic condition: $\partial_t S + w(S,z)\partial_z S = u(S,z)$. Introducing u and w into this condition,

$$\partial_t S + (w_s(S,z) + V)\partial_z S = u_s(S,z) \tag{9.2}$$

Recall that we are interested in writing an equation of the form $8\partial_t(S^2) = \partial_z(F(S,z))$, as in (4.16), and from there we have already derived an $F_s(S,z)$ such that

$$8\partial_t(S^2) = \partial_z(F_s(S,z)) \Longleftrightarrow \partial_t S + w_s(S,z)\partial_z S = u_s(S,z) \tag{9.3}$$

Thus in our new case, we can write

$$\begin{aligned} \partial_t S + (w_s(S,z) + V)\partial_z S = u_s(S,z) \Longrightarrow \partial_t S + w_s(S,z)\partial_z S = u_s(S,z) - V\partial_z S \\ 16S\partial_t S + 16Sw_s(S,z)\partial_z S = 16Su_s(S,z) - 16VS\partial_z S \end{aligned} \tag{9.4}$$

now the stationary part can be written as $16\partial_t(S^2) = \partial_z(F_s(S,z))$, leading to

$$16\partial_t(S^2) = \partial_z(F_s(S,z)) - 16VS\partial_z S \tag{9.5}$$

and noting that

$$-16VS\partial_z S = -\partial_z(8VS^2) \Longrightarrow 16\partial_t(S^2) = \partial_z(F_s(S,z)) - \partial_z(8VS^2) = \partial_z(F_s(S,z) - 8VS^2) \tag{9.6}$$

The conservation equation is slightly different from the zero velocity case. In particular, when we substitute $F_s(S,z)$ from (4.16), we find

$$8(S^2)_t = \frac{\partial}{\partial z}\left((p_z - 1)\left(2S^2(\alpha^2 - S^2 + 2S^2\log\left(\frac{S}{\alpha}\right)\right) - (\alpha^2 - S^2)^2) - 8VS^2\right) \tag{9.7}$$

and the same equation for the pressure $p(S,z,T)$ as in the long wave section, obtained by taking the long wave limit of the normal stress condition.

9.2. Thin film limit

Proceeding as in the stationary case, it is interesting to consider the behaviour of the equation when the film is thin. As in chapter 4, we introduce $S = \alpha + \eta$ and consider the case $|\eta| \ll 1$. We can reach a similar equation as the Benney type eq. (4.20), and indeed the derivation is mostly the same so it is ommited here.

$$\eta_t + \frac{1}{3}\frac{\partial}{\partial z}\left[\eta^3(1 + \eta_z + \epsilon^2\eta_{zzz})\right] + \frac{V\alpha}{2}\frac{\partial}{\partial z}\left(\left(1 + \frac{\eta}{\alpha}\right)^2\right) = 0 \tag{9.8}$$

In particular, it is interesting to note that the moving cylinder does not have a effect on the linear stability of the system, as the new terms in the equations only obtain first order spatial derivatives, which act as transport terms when linearised, i.e. only contribute to the imaginary part of the dispersion relation.

However, this means we can now find values of V such that the transport part of the dispersion relation is zero, meaning the speed required for the cylinder to move up to exactly counteract gravity at the linear order. In particular, the value of V required for this is is given by

$$V = \frac{1}{2}(\alpha^2 - 1 - 2\log\alpha) \approx (1 - \alpha)^2 \quad \alpha \to 1 \tag{9.9}$$

9.3. Numerical Results

We can compare the thin film equation for the static (eq. (4.20)) and translating cylinder case (eq. (9.8)). Several cases are presented for different values of V in fig. 9.1, fig. 9.2 and fig. 9.3, where the system is set up at the stability threshold, Ma = 0.5. As is the case in other chapters, the initial condition is given by:

$$\eta(z, 0) = (1 - \alpha)(1 + \delta\sin(k^* z)) \tag{9.10}$$

Where k^* is the fastest growing mode according to linear theory and $\delta = 0.95$. The film thickness is chosen to be $\alpha = 0.5$ in all simulations.

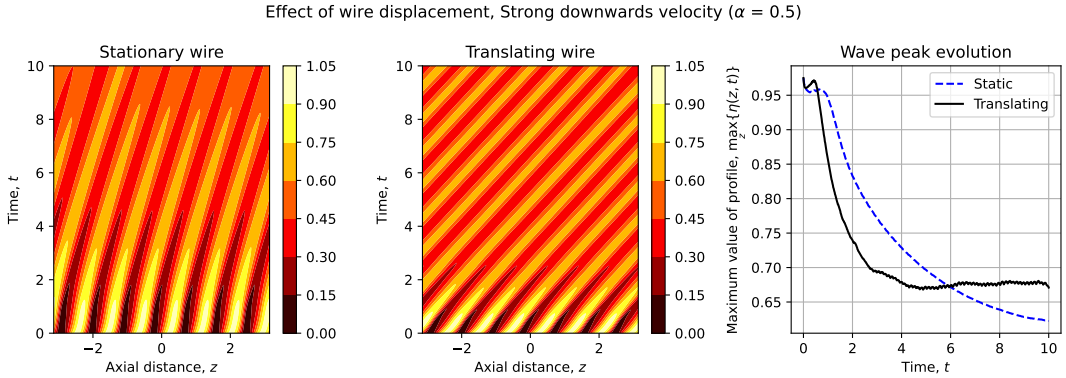

Figure 9.1.: The translation velocity is chosen so that it acts in the same direction as gravity, accelerating the film's fall. Here $\epsilon = 0.1$, Ma $= 0.5$ and $V = 2(1-\alpha)^2$

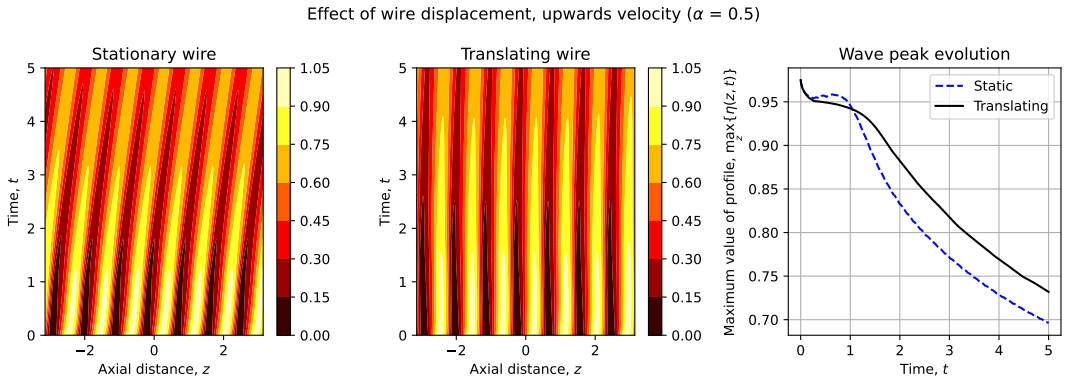

Figure 9.2.: The translation velocity given exactly as in eq. (9.9), so that the fluid film does not move upwards or downwards at linear order. Here $\epsilon = 0.1$, Ma $= 0.5$ and $V = (1-\alpha)^2$

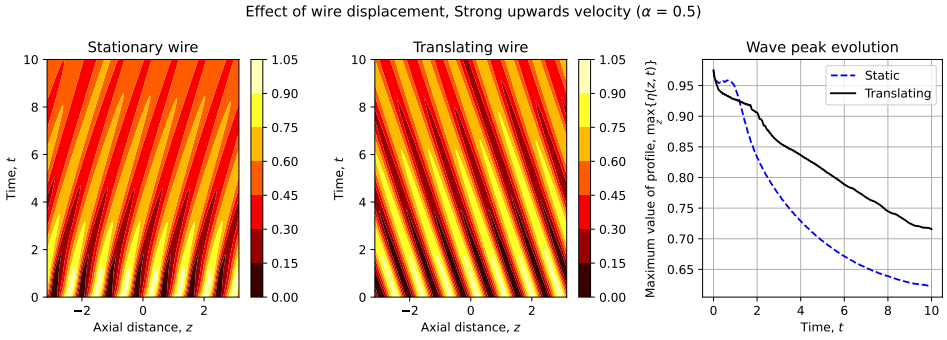

Figure 9.3.: The translation velocity is chosen so that it is much stronger than gravity, and the fluid film advances upwards. Here $\epsilon = 0.1$, Ma $= 0.5$ and $V = -(1-\alpha)^2$. (Recall gravity acts in the positive z direction.)

As a comparison to the results in section 6.2, travelling waves still form but their morphology

is altered by the wire translation. In the same spirit as before, numerical experiments were conducted for 3 distinct values of V, and $\epsilon = 0.1$ for all cases and $\mathrm{Ma} = 0.2$.

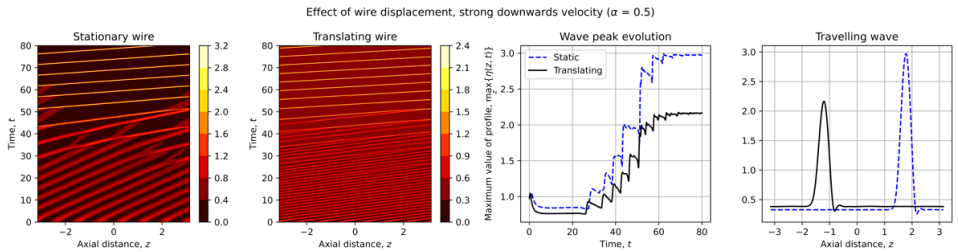

Figure 9.4.: The translation velocity is chosen so that it acts in the same direction as gravity, accelerating the film's fall. Here $\epsilon = 0.1$, $\mathrm{Ma} = 0.2$ and $V = 2(1-\alpha)^2$. The wave forms at a similar time compared to the static case.

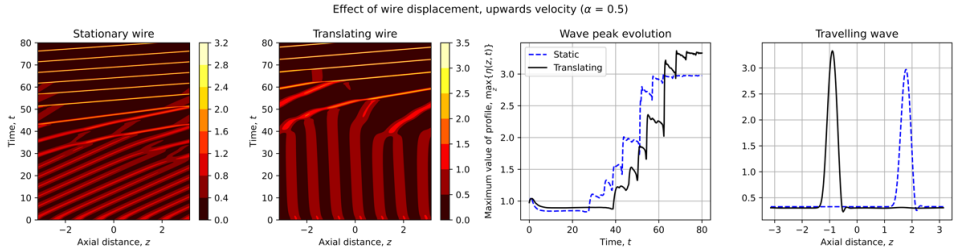

Figure 9.5.: The translation velocity given exactly as in eq. (9.9), so that the fluid film does not move upwards or downwards at linear order. Here $\epsilon = 0.1$, $\mathrm{Ma} = 0.2$ and $V = (1-\alpha)^2$.

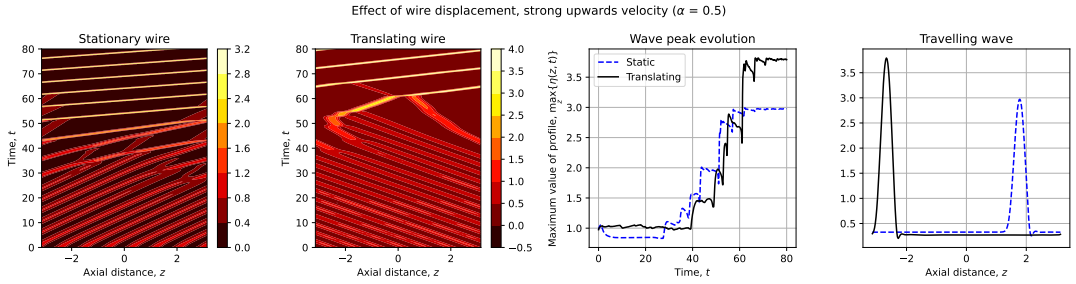

Figure 9.6.: The translation velocity is chosen so that it is much stronger than gravity, and the fluid film advances upwards, until it reaches a critical time where the wave direction is reversed and a travelling wave is formed, but this happens later than in the static case. Here $\epsilon = 0.1$, $\mathrm{Ma} = 0.2$ and $V = -(1-\alpha)^2$.

As a general observation, we see that when the cylinder travels upwards gives travelling waves of larger amplitude than when the cylinder travels downwards.

10. Stochastically driven currents

Stochastic partial differential equations have received an immense amount of attention in recent decades thanks to their exotic properties and wide applicability in the physical, biological and engineering sciences (11; 19). However, in many cases their derivation from physical problems requires complicated constructions and sometimes unrealistic assumptions (33; 40; 41). In the ferrofluids problem however they can be naturally derived just by assuming the current is stochastic, an exceedingly natural assumption to make considering the nature of electricity.

Thus, in this section we model the current intensity as a Brownian motion, $I_t = I_0 + \sigma W_t$, where W_t is a standard Brownian motion (14; 27; 36) and σ is the standard deviation. We aim to understand the role stochasticity plays in the linear stability results derived in chapter 4 as well as the travelling waves from section 6.2. This simple and realistic modelling assumption will lead to novel results not seen as of yet in the deterministic setting.

Two different situations will be analysed in this chapter. First, a brief investigation into the effect stochasticity has on the linear stability results derived in chapter 4, where we verify random currents only have mild effects. This is not the case however in the second situation, where it is shown that stochastic currents can lead to the decay of the travelling wave derived in section 6.2. This is a nonlinear phenomenom that has not been described in systems of thin films equations.

10.1. At the linear stability threshold

In this section we analyse the role random currents play in the linear stability results derived for the long wave equations. In order to simplify the physics involved it is assumed $\sigma << 1$.

This means that we can neglect the electric field induced by the time dependent magnetic field, as discussed in section 2.1.5. We solve eq. (4.20), but instead of having a constant magnetic bond number, this parameter is now stochastic, and in particular Ma(t) $\sim I(t)^2 = (I_0 + \sigma W_t)^2$. The equation is repeated here for convenience.

$$\partial_t \eta + \frac{1}{3}\frac{\partial}{\partial z}(\eta^3(1 + (1 - 2\mathrm{Ma})\eta_z + \epsilon^2 \eta_{zzz}) = 0 \tag{10.1}$$

In the numerical scheme, we initialize the system by the fastest growing linear perturbation, but we round the wavenumber to an integer to ensure the initial condition satisfies the periodic boundary conditions. Thus the initial conditions are the same as for the previous chapter. The system is then iterated until a final time of $t = 200$ and the results are averaged. In particular, $N = 2024$ realisations were simulated. In fig. 10.1 a graph is presented that shows the maximum value of the wave profile at the final iteration plotted against the averaged current for that particular realization of the Brownian motion W_t. The interesting behaviour present here is that when the average current is smaller than expected the maximum value is larger than the equivalent deterministic case for the same average current.

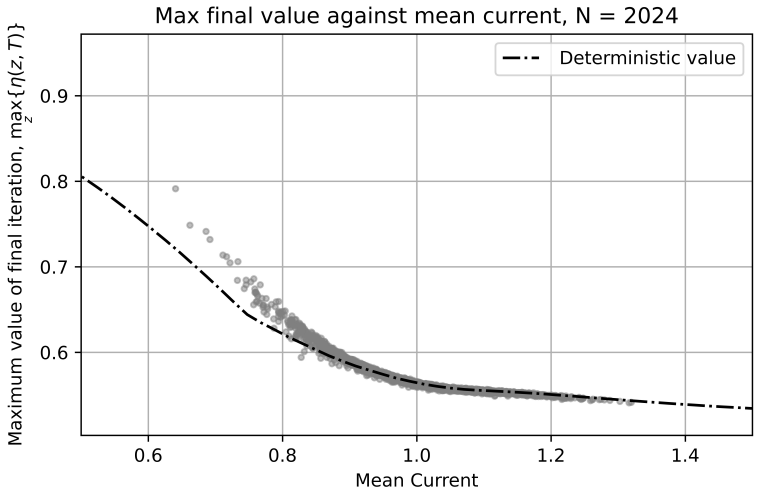

Figure 10.1.: Maximum value of profile at final iteration against mean current, $N = 2024$. Note how the stochastic realizations where the mean current is below the average of $I_0 = 1$ showcase larger maximum values than what would be expected in the deterministic case for the same current.

The data can be further analysed by constructing a histogram of the maximum values at the final

iteration. This is done in fig. 10.2, where we observe the distribution is skewed towards larger values, i.e. the tails are heavier in the right hand side. This is confirmed by computing the skew, that comes out to $2.615 > 0$, confirming the distribution is skewed to the right. Furthermore, the excess kurtosis value of 10.44 indicates the tails are very heavy, and the distribution is far from being normal, unlike the case for standard brownian motion. This is expected from the nonlinearity inherent to the problem.

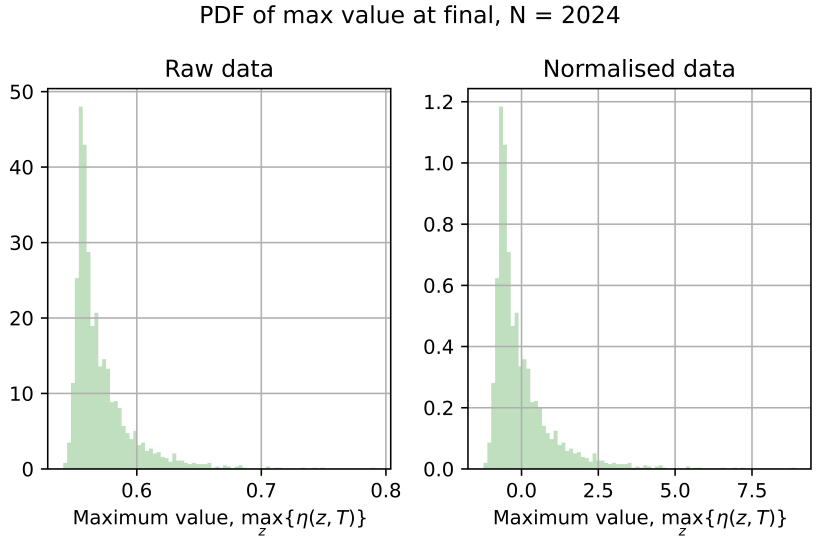

Figure 10.2.: Histogram of max values at final iteration

10.2. Stochastically driven decay of travelling waves

In section 6.2 it was shown that the long wave equation eq. (4.20) can develop localised travelling waves that do not change shape with time. Further, it was shown that they are stable to perturbations in the initial conditions. Moreover, in section 6.2.1 that travelling waves can still be developed if the intensity varies periodically. Hence, in this section we analyse the stability of these solitary waves to stochastic perturbations to the current, of the form $I_t = I_0 + \sigma W_t$.

10.2.1. Results

The main result is that the travelling wave solutions discussed previously are unstable to stochastic perturbations to the current. Furthermore as the volatility σ increases, the travelling wave

decays faster. This can clearly be observed in fig. 10.3.The stochastically driven decay can also visualised using a two dimensional contour as well, as presented in fig. 10.4.

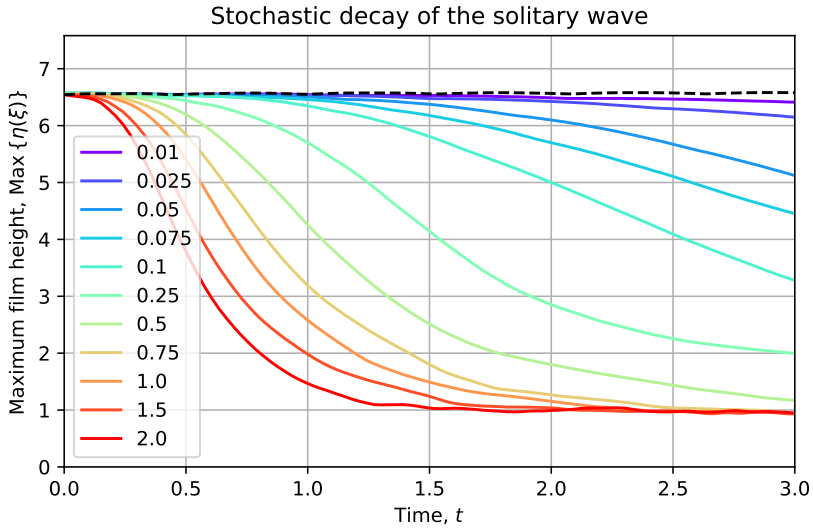

Figure 10.3.: Stochastic decay of traveling wave. The color gradient represents the different volatility values. The vertical axis shows the average maximum value of the wave profile at any given time. It is clear that a larger volatility leads to a faster decay. Each of the "lines" is the average of thousands of realisations.

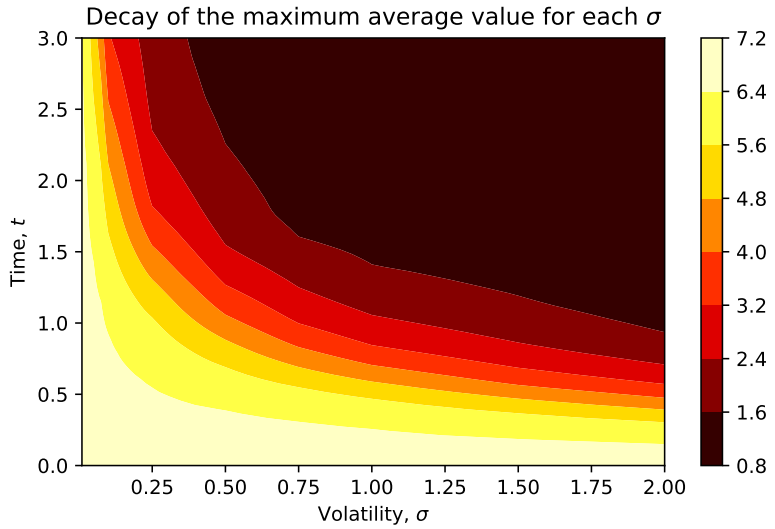

Figure 10.4.: Stochastic decay of traveling wave. Volatility σ on the horizontal axis and time in the vertical axis, and the maximum height given by the colormap.

These novel results showcase stochastic forcing can have effects on stability of solutions unattainable for deterministic systems. The instability can be understood by considering the following

argument. The travelling wave solution is a homoclinic orbit (an orbit that starts and finishes in the same point) in the phase space diagram of the thin film equation (4.20) when transformed into the coordinate $\xi = x - ct$. Some example orbits are showcased in fig. 10.5. This orbit is an attractor as discussed in section 6.2, but the exact shape of the orbit depends on the values of the parameters, in particular on Ma. In the stability analysis in section 6.2 all parameters are held constant, but now Ma varies with time as a result of the stochastic forcing. This means the exact shape of the orbit continuously changes, and in particular the system is unstable.

However, we saw in section 6.2.1 that this does not necessarily mean travelling waves can not develop, but they have some time structure as well, i.e. periodicity. Thus, we must conclude that the stochasticity has a stronger effect than the deterministic time dependence in eq. (7.8), as the travelling disappears completely. This qualitative difference between the deterministic and the stochastic problem is the key difference that allows these mathematical phenomena to occur. Compared to other similar stochastic problems, i.e. (40; 41), this problem is more nonlinear. We can hypothesise that the nonlinearity distributes the stochastic forcing to stabilise the unstable modes.

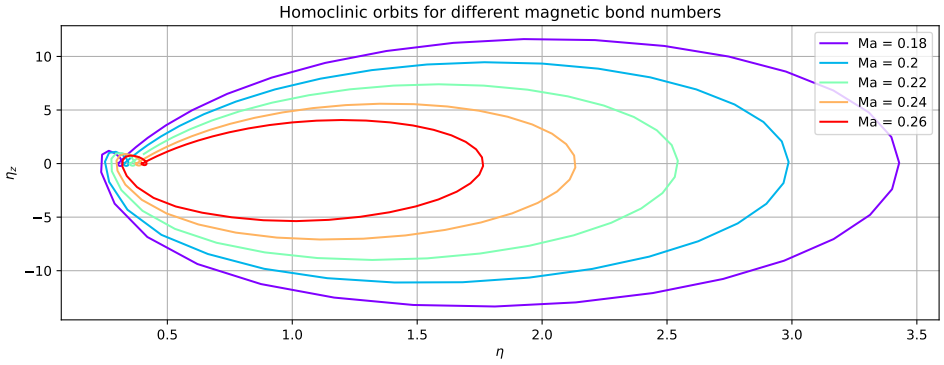

Figure 10.5.: The projection of some periodic orbits for different values of the magnetic bond number. As a remark, the careful observer might be concerned that the orbits cross, but this is because this plot is a projection of a four dimensional dynamical system into two dimensions, so the orbits are not necessarily crossing.

Further, in fig. 10.5 we observe that as the magnetic bond number is increased towards the stability threshold the orbits shrink, to the point that at $\mathrm{Ma} = \frac{1}{2}$ they will collapse to the perfectly cylindrical solution (i.e. the a flat profile, which is a single point in the phase space).

11. Numerical Methods

In this short chapter we comment and describe the numerical methods and algorithms used throughout the project. Numerical schemes are essential in modern applied mathematics, for most problems are intractable analytically and even when simplified they require a computational method to solve them.

11.1. The pseudospectral method

The main method used to solve the nonlinear partial differential equations present in this investigation is the pseudospectral method (17). The pseudospectral method is very useful for solving problems with nonlinear terms and periodic boundary conditions, such as eq. (4.16) and eq. (4.20). This method is optimal for this task as it treats the derivatives in frequency space (recall the FFT diagonalises the derivative operator (49)), and the nonlinearities are evaluated in a natural way in real space. In particular, for a PDE of the form $\partial_t u(x,t) = f(u, u_x, u_{xx}, \dots)$ the equation is discretised in space (thus using the method of lines, where $(\tilde{\mathbf{u}})_k(t) = u^{(k)}(t) = u(x_k, t)$ is the discretised vector of unknowns)

$$\partial_t u^{(k)} = f(u^{(k)}, u_x^{(k)}, u_{xx}^{(k)}, \dots) \tag{11.1}$$

where the j^{th} spatial derivative is computed according to (17)

$$\partial_x^j(\tilde{\mathbf{u}}) = \text{IFFT}\left(\left(\frac{2\pi i n}{L}\right)^j \text{FFT}(\tilde{\mathbf{u}})\right) \tag{11.2}$$

Where the FFT is the Fast Fourier Transform (of a vector) and the IFFT is the inverse Fourier Transform. This is a system of ordinary differential equations, which in vector form may be written as

$$\frac{d\tilde{\mathbf{u}}}{dt} = \mathbf{f}(\tilde{\mathbf{u}}, \dots, \partial_x^j(\tilde{\mathbf{u}}), \dots) \tag{11.3}$$

Finally, this coupled system of nonlinear ordinary differential equations is evolved in time using a stiff solver. In particular, in this investigation the method 'BDF' (21; 24) was used. This algorithmic combination is flexible, robust to stiff problems and relatively fast thanks to the spectral evaluation of the derivatives. Python was the programming language of choice, and abundant use was made of `Scipy` (15) and `Numpy` (23). In terms of the discretisation accuracy, most problems were solved with either $N = 256$ or $N = 512$ modes.

12. Conclusion and further work

The problem of falling axisymmetric ferrofluids has been analysed from a plethora angles. In particular, from a long wave formulation where we discovered the magnetic field plays a stabilising role, to a more traditional hydrodynamic stability framework that confirmed our findings.

Interesting mathematical solutions to the reduced order partial differential equations were presented in the form of shape preserving travelling waves, which were present even under the influence of time dependent magnetic fields and a translating cylinder, and were shown to be stable to perturbations using numerical methods.

Moreover, the natural incorporation of randomness into the problem opened up new exciting research avenues, by showing how the aforementioned travelling waves can be damped or completely eliminated by introducing a stochastically forced electric current, a behaviour unseen in the deterministic case.

A natural extension to the linear stability for the Stokes limit is considering the problem for an arbitrary and finite, Reynolds numbers. This is a considerably harder problem than the Stokes flow limit, as the background flow will appear in the linearised equations through the advection term $\mathbf{u} \cdot \nabla \mathbf{u}$. In particular, this means that the pressure field will not be harmonic, as it was the case in eq. (8.8). This in term means that we cannot solve for the stream function or the pressure field analytically, and we must consider the problem numerically. The author proposes finding the correction to the Stokes dispersion relation by solving for $\Lambda = \Lambda_0 + \mathrm{Re}\,\Lambda_1$, in an asymptotic fashion and using the Fredholm Alternative as a solvability condition as a natural next step.

An interesting avenue to pursue further is to more precisely understand the role oscillating

currents play in the stability of thin ferrofluid films, in particular by considering the full form of the Maxwell stress tensor for fields as given in section 2.1.6. We suspect the bulk equations will still be standard Navier-Stokes for the same assumptions, but the normal stress balance will have additional terms.

Further, methods such as those presented in chapter 5, where differential equations were obtained for the effective growth rates could be implemented to the Stokes problem, although the ODE system would be considerably harder to solve analytically.

Understanding the stability of the travelling waves found for the long wave problem from a more theoretical perspective is also desirable, although the intrinsic nonlinearity of the solution makes this a daunting task.

Finally, this thesis has successfully bridged the gap between the ferrofluid research area with the more traditional problem of falling viscous fluid films, attacking the problem from several angles to ensure the consistency and applicability of the solutions.

A. Appendix

A.1. Code

The code for all the simulations, solvers and numerical schemes has been made available in the authors `Github` profile, and can be accessed using this link. (`https://github.com/JavierChico/M4R-codes`).

A.2. Jefimenko integrals

A.2.1. Liénard-Wiechert potentials

In the appendix the hat notation has been dropped for the dimensional variables. To derive the Jefimenko integrals eq. (2.4), we consider the Liénard-Wiechert potentials (32; 52).

$$\begin{aligned} \phi(\mathbf{r},t) &= \frac{1}{4\pi\epsilon_0}\int \frac{\rho(\mathbf{r}',t_r)}{|\mathbf{r}-\mathbf{r}'|}d\mathbf{r}' \\ \mathbf{A}(\mathbf{r},t) &= \frac{\mu_0}{4\pi}\int \frac{\mathbf{J}(\mathbf{r}',t_r)}{|\mathbf{r}-\mathbf{r}'|}d\mathbf{r}' \end{aligned} \tag{A.1}$$

Here, $t_r = t - |\mathbf{r}-\mathbf{r}'|/c$ is the retarded time and the integrals are over the entire space. Finally, we obtain the Jefimenko integrals eq. (2.4) with the equations (20; 25)

$$\begin{aligned} \mathbf{E} &= -\nabla\phi - \partial_t\mathbf{A} \\ \mathbf{H} &= \nabla\times\mathbf{A} \end{aligned} \tag{A.2}$$

A.2.2. Electric field

Although the leading order behaviour is sufficient for our setting, using power symbollic calculators we can integrate the Jefimenko equations 2.4. Recall that the current density is non-zero in the longitudinal direction, and in particular given by

$$\mathbf{J} = \left(0, 0, \frac{I_0}{\text{Wire cross sectional area}}\cos(\Omega t)\right)^\intercal$$

We can first integrate the second Jefimenko equation, listed here for convenience

$$\mathbf{E} = -\frac{\mu_0}{4\pi}\int \frac{1}{|\mathbf{x}-x'|}\frac{\partial\mathbf{J}(\mathbf{x}',t_r)}{\partial t}d^3x'$$

Introducing cylindrical coordinates, the volume integral can be explicited and factored to

$$E_z = \frac{\mu_0 I_0 \Omega}{4\pi A} \int_0^{2\pi} d\varphi' \int_0^a r' dr' \int_{-\infty}^{\infty} dz' \left[\frac{1}{\sqrt{r^2 + (z-z')^2}} \sin \Omega (t - \frac{\sqrt{r^2 + (z-z')^2}}{c}) \right]$$

integrating along the radial and azimuthal directions leads to an expression involving a single integral

$$= \frac{I_0 \mu_0 \Omega 2\pi}{4\pi A} a^2/2 \int_{-\infty}^{\infty} dz' \left[\frac{1}{\sqrt{r^2 + (z-z')^2}} \sin \Omega (t - \frac{\sqrt{r^2 + (z-z')^2}}{c}) \right]$$

Now, let $u^2 = r^2 + (z-z')^2 = |\mathbf{x} - \mathbf{x}'|^2$. Then $udu = -(z-z')dz'$, or $dz'/u = -du/(z-z')$, the limits change to r and ∞ and we need to account for an extra 2 for the negative z'. Thus, the integral is now equal to

$$= \frac{I_0 \mu_0 \Omega 2\pi}{4\pi A} a^2 \int_r^{\infty} du \left[\frac{1}{\sqrt{u^2 - r^2}} \sin \Omega (t - \frac{u}{c}) \right]$$

Expanding the sin function using the sum formulas,

$$\sin \Omega (t - \frac{u}{c}) = \sin \Omega t \cos(\Omega \frac{u}{c}) - \cos \Omega t \sin(\Omega \frac{u}{c})$$

so that we can write the electric field as the sum of two different integrals that depend only on r (and not on t)

$$E_z = \frac{I_0 \mu_0 \Omega}{2\pi} \left(\sin(\Omega t) I_1(r) - \cos(\Omega t) I_2(r) \right)$$

with

$$I_1(r) = \int_r^{\infty} du \left[\frac{1}{\sqrt{u^2 - r^2}} \cos \Omega (\frac{u}{c}) \right] \quad I_2(r) = \int_r^{\infty} du \left[\frac{1}{\sqrt{u^2 - r^2}} \sin \Omega (\frac{u}{c}) \right] \tag{A.3}$$

We can proceed with the aid of `Mathematica` (43) or Python's symbollic algebra library, `Sympy`. The integrals are given by

$$\begin{aligned} I_1(r) &= \frac{\pi c}{\Omega r} G^{0,2}_{3,1} \left(\begin{matrix} \frac{1}{2}, \frac{1}{2} & 0 \\ & 0 \end{matrix} \middle| \frac{4c^2}{\Omega^2 r^2} \right) \\ &= \log \left(\frac{2c}{r\Omega} \right) J_0 \left(\frac{r\Omega}{c} \right) - \text{Hypergeometric0F1Regularized}^{(1,0)} \left(1, -\frac{r^2 \Omega^2}{4c^2} \right) \end{aligned} \tag{A.4}$$

$$I_2(r) = \frac{\pi J_0 \left(\frac{\Omega r}{c} \right)}{2}$$

Where G is the Meijer-G function and J_1 is a Bessel function of the first kind of order 0. Hence we have obtained an exact expression for the electric field $\mathbf{E}$. In our case however, c is large compared to the other physical variables so we can expand $I_2(r)$ in powers of c

$$I_2 = \frac{\pi}{2} - \frac{\pi \Omega^2 r^2}{8c^2} + \mathcal{O}\left(\frac{1}{c^3} \right) \tag{A.5}$$

repeating the same expansion for $I_1(r)$ we discover the leading order solution has the expected

logarithmic dependence on r from 2.13, and furthermore, there is no $\mathcal{O}(c^{-1})$ term in any of the expansions. (If you stare at Ampere's law this makes sense, because the electric field there acts in second order in c^{-1}, so there is no "room" for an $\mathcal{O}(c^{-1})$ term in any of the fields, as this would mean automatically mean they have an $\mathcal{O}(c)$ term)

$$\begin{aligned} I_1 &= \left(-\text{Hypergeometric0F1Regularized}^{(1,0)}(1,0) + \log(c) - \log(r\Omega) + \log(2)\right) + O\left(\frac{1}{c^2}\right) \\ &= (-\gamma + \log(c) - \log(r\Omega) + \log(2)) + O\left(\frac{1}{c^2}\right) \end{aligned} \tag{A.6}$$

Further, from the leading order terms for I_1 and I_2 we can deduce the $f(t)$ term hypothesized in the previous section. Indeed, we see

$$f(t) = \frac{I_0\mu_0\Omega}{2\pi}\left(\sin(\Omega t)(\log(2c) - \log(\Omega) - \gamma) - \cos(\Omega t)\frac{\pi}{2}\right)$$

A.2.3. Magnetic field

This is slightly more convoluted than the calculation for the electric field, as we must consider the contribution from both $\mathbf{J}$ and $\partial_t\mathbf{J}$ terms to the Jefimenko integral (2.4) First we consider the contribution from the current density, given by

$$\frac{\mu_0}{4\pi}\int\left[\frac{\mathbf{J}(\mathbf{x}', t_r)\times(\mathbf{x}-x')}{|\mathbf{x}-x'|^3}\right]d^3x'$$

proceeding as before we obtain that only the angular component is non zero, as this the direction if the cross product. Integrating out the radial and azimuthal contributions, we reach

$$= \frac{\mu_0}{4\pi}\int_{-\infty}^{\infty}\left[\frac{I(t_r)r}{(r^2+(z-z')^2)^{3/2}}\right]dz'$$

Using the same change of variables as for the electric field this simplifies to

$$\frac{\mu_0 I_0 r}{2\pi}\int_r^{\infty}\left[\frac{\cos(\Omega(t-\frac{u}{c}))}{u^2\sqrt{u^2-r^2}}\right]du$$

We can now proceed with the symbolic calculations, reaching a very complicated analytical expression.

$$\begin{aligned} &\frac{1}{8}I_0\mu\left(\frac{2}{r}\cos(t\Omega)G^{2,0}_{1,3}\left(\frac{r^2\Omega^2}{4c^2}\middle|\begin{matrix}\frac{3}{2}\\ 0,1,\frac{1}{2}\end{matrix}\right)\right) \\ &+\frac{\Omega\sin(t\Omega)\left(-\pi r\Omega\boldsymbol{H}_0\left(\frac{r\Omega}{c}\right)J_1\left(\frac{r\Omega}{c}\right)+\pi r\Omega\boldsymbol{H}_1\left(\frac{r\Omega}{c}\right)J_0\left(\frac{r\Omega}{c}\right)+2cJ_1\left(\frac{r\Omega}{c}\right)-2r\Omega J_0\left(\frac{r\Omega}{c}\right)+2c\right)}{c^2} \end{aligned} \tag{A.7}$$

Where $\boldsymbol{H}$ is the Struvel H function (1). And we can expand this to

$$\frac{I_0\mu\cos(t\Omega)}{2\pi r}+\frac{I_0\mu\Omega\sin(t\Omega)}{4c}+O\left(\frac{1}{c^2}\right)$$

so in particular we recover the expected solution to leading order. Now moving on the second part of the integral in Jefimenko's formula, we consider the contribution of $\partial_t\mathbf{J}$. The integral is given by

$$-\frac{\mu_0}{4\pi}\int\left[\frac{\mathbf{x}-x'}{|\mathbf{x}-x'|^2}\times\frac{1}{c}\frac{\partial\mathbf{J}(\mathbf{x}',t_r)}{\partial t}\right]d^3x'=-\frac{\mu_0}{4\pi c}\int_{-\infty}^{\infty}\left[\frac{I'(t_r)r}{r^2+(z-z')^2}\right]dz' \tag{A.8}$$

We will proceed in the same way as for the other two integrals. Integrating out the radial and azimuthal components we apply the same change of variables. The result after the aforementioned change of variables is

$$\frac{\mu_0 I_0 r\Omega}{2\pi c}\int_r^{\infty}\left[\frac{\sin(\Omega(t-\frac{u}{c}))}{u\sqrt{u^2-r^2}}\right]du$$

we can split the integral in two with the angle sum identity for the sum

$$\begin{aligned}&\frac{\mu_0 I_0 r\Omega}{2\pi c}\left(\sin\Omega t\int_r^{\infty}\left[\frac{\cos(\frac{\Omega u}{c})}{u\sqrt{u^2-r^2}}\right]du-\cos\Omega t\int_r^{\infty}\left[\frac{\sin(\frac{\Omega u}{c})}{u\sqrt{u^2-r^2}}\right]du\right)\\&=\frac{\mu_0 I_0 r\Omega}{2\pi c}\left(\sin\Omega t I_3(r)du-\cos\Omega t I_4(r)\right)\end{aligned} \tag{A.9}$$

Again, we compute two different integrals here. First, we compute

$$\begin{aligned}I_3(r)=\int_r^{\infty}\left[\frac{\cos(\frac{\Omega u}{c})}{u\sqrt{u^2-r^2}}\right]du&=\frac{\pi\left(-\pi r\Omega\boldsymbol{H}_0\left(\frac{r\Omega}{c}\right)J_1\left(\frac{r\Omega}{c}\right)+r\Omega\left(\pi\boldsymbol{H}_1\left(\frac{r\Omega}{c}\right)-2\right)J_0\left(\frac{r\Omega}{c}\right)+2c\right)}{4cr}\\&=\frac{\pi}{2r}\left(-\frac{\Omega r}{c}{}_1F_2\left(\begin{matrix}\frac{1}{2}\\1,\frac{3}{2}\end{matrix}\middle|-\frac{\Omega^2r^2}{4c^2}\right)+1\right)\end{aligned} \tag{A.10}$$

This is expanded in inverse powers of the speed of light to give

$$I_3(r)=\frac{\pi}{2r}-\frac{\pi\Omega}{2c}+\mathcal{O}\left(\frac{1}{c^2}\right)$$

It is important to note the $1/c$ factor in equation 2.23, so only the leading order term is relevant to approximated the first order corrections to the magnetic field. Now, for the second integral, that associated with the sin, we reach

$$I_4(r)=\int_r^{\infty}\left[\frac{\sin(\frac{\Omega u}{c})}{u\sqrt{u^2-r^2}}\right]du=\frac{\pi}{2r}G^{0,2}_{3,1}\left(\begin{matrix}\frac{1}{2},\frac{1}{2}&1\\&0\end{matrix}\middle|\frac{4c^2}{\Omega^2r^2}\right)$$

expanding in powers of c

$$I_4(r) = -\frac{(\Omega(-\log(c)+\log(r)+\log(\Omega)+\gamma-1-\log(2)))}{c} + \mathcal{O}\left(\frac{1}{c^2}\right)$$
$$= -\frac{\Omega}{c}(\gamma - 1 + \log(\frac{\Omega r}{2c})) + \mathcal{O}(c^{-2})$$

Considering again the $1/c$ factor in 2.23 we see this does not contribute to the first order correction.

A.3. Computation of components of the stress tensor for the free-boundary

A.3.1. Tangential stress balance

For the tangential stress balance the following term is required:

$$\mathbf{n} \cdot T_v \cdot \mathbf{t}$$

first we compute the components of the viscous stress tensor

$$T_v = \mu \begin{pmatrix} 2\partial_r u & 0 & \partial_z u + \partial_r w \\ 0 & \frac{2u(r,z)}{r} & 0 \\ \partial_z u + \partial_r w & 0 & 2\partial_z w \end{pmatrix}$$

Then, we can proceed to compute $T_v \cdot \mathbf{t}$

$$T_v \cdot \mathbf{t} = \mu \begin{pmatrix} \frac{2S_z \partial_r u}{\sqrt{S(z)^2+1}} + \frac{\partial_z u + \partial_r w}{\sqrt{S(z)^2+1}} \\ 0 \\ \frac{S_z(\partial_z u + \partial_r w)}{\sqrt{S(z)^2+1}} + \frac{2\partial_z w}{\sqrt{S(z)^2+1}} \end{pmatrix}$$

we can take the dot product of this vector with $\mathbf{n}$ to obtain the desired term:

$$\mathbf{n} \cdot T_v \cdot \mathbf{t} = \mu \frac{\frac{\partial_z u + \partial_r w}{\sqrt{S(z)^2+1}} - \frac{2S_z \partial_z w}{\sqrt{S(z)^2+1}}}{\sqrt{S(z)^2+1}} + \frac{S_z\left(\frac{2\partial_r u}{\sqrt{S(z)^2+1}} - \frac{S_z(\partial_z u + \partial_r w)}{\sqrt{S(z)^2+1}}\right)}{\sqrt{S(z)^2+1}}$$

this can be significantly manipulated to obtain

$$\frac{-2S_z\left(\partial_z w - \partial_r u\right) - \left(S_z^2 - 1\right)\partial_z u + S_z^2\left(-\partial_r w\right) + \partial_r w}{S(z)^2+1}$$

A.3.2. Normal Stress Balance

We must consider all the terms in the stress tensor now, to understand the condition:

$$\mathbf{n} \cdot [T] \cdot \mathbf{n} = \sigma \nabla \cdot \mathbf{n}$$

The pressure term is trivial, as it is an isotropic diagonal tensor, so it is simply p First we compute the curvature, or the divergence of the normal vector:

$$\kappa = \nabla \cdot \mathbf{n} = \frac{1}{r\sqrt{S_z^2+1}} + \frac{S_z^2 S_{zz}}{(S_z^2+1)^{3/2}} - \frac{S_{zz}}{\sqrt{S_z^2+1}}$$

this is evaluated at the free boundary, $r = S$ and it can thus be simplified to

$$\kappa = \nabla \cdot \mathbf{n} = \frac{1}{\sqrt{1+S_z}}\left(\frac{1}{S} - \frac{\partial_z^2 S}{1+S_z^2}\right)$$

Moving on to the contribution from the viscous stress tensor, we need $\mathbf{n}\cdot T_v \cdot \mathbf{n}$. The components of the viscous stress tensor where computed in the previous section so we focus on

$$T_v \cdot \mathbf{n} = \begin{pmatrix} \frac{2\partial_r u - S_z(\partial_z u + \partial_r w)}{\sqrt{S_z^2+1}} \\ 0 \\ \frac{-2S_z\partial_z w + \partial_z u + \partial_r w}{\sqrt{S_z^2+1}} \end{pmatrix}$$

and finally, dotting this with the normal vector again,

$$\mathbf{n}\cdot T_v \cdot \mathbf{n} = \frac{\frac{2\partial_r u}{\sqrt{S_z^2+1}} - \frac{S_z(\partial_z u+\partial_r w)}{\sqrt{S_z^2+1}}}{\sqrt{S_z^2+1}} - \frac{S_z\left(\frac{\partial_z u+\partial_r w}{\sqrt{S_z^2+1}} - \frac{2S_z\partial_z w}{\sqrt{S_z^2+1}}\right)}{\sqrt{S_z^2+1}}$$

which simplifies to

$$\frac{2\left(-S_z\left(\partial_z u + \partial_r w\right) + S_z^2\partial_z w + \partial_r u\right)}{S_z^2+1}$$

A.4. Long-wave expansions

Starting from eq. (4.16), we can substitute $S = \alpha + \eta$, and take the limit as η is small. Considering the left hand side first,

$$8\partial_t(S^2) = 16S\partial_t S = 16(\alpha+\eta)\partial_t\eta = 16\alpha\partial_t\eta\left(1+\frac{\eta}{\alpha}\right)$$

Moving on to the right hand side, first we must consider the $\partial_z p$

$$p = \frac{1}{S} - \epsilon^2 S_{zz} - \frac{\mathrm{Ma}}{S^2}$$

thus we reach that

$$\partial_z p - 1 = \frac{2\mathrm{Ma}\partial_z\eta}{(\alpha+\eta(z))^3} - \frac{\partial_z\eta)}{(\alpha+\eta)^2} + \epsilon^2\left(-\partial_z^3\eta\right) - 1 = -\left(1 + \frac{\partial_z\eta}{(\alpha+\eta)^2}\left(1 - \frac{2\mathrm{Ma}}{\alpha+\eta}\right) + \epsilon^2\partial_z^3\eta\right)$$

Considering the second term in the parenthesis, first we expand

$$(\alpha^2 - S^2)^2 = 4\alpha^2\eta^2 + 4\alpha\eta^3 + \eta^4$$

and then, the other term is

$$2(\alpha+\eta(z))^2\left(\alpha^2-(\alpha+\eta(z))^2+2(\alpha+\eta(z))^2\log\left(\frac{\alpha+\eta(z)}{\alpha}\right)\right)=4\alpha^2\eta^2+\frac{28}{3}\alpha\eta^3+\frac{19\eta^4}{3}+\mathcal{O}\left(\eta(z)^5\right)$$

subtracting both of this we obtain the second factor in the parenthesis is (higher order terms truncated)

$$\frac{16}{3}\alpha\eta^3+\frac{16\eta^4}{3}=\frac{16\eta^3\alpha}{3}\left(1+\frac{\eta}{\alpha}\right)$$

Thus, reassembling eq. (4.16), we reach

$$16\alpha\partial_t\eta\left(1+\frac{\eta}{\alpha}\right)=-\frac{\partial}{\partial z}\left\{\frac{16\eta^3\alpha}{3}(1+\frac{\eta}{\alpha})\left(1+\frac{\partial_z\eta}{(\alpha+\eta)^2}\left(1-\frac{2\mathrm{Ma}}{\alpha+\eta}\right)+\epsilon^2\partial_z^3\eta\right)\right\}$$

we can now divide by 16α and move all terms to the left hand side to obtain

$$\partial_t\eta\left(1+\frac{\eta}{\alpha}\right)+\frac{1}{3}\frac{\partial}{\partial z}\left\{\eta^3(1+\frac{\eta}{\alpha})\left(1+\frac{\partial_z\eta}{(\alpha+\eta)^2}\left(1-\frac{2\mathrm{Ma}}{\alpha+\eta}\right)+\epsilon^2\partial_z^3\eta\right)\right\}=0$$

A.5. Long wave dispersion relation

$$\begin{aligned}\partial_z p=-\frac{1}{S^2}\partial_z S-\epsilon^2\partial_z^3 S+2\mathrm{Ma}\frac{1}{S^3}\partial_z S&=-(1-2\mathrm{Ma})ik\delta\tilde{S}\phi-\epsilon^2(ik)^3\delta\tilde{S}\phi+\mathcal{O}(\delta^2)\\&=(-(1-2\mathrm{Ma})ik-\epsilon^2(ik)^3)\delta\tilde{S}\phi+\mathcal{O}(\delta^2)\\8\partial_t(S^2)=8\partial_t(1+2\delta\tilde{S}\phi+\mathcal{O}(\delta^2))&=16\delta\tilde{S}\lambda\phi+\mathcal{O}(\delta^2)\end{aligned}$$

we further consider

$$2S^2\left(\alpha^2-S^2+2S^2\log\left(\frac{S}{\alpha}\right)\right)-(\alpha^2-S^2)^2$$

$$\begin{aligned}(\alpha^2-S^2)^2=\alpha^4-2S^2\alpha^2+S^4&=\alpha^4-2\alpha^2(1+\delta\tilde{S}\phi)^2+(1+\delta\tilde{S}\phi)^4\\&=\alpha^4-2\alpha^2(1+2\delta\tilde{S}\phi)+(1+4\delta\tilde{S}\phi)+\mathcal{O}(\delta^2)\\&=(\alpha^2-1)^2+\mathcal{O}(\delta^2)\end{aligned}$$

for the first part, we directly use $1+2\delta\tilde{S}\phi$ instead of S^2

$$2S^2\left(\alpha^2-S^2+2S^2\log\left(\frac{S}{\alpha}\right)\right)=$$

$$2(1+2\delta\tilde{S}\phi)\left(\alpha^2-(1+2\delta\tilde{S}\phi)+2(1+2\delta\tilde{S}\phi)\log(1+\delta\tilde{S}\phi)-2(1+2\delta\tilde{S}\phi)\log\alpha\right)$$

now

$$\log(1+\delta\tilde{S}\phi)=\delta\tilde{S}\phi$$

thus

$$2(1+2\delta\tilde{S}\phi)\left(\alpha^2-(1+2\delta\tilde{S}\phi)+2(1+2\delta\tilde{S}\phi)\delta\tilde{S}\phi-2(1+2\delta\tilde{S}\phi)\log\alpha\right)$$

keeping only linear terms

$$2(\alpha^2-1-2\log\alpha-4\delta\tilde{S}\phi-\delta\tilde{S}\phi\log\alpha)+4\delta\tilde{S}\phi(\alpha^2-1-2\log\alpha)=$$

$$2(\alpha^2 - 1 - 2\log\alpha) + \delta\tilde{S}\phi(-8 - 2\log\alpha + 4((\alpha^2 - 1 - 2\log\alpha))$$

Considering the linear terms of the product inside the derivative in equation (4.16)

$$(\partial_z p - 1)\left(2S^2\left(\alpha^2 - S^2 + 2S^2\log\left(\frac{S}{\alpha}\right)\right) - (\alpha^2 - S^2)^2\right)$$

$$-(2(\alpha^2 - 1 - 2\log\alpha) - 8\delta\tilde{S}\phi(\alpha^2 - 1 - 2\log\alpha) - (\alpha^2 - 1)^2$$

$$+(-(1 - 2\mathrm{Ma})ik - \epsilon^2(ik)^3)\delta\tilde{S}\phi(2(\alpha^2 - 1 - 2\log\alpha) - (\alpha^2 - 1)^2)$$

taking a derivative with respect to z annihilates all the constant terms, and gives us

$$-8ik\delta\tilde{S}\phi(\alpha^2 - 1 - 2\log\alpha) - ((1 - 2\mathrm{Ma})ik + \epsilon^2(ik)^3)\delta\tilde{S}\phi(2(\alpha^2 - 1 - 2\log\alpha) - (\alpha^2 - 1)^2)$$

reconstructing the equation and cancelling $\delta\tilde{S}\phi$ we reach the linear dispersion relation:

$$\lambda(k) = \frac{k^2}{16}\left(\epsilon^2k^2 + 2\mathrm{Ma} - 1\right)((\alpha^2 - 1)^2 + 2(2\log\alpha + 1 - \alpha^2)) - \frac{ik}{2}(2\log\alpha + 1 - \alpha^2) \quad \text{(A.11)}$$

A.6. Computation of the stream function

From the equations obtained for the radial and axial velocities, $u(r, z)$ and $w(r, z)$ the Stokes stream function can be computed by integration. Writing

$$w = -\frac{1}{r}\frac{\partial\psi}{\partial r}$$

We can integrate this to

$$\psi(r, z) = -\frac{1}{16}r^2\left(p_z - 1\right)\left(-2\alpha^2 + r^2 + S^2\left(2 - 4\log\left(\frac{r}{\alpha}\right)\right)\right) + f(z)$$

where $f(z)$ is an arbitrary function of z. Substituting into the second velocity-stream function relation we find an expression for $f'(z)$

$$u(r, z) = \frac{1}{r}\frac{\partial\psi}{\partial z} =$$

$$= \frac{1}{r}\left[\frac{1}{16}r^2\left(4S\left(p_z - 1\right)\left(2\log\left(\frac{r}{\alpha}\right) - 1\right)S_z - p_{zz}\left(-2\alpha^2 + r^2 + S^2\left(2 - 4\log\left(\frac{r}{\alpha}\right)\right)\right)\right) + f'(z)\right]$$

Solving for $f'(z)$

$$f'(z) = \frac{1}{16}\alpha^2\left(2S^2p_{zz} - \alpha^2p_{zz} + 4S\left(p_z - 1\right)S_z\right)$$

and finally integrating (the integration constant is unimportant)

$$f(z) = \frac{1}{8}\alpha^2S^2\left(p_z - 1\right) - \frac{1}{16}\alpha^4p_z$$

This can be reassembled to obtain the stream function.

$$\psi(r, t) = \frac{1}{16}\left(2S^2\left(p_z - 1\right)\left(\alpha^2 + 2r^2\log\left(\frac{r}{\alpha}\right) - r^2\right) - \left(r^2 - \alpha^2\right)^2p_z + r^4 - 2\alpha^2r^2\right) \quad \text{(A.12)}$$

We can add a constant, α^4, without altering the dynamics, to obtain a more compact final form for the stream function

$$\psi(r,t) = \frac{(\partial_z p - 1)}{16}\left(2S^2\left(\alpha^2 + 2r^2\log\left(\frac{r}{\alpha}\right) - r^2\right) - \left(r^2-\alpha^2\right)^2\right) \tag{A.13}$$

A.7. Linearised boundary conditions in terms of the stream function

Recall all of the below equations are evaluated at $r = 1$. The tangential stress balance is transformed from

$$\partial_r w_1 + \partial_z u_1 = S_1$$

to

$$\frac{\frac{\partial}{\partial r}\psi(r,t)}{r^2} - \frac{\frac{\partial^2}{\partial r^2}\psi(r,t)}{r} - \frac{k^2\psi(r,t)}{r} = S_1$$

using this expression for S in the kinematic equation, that reads

$$\partial_t S + i\kappa w_0(1)S = u_1(1) \Longrightarrow \partial_t S + i\kappa w_0(1)S = i\kappa\psi(r=1)$$

is transformed to

$$\frac{\frac{\partial^2}{\partial r\partial t}\psi(r,t)}{r^2} - \frac{\frac{\partial^3}{\partial r^2\partial t}\psi(r,t)}{r} - \frac{k^2\left(\frac{\partial}{\partial t}\psi(r,t)\right)}{r} + ikW\left(\frac{\frac{\partial}{\partial r}\psi(r,t)}{r^2} - \frac{\frac{\partial^2}{\partial r^2}\psi(r,t)}{r} - \frac{k^2\psi(r,t)}{r}\right) - \frac{ik\psi(r,t)}{r}$$

which is the required equation as presented in section 7.5. Now, using the normal stress balance that in velocity-pressure variables reads

$$\mathrm{Bo}\, p - 2\mathrm{Ca}\partial_r u_1 = -(D-\kappa^2)S_1$$

is first transformed to streamfunction-pressure variables to

$$\mathrm{Bo}\, p + 2i\kappa\mathrm{Ca}(\psi(1) - \psi'(1)) = -(D-\kappa^2)S_1$$

to obtain an expression that only involves ψ we must solve for p in the Navier-Stokes equation in the z direction

$$\begin{aligned} &i\left(\frac{\partial}{\partial r}\psi(r,t)\right)W(r)\,Rk\,r^2 - i\psi(r,t)\left(\frac{d}{dr}W(r)\right)Rk\,r^2 + k^2\left(\frac{\partial}{\partial r}\psi(r,t)\right)r^2 \\ &+\left(\frac{\partial^2}{\partial r\partial t}\psi(r,t)\right)R\,r^2 - \left(\frac{\partial^3}{\partial r^3}\psi(r,t)\right)r^2 + \left(\frac{\partial^2}{\partial r^2}\psi(r,t)\right)r - \frac{\partial}{\partial r}\psi(r,t) = 0 \end{aligned} \tag{A.14}$$

with a simple substitution we will recover the equation as presented in section 7.5.

A.8. Matrix for Stokes stability

The matrix $M(\Lambda)$ is given by

$$\begin{pmatrix} \dots & \mathbf{v}^\intercal(\alpha) & \dots \\ \dots & \frac{\partial \mathbf{v}^\intercal}{\partial r}(\alpha) & \dots \\ \dots & \mathbf{v}^\intercal(1)(-\Lambda\kappa^2 - w_0(1)i\kappa^3 - i\kappa) + \frac{\partial \mathbf{v}^\intercal}{\partial r}(1)(\Lambda + i\kappa w_0(1)) + \frac{\partial^2 \mathbf{v}^\intercal}{\partial r^2}(1)(-\Lambda - i\kappa w_0(1)) & \dots \\ \dots & \mathrm{Bo}\,\mathbf{q}^\intercal(1) + \mathbf{v}^\intercal(1)(-2i\kappa\mathrm{Ca} - D\kappa^2 + \kappa^4) + \frac{\partial \mathbf{v}^\intercal}{\partial r}(1)(-2i\kappa\mathrm{Ca} - \kappa^2 + D) + \frac{\partial^2 \mathbf{v}^\intercal}{\partial r^2}(1)(\kappa^2 - D) & \dots \end{pmatrix} \tag{A.15}$$

A.9. Chebyshev Spectral Method.

To discretise the linear system in section 7.5, the Chebyshev spectral method was used (49). The unknown function is expanded as a (finite) Chebyshev series

$$\psi(r) = \sum_{j=0}^{N} \mu_j T_j(r) \tag{A.16}$$

so that we are now interested in solving for the $N+1$ unknowns $\{\mu_j\}_j$. Taking into account that we have 4 boundary conditions for ψ, we evaluated the differential equation at $N-3$ Gauss-Lobato points (46). Considering we can write the derivatives of a Chebyshev polynomial in terms of other Chebyshev polynomials, this will give us a linear system of $N+1$ linear equations for the $N+1$ unknowns. In practice, we first evaluate the Chebyshev polynomials and their derivatives using the three term recurrence relation (49).

$$T_{j+1}(x) = 2xT_j(x) - T_{j-1}(x) \tag{A.17}$$

and this is directly substituted into the equations to build the matrix for the linear system.

Bibliography

[1] M. Abramowitz and I. A. Stegun. *Handbook of Mathematical Functions: With Formulas, Graphs, and Mathematical Tables*. Dover Publications, 1972.

[2] V. S. Ajaev and G. M. Homsy. Spreading of thin volatile liquid films on uniformly heated surfaces. *Journal of Fluid Mechanics*, 560:229–240, 2006.

[3] V. I. Arkhipenko, Yu D. Barkov, V. G. Bashtovoi, and M. S. Krakov. Investigation into the stability of a stationary cylindrical column of magnetizable liquid. *Fluid dynamics*, 15(4):477–481, 1981. ISBN: 0015-4628.

[4] S. G. Bankoff and S. H. Davis. A systematic approach to falling film flows. *Journal of Fluid Mechanics*, 267:173–191, 1994.

[5] V. G. Bashtovoi and M. S. Krakov. Stability of an axisymmetric jet of magnetizable fluid. *Journal of applied mechanics and technical physics*, 19(4):541–545, 1974. ISBN: 0021-8944.

[6] G. K. Batchelor. *An introduction to fluid dynamics*. Cambridge University Press, 1973.

[7] M. G. Blyth and E. I. Părău. Solitary waves on a ferrofluid jet. *Journal of Fluid Mechanics*, 750:401–420, 2014.

[8] Michael Cornish. *Viscous and inviscid nonlinear dynamics on an axisymmetric ferrofluid jet*. Imperial College London, 2018.

[9] M. D. Cowley and R. E. Rosensweig. The interfacial stability of a ferromagnetic fluid. *Journal of Fluid Mechanics*, 30(4):671–688, 1967.

[10] R. V. Craster and O. K. Matar. On viscous beads flowing down a vertical fibre. *Journal of Fluid Mechanics; J.Fluid Mech*, 553(1):85–105, 2006. ISBN: 0022-1120.

[11] G. Da Prato and J. Zabczyk. *Stochastic Partial Differential Equations: An Introduction*. Springer, 2014.

[12] P. A. Davidson. *An Introduction to Magnetohydrodynamics*. Cambridge University Press, 2001.

[13] C. Duprat, C. Ruyer-Quil, S. Kalliadasis, and F. Giorgiutti-Dauphiné. Absolute and convective instabilities of a viscous film flowing down a vertical fiber. *Physical Review Letters; Phys Rev Lett*, 98(24):244502, 2007. ISBN: 0031-9007.

[14] A. Einstein. *Investigations on the Theory of the Brownian Movement*. Dover Publications, 1956.

[15] Pauli Virtanen et. al. Scipy 1.0: Fundamental algorithms for scientific computing in python, 2020.

[16] Sarah Helen Ferguson-Briggs. *Linear stability of ferrofluids in a non-uniform magnetic field*. Imperial College London, 2022.

[17] B. Fornberg. *A Practical Guide to Pseudospectral Methods*. Cambridge University Press, 1996.

[18] A. L. Frenkel. Nonlinear theory of strongly undulating thin films flowing down vertical cylinders. *Europhysics Letters*, 18(7):583–588, 1992. ISBN: 0295-5075.

[19] C. W. Gardiner. *Stochastic Methods: A Handbook for the Natural and Social Sciences*. Springer Science & Business Media, 4 edition, 2009.

[20] I. S. Grant and W. R. Phillips. *Electromagnetism*. The Manchester physics series. Wiley, 2nd ed edition, 1990.

[21] E. Hairer and G. Wanner. *Solving Ordinary Differential Equations II: Stiff and Differential-Algebraic Problems*. Springer-Verlag, 1996.

[22] Damian P. Hampshire. A derivation of maxwell's equations using the heaviside notation. *Philosophical Transactions of the Royal Society A: Mathematical, Physical and Engineering Sciences*, 376(2134):20170447, 2018.

[23] Charles R Harris, K Jarrod Millman, Stéfan J van der Walt, Ralf Gommers, Pauli Virtanen, David Cournapeau, Eric Wieser, Julian Taylor, Sebastian Berg, Nathaniel J Smith, et al. Array programming with numpy. *Nature*, 585(7825):357–362, 2020.

[24] A. C. Hindmarsh. Odepack, a systematized collection of ode solvers. *Scientific Computing*, pages 55–64, 1983.

[25] J. D. Jackson. *Classical Electrodynamics*. John Wiley & Sons, 3 edition, 1999.

[26] S. Kalliadasis, C. Ruyer-Quil, B. Scheid, and M. G. Velarde, editors. *Falling Liquid Films*. Springer Science & Business Media, 2012.

[27] I. Karatzas and S. E. Shreve. *Brownian Motion and Stochastic Calculus*. Springer Science & Business Media, 2 edition, 2012.

[28] I. L. Kliakhandler, S. H. Davis, and S. G. Bankoff. Viscous beads on vertical fibre. *Journal of Fluid Mechanics*, 429:381–390, 2001.

[29] H. Lamb. *Hydrodynamics*. Cambridge University Press, 6 edition, 1932.

[30] B. Levich and L. Landau. Dragging of a liquid by a moving plate. *Acta Physicochimica U.R.S.S.*, 17(1-2):42–54, 1942.

[31] V. G. Levich. *Physicochemical Hydrodynamics*. Prentice Hall, 1962.

[32] A. Liénard. Champ électrique et magnétique produit par une charge concentrée en un point et animée d'un mouvement quelconque. *L'Éclairage Électrique*, 16(27, 28, 29):5–14, 53–59, 106–112, 1898.

[33] G. J. Lord, C. E. Powell, and T. Shardlow. *An Introduction to Computational Stochastic PDEs*. Cambridge University Press, 2014.

[34] J. E. Marsden and A. J. Tromba. *Vector Calculus*. W. H. Freeman, 6 edition, 2012.

[35] A. M. Mathai. *A Handbook of Generalized Special Functions for Statistical and Physical Sciences*. Oxford University Press, New York, 1993.

[36] P. Mörters and Y. Peres. *Brownian Motion*. Cambridge University Press, 2010.

[37] D. T. Papageorgiou. Nonlinear dynamics of films and filaments on vertical fibers subject to a gravitational field. *Physics of Fluids A: Fluid Dynamics*, 2(9):1499–1508, 1990.

[38] D. T. Papageorgiou. On the breakup of viscous liquid threads. *Physics of Fluids A: Fluid Dynamics*, 4(2):258–267, 1992.

[39] D. T. Papageorgiou, C. Maldarelli, and D. S. Rumschitzki. Dynamics of liquid films on inclined planes: I. development of a quasi-2d model. *Physics of Fluids*, 7(4):787–804, 1995.

[40] M. Pradas, G.A. Pavliotis, S. Kalliadasis, D.T. Papageorgiou, and D. Tseluiko. Additive noise effects in active nonlinear spatially extended systems. *European Journal of Applied Mathematics*, 23(5):563–591, 2012,.

[41] M. Pradas, D. Tseluiko, S. Kalliadasis, D. T. Papageorgiou, and G. A. Pavliotis. Noise induced state transitions, intermittency, and universality in the noisy kuramoto-sivashinksy equation. *Physical Review Letters*, 106(6):060602, 2011.

[42] E. R. Priest and T. G. Forbes. *Magnetic Reconnection: MHD Theory and Applications*. Cambridge University Press, 2000.

[43] Wolfram Research. Mathematica.

[44] Wolfram Research. Hypergeometric0f1regularized, 1996. Updated in 2021.

[45] R. E. Rosensweig. *Ferrohydrodynamics*. Cambridge University Press, 1985.

[46] J. Shen. Efficient spectral-galerkin method i. direct solvers of second-and fourth-order equations using legendre polynomials. *SIAM Journal on Scientific Computing*, 15(6):1489–1505, 1994.

[47] D. Ter Haar. *Collected papers of LD Landau*. Elsevier, 2013.

[48] U. Thiele and E. Knobloch. Driven drops on heterogeneous substrates: Onset of sliding motion. *Physical Review Letters*, 95(7):076104, 2005.

[49] L. N. Trefethen. *Spectral Methods in MATLAB*. SIAM, 2000.

[50] Q. Wang and D. T. Papageorgiou. Dynamics of a viscous thread surrounded by another viscous fluid in a cylindrical tube under the action of a radial electric field: breakup and touchdown singularities. *Journal of Fluid Mechanics; J.Fluid Mech*, 683:27–56, 2011. ISBN: 0022-1120.

[51] F. M. White. *Viscous Fluid Flow*. McGraw-Hill, 3 edition, 2006.

[52] E. Wiechert. Elektrodynamische elementargesetze. *Annalen der Physik*, 309(4):667–689, 1901.

[53] Liyan Yu and John Hinch. The velocity of 'large' viscous drops falling on a coated vertical fibre. *Journal of Fluid Mechanics*, 737:232–248, 2013.

[54] Andrew Zangwill. *Modern electrodynamics*. Cambridge University Press, 2013.